AXON DEGENERATION IN *C. ELEGANS*

by

Randi L. Rawson

A dissertation submitted to the faculty of
The University of Utah
in partial fulfillment of the requirements for the degree of

Doctor of Philosophy

Interdepartmental Program in Neuroscience

The University of Utah

August 2014

The University of Utah Graduate School

STATEMENT OF DISSERTATION APPROVAL

The dissertation of **Randi L. Rawson**

has been approved by the following supervisory committee members:

Erik M. Jorgensen	, Chair	**March 7, 2014** Date Approved
Michael Bastiani	, Member	**March 7, 2014** Date Approved
Sabine Fuhrmann	, Member	**March 7, 2014** Date Approved
Andres V. Maricq	, Member	**March 7, 2014** Date Approved
Jody Rosenblatt	, Member	**March 7, 2014** Date Approved

and by **Kristen A. Keefe** , Chair/Dean of

the Department/College/School of **Interdepartmental Program in Neuroscience**

and by David B. Kieda, Dean of The Graduate School.

ABSTRACT

Axons degenerate following injury and during “dying-back” neurodegenerative diseases, which are characterized by early degeneration of synapses and axons. While injury and disease are clearly distinct events, they share some common regulators. Although these problems have been extensively studied, very little is known about which molecules initiate and execute the degeneration process. Uncovering mediators of axonal degeneration could provide new therapeutic targets for the treatment of neurodegenerative disease.

This dissertation studies axon degeneration in the nematode *Caenorhabditis elegans,* where degeneration can be induced genetically or by injury. Axons degenerate in a manner consistent with Wallerian degeneration; they swell and fragment into debris particles that are engulfed by other cells. I have studied two main aspects of axon degeneration. First, I have shown that mitochondria are required to prevent the initiation of axon degeneration. I characterize a novel gene *ric-7*, which is required for mitochondrial export from neuronal cell bodies. In both *ric-7* mutant and wild-type axons, degeneration is enhanced in the absence of mitochondria. Thus, mitochondria primarily protect axons and are not required for the execution of degeneration. Second, I have identified genes required for nonprofessional phagocytes to engulf neuronal

debris following degeneration. I demonstrate that hypodermal cells engulf degenerating axons in *C. elegans* and that only some of the programmed cell death (*ced*) genes are involved. There are two parallel pathways that mediate engulfment of cell corpses during apoptosis; *ced-1, -6, -7* and *ced-2, -5, -10, -12*. Both *ced-1* and *ced-6* are required for engulfment of degenerating axons, but not the parallel *ced-2, -5, -12* pathway. Thus, epithelial cells engulf degenerating axons in a manner that is distinct from both apoptosis and macrophage/glia-mediated engulfment of degenerating axons. *C. elegans* will be a useful model system for uncovering novel regulators of mitochondria-mediated axon protection and epithelia-mediated engulfment.

TABLE OF CONTENTS

LIST OF FIGURES

ACKNOWLEDGMENTS

First and foremost, I would like to thank my advisor Erik Jorgensen for his continued support and enthusiasm, and perhaps most of all, for throwing me into the deep end of the pool right from the beginning. Thank you for providing inspiration and the freedom to explore. I've learned a deeper joy for science than I ever imagined possible.

I would also like to thank all of my colleagues in the Jorgensen lab for providing such an intellectually stimulating and supportive environment. I would especially like to thank Marc Hammarlund, Michael Ailion, and Gunther Hollopeter for providing the most training and guidance; Erik and Wayne Davis for teaching me the art of communicating science; and Eric Bend, Josh Jackson, Qiang Liu, and Shigeki Watanabe for collaboration on experiments. Many thanks to Becky McKean, Amrita, Sarah Bodian, and Janice; you lift us all higher. I'm also grateful to Patrick, Eddie, Sean, and Christian for taking the time to review my dissertation. I'd like to give a huge shout out to my science brother P. Mac for moral support and for always being someone to dream big with, as well as to Mark Palfreyman and Hsiao-Fen Han. I was so fortunate to have three wonderful baymates who made each day a delight.

I am grateful to each of my thesis committee members for all their time and thoughtful advice over the years; Mike Bastiani, Chi-Bin Chien, Sabine

Fuhrmann, Villu Maricq, and Jody Rosenblatt. I especially want to thank Mike Bastiani and Villu Maricq for so generously providing me with access to their microscopy equipment, without which this dissertation would not have been possible. My sincerest thanks to the Neuroscience program directors Mary Lucero and Kristin Keefe, and to Tracy Marble. Thank you for the support that each of you has provided; it has been wonderful to be a part of this program. I would also like to thank the Neuroscience training grant and the Dale A. Stringfellow Award for financial support.

I express my sincerest gratitude to John E. Kelsey, José Lemos, Nils Brose, and Frederique Varoqueaux, without whom this journey may have never happened. Many thanks to Shaili Johri, Anand Mukhopadhyay, Eric & Renee Bend, Shushruth, Annie Schwager, Sean Flynn, Eric Stembridge, and Michael Manhard for all the memories and fun times away from the lab bench. Most importantly, I would like to thank my family for all their love and unwavering support of any and all dream chasing.

CHAPTER 1

INTRODUCTION

Breakdown of neuronal processes occurs during developmental pruning, neurodegenerative disease, and following an injury. While degeneration is typically thought of as detrimental, it can serve a beneficial purpose. The pruning of axons and dendrites during development is essential for establishing functional neuronal networks (Luo and O'Leary, 2005). Degeneration of injured axons is also beneficial to an organism because regrowth is impaired if damaged axons are not removed (Hosmane et al., 2012; Tanaka et al., 2009). However, axon destruction programs are inappropriately activated in neurodegenerative diseases. Some diseases clearly involve the death of the whole cell, while others are considered "dying-back" neurodegeneration (Coleman and Freeman, 2010; Dadon-Nachum et al., 2011; Han et al., 2010; Kanaan et al., 2013). In "dying-back" diseases, the synapses and axons break down a substantial time before the cell body dies. One model to explain the "dying-back" phenomenon is that a prodegeneration signal in distal axons is transmitted back to the cell body over time. In this model, preventing the degeneration of synapses and axons may quell the disease as a whole.

Although pruning, neurodegenerative disease, and injury-induced degeneration are clearly distinct events, they do share multiple characteristics. First, the breakdown process in all three of these events follows a progression of stereotyped morphological changes commonly referred to as Wallerian degeneration. They swell and fragment into smaller particles that are cleared away by other cells through engulfment. Second, caspase signaling mediates both pruning and degeneration following injury (Kuo et al., 2006; Nikolaev et al., 2009; Schoenmann et al., 2010; Williams et al., 2006). Third, the protective chimeric protein Wlds can suppress degeneration in both disease and injury models (Beirowski et al., 2004; Ferri et al., 2003; Howell et al., 2007). Lastly, genes required for the clearance of fragmented neurites are shared between pruning, injury-induced degeneration, and neurodegeneration (Awasaki et al., 2006; Chung et al., 2000; Macdonald et al., 2006). Thus, investigating the molecular underpinnings of axon degeneration is a means to understand neuronal development and response to injury, as well as to uncover therapeutic targets for the treatment of neurodegenerative diseases.

Wallerian Degeneration

Augustus Waller (1816-1870) characterized the destruction of axons following an injury. Waller severed the glossopharyngeal and hypoglossal nerves of the frog tongue and observed the morphological changes occurring over time (Waller, 1850). He made three critical observations that have proven over the past century and a half to be hallmarks of axon degeneration. First, he noted that

the nerves break down by dissociating into increasingly smaller granules. Second, he observed that this fragmentation process was most severe at the extremities of the nerves. And third, he stated that the granules were “removed by absorption.” He also aptly speculated that the destruction he was observing might be related to prolonged disease states in humans. Due to the seminal nature of this work, the breakdown of nerve fibers has subsequently been referred to as Wallerian degeneration. A legion of studies has since corroborated Waller’s foundational discoveries. Injured axons first swell and then fragment into dissociated granules of debris that are eventually cleared away by other cells through engulfment (Wang et al., 2012). Fragmentation progresses anterograde from the lesion site after complete transection of an axon and retrograde from the distal tip after a crush injury (Beirowski et al., 2005).

Wld^{S}

The study of Wallerian degeneration took a profound turn with the discovery of a spontaneous mutation that protected mice against neuronal injury (Lunn et al., 1989). The mutation was named Wld^{S} for slow Wallerian degeneration. Wld^{S} is a tandem triplication that creates a chimeric protein fusion between the N-terminal 70 amino acids of ubiquitination factor E4B (Ube4b) and nicotinamide mononucleotide adenylyltransferase 1 (Nmnat1) (Coleman et al., 1998; Mack et al., 2001). The discovery of the neuroprotected Wld^{S} mice provided evidence that Wallerian degeneration is a genetically encoded and regulated process, rather than the passive decay of tissue.

The specific mechanism of Wld^S neuroprotection is not clear. However, Nmnat is known to provide the neuroprotective activity, while the Ube4b domain mediates subcellular localization. Nmnat is an NAD^+ synthesis enzyme. There are three Nmnat proteins in mice, each with a unique subcellular localization; nucleus (Nmnat1) (Berger et al., 2005), Golgi transport vesicles (Nmnat2) (Gilley and Coleman, 2010; Milde et al., 2013), and mitochondria (Nmnat3) (Berger et al., 2005). Both Nmnat1 and 3 are axon protective when overexpressed, whereas Nmnat2 is not protective unless highly overexpressed due to its short half-life (Avery et al., 2009; Gilley and Coleman, 2010; Sasaki et al., 2006). The Ube4b fragment in Wld^S increases the axon localization of the fusion protein. Localizing Wld^S to axons must be the important contribution of the Ube4b fragment, since Nmnat1 is just as potent as Wld^S at protecting axons if its endogenous nuclear localization signal is replaced with an axon localization signal (Babetto et al., 2010; Beirowski et al., 2009; Sasaki et al., 2009a). Despite the multitude of studies on Wld^S over the past decade, its mechanism of action is still widely debated. There are three models for Wld^S mechanism of protection: NAD^+ synthesis, altering mitochondria dynamics, and chaperoning synaptic proteins.

NAD^+ synthesis

The importance of Nmnat's enzymatic activity remains controversial. Several studies have shown that Nmnat enzyme activity is required for its axon protection effects (Araki et al., 2004; Avery et al., 2009; Jia et al., 2007; Sasaki et al., 2009b; Yan et al., 2010). In contrast, two studies from Drosophila have

demonstrated that enzymatically dead Nmnat can still robustly protect axons after an injury (Kitay et al., 2013; Zhai et al., 2006). Exogenous application of the enzymatic product, NAD^+, can protect axons (Araki et al., 2004; Wang et al., 2005a), although this result is not consistent between different studies (Conforti et al., 2007; Sasaki et al., 2009b). And while Nmnat activity is increased in Wld^S neurons, the NAD^+ levels are not (Mack et al., 2001). In conclusion, the conflicting results regarding the importance of Nmnat's enzymatic activity suggest that while NAD^+ likely affects neuronal stability, NAD^+ synthesis is not likely to be the only mechanism of protection for Wld^S.

Mitochondria

Recent reports suggest that an important function of Wld^S is to regulate mitochondria function or trafficking. Nmnat3 is localized to mitochondria and can robustly protect axons when overexpressed (Avery et al., 2009; Berger et al., 2005; Sasaki et al., 2006). RNAi against *Drosophila* Nmnat results in age-dependent depletion of mitochondria from axons in the wing (Fang et al., 2012). Wld^S mitochondria are capable of buffering a greater amount of calcium and have increased mobility in axons following an injury compared to wild-type mitochondria (Avery et al., 2012; O'Donnell et al., 2013).

Wld^S axon protection depends on proper mitochondria transport. Decreased Wld^S mitochondria mobility in hypomorphic mutants of the transport adaptor *miro* suppresses the axon protective effects of Wld^S (Avery et al., 2012). In a separate study, knockdown of another mitochondria transport adaptor milton

resulted in spontaneous degeneration of axons in the adult fly wing. The spontaneous axon degeneration could not be suppressed with Wld^S or overexpression of Nmnat (Fang et al., 2012). These data suggest that mitochondria are critical for the protective mechanism of Wld^S.

Chaperone

Perhaps the most intriguing model for Wld^S function is its proposed action as a chaperone. Grace Zhai's laboratory has demonstrated that an enzymatically dead Wld^S can still protect axons, even in the complete absence of mitochondria (Kitay et al., 2013; Zhai et al., 2006). They demonstrate that in the absence of Nmnat, the synaptic protein Bruchpilot is degraded and synapses are destabilized (Zang et al., 2012). However, while loss of Nmnat destabilized Bruchpilot T-bar structures at the active zone, neuromuscular junction and motor neuron axon degeneration were not demonstrated. Similarly, there have not been reports of Bruchpilot mutants exhibiting neurodegeneration. Perhaps Nmnat is stabilizing multiple synaptic proteins and the loss of Bruchpilot alone is insufficient to induce the neurodegeneration frequently observed after loss of Nmnat.

Towards an integrated model

Our current understanding of Wld^S-mediated neuronal protection comes from *Drosophila* and mammalian model organisms using several different experimental protocols for inducing degeneration. It is plausible that different

neuronal insults require protective factors like Wld^S to varying degrees. To properly interpret the results above, we must consider the three methods used to induce neurodegeneration: axon damage (crushing), axon transection, and degeneration in the absence of injury.

Studies from *Drosophila* present conflicting results for the role of mitochondria in Nmnat-mediated axon protection. Hypomorphic mutations in *miro* suppress the protective effects of Wld^S after laser axotomy of the olfactory receptor neurons (Avery et al., 2012); but, knockout of milton has no effect on Wld^S protection of crushed motor neuron axons. Perhaps Wld^S protects axons through multiple mechanisms and the type of injury is critical. Crush injuries proceed retrogradely from the distal axon (Beirowski et al., 2005). Thus, in a motor neuron crush injury, Wld^S may be protecting the axons by stabilizing Bruchpilot at the neuromuscular junctions. By contrast, complete transection of an axon leads to fragmentation proceeding anterogradely, beginning at the lesion site (Beirowski et al., 2005). Complete transection likely results in a larger calcium influx at the lesion site, and protecting axons from transection may therefore require mobilizing mitochondria and increasing their buffering capacity. However, Wld^S was also unable to protect against retrograde degeneration of axons in the fly wing after knockdown of milton (Fang et al., 2012). In this case, there was no injury to the cell; thus, these experiments represent yet another class of axon degeneration. It will be important for future studies to resolve whether these discrepancies are due to variations in the injury method or neuron type. It will also be interesting to see if roles for Wld^S in both chaperoning and

mitochondria dynamics can be observed in mammalian systems as well.

Limitations of Wld^S

Wld^S is not always protective. Perhaps most intriguing are the results for Wld^S in developmental pruning. Wld^S does not suppress axon pruning in *Drosophila* (Hoopfer et al., 2006), but surprisingly, it can inhibit dendritic pruning (Schoenmann et al., 2010; Tao and Rolls, 2011). In addition to axon pruning, Wld^S has been reported to have no effect on various neurodegenerative disease models, including ALS and spinal muscular atrophy, both of which are considered to be dying-back diseases with axonal defects arising before the death of the cell (Kariya et al., 2009; Rose Jr. et al., 2008; Velde et al., 2004).

The rules governing the degeneration of neuronal processes are still murky at best. There are undoubtedly different types of degeneration with unique molecular mediators of destruction. However, at this time it is unclear as to how various types of degeneration can be categorized. Where do they overlap and differentiate from one another? For example, does dendritic pruning have more in common with axon degeneration than axon pruning? Because Wld^S is one of the most widely tested molecules in degeneration, it may be the first step in categorizing types of neural degeneration. Elucidation of the mechanisms behind Wld^S may help parse the various forms of axon degeneration into functional categories.

Up until the last couple of decades, Wallerian degeneration was defined exclusively by its characteristic morphological changes. In recent years, Wld^S has

become the gold standard of Wallerian degeneration. However, it is important to acknowledge that Wld^S represents a mechanism of axon protection, and not necessarily a mechanism of axon destruction. Wld^S could be acting to directly inhibit an axon destruction program (Figure 1.1A), in which case it is a reliable readout of the actual degeneration process. Alternatively, Wld^S could be acting in parallel to destruction programs by over-activating a survival mechanism (Figure 1.1B). In other words, it could be promoting a protective function within the axon that is independent of the executers of axon degeneration. There are undoubtedly multiple ways to kill an axon. Do each of these mechanisms end with the same fragmentation, beading, and removal of axons, i.e., Wallerian degeneration? How likely is it that Wld^S will also suppress each mechanism of axon destruction? Wld^S has provided a valuable inroad to the molecular study of Wallerian degeneration, but until its function is finally resolved, it is difficult to know whether it is an appropriate redefinition of Wallerian degeneration.

The Role of Mitochondria in Degeneration

Many neurodegenerative disorders are associated with mitochondrial defects. However, due to the vast complexity of most neurological diseases, it is difficult to resolve the role of mitochondria within degeneration. While a select number of diseases do arise directly from mutations affecting mitochondria (Alexander et al., 2000; Delettre et al., 2000; Züchner et al., 2004), the vast majority of diseases involve indirect impairment of mitochondria. But even the indirect mitochondrial deficits may be playing an early and influential role in

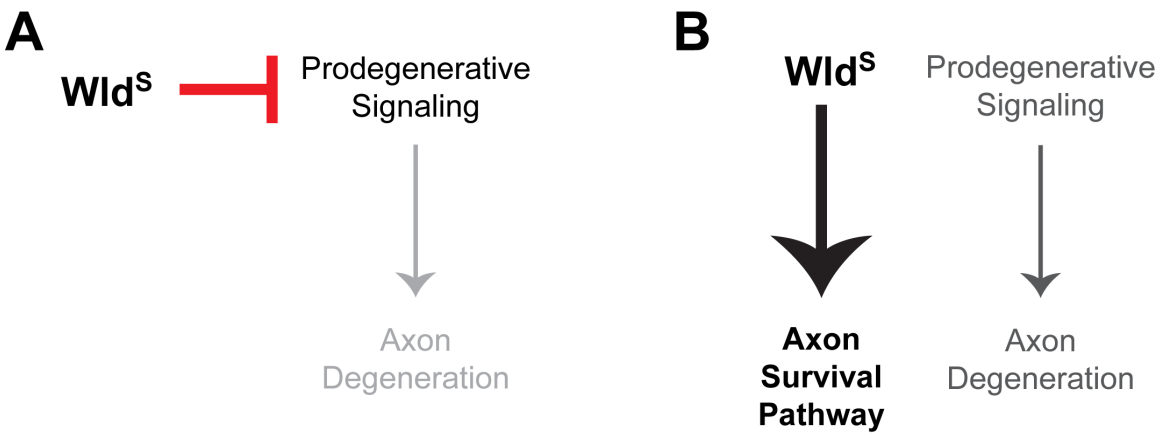

Figure 1.1 Wld^S models. (A) Wld^S may be functioning to inhibit molecules that are involved in breaking down axons. In this model, Wld^S is suppressing the prodegenerative signaling to prevent axon degeneration from occurring. (B) Wld^S may be functioning in parallel to an axon degeneration pathway. In this model, Wld^S is augmenting an axon survival pathway such that it overwhelms any prodegenerative signaling.

disease progression. In diseases that are primarily sporadic, such as Alzheimer's, mitochondrial defects are often observed before other hallmarks of pathology become detectable (Manczak, 2006; Nunomura et al., 2001; Praticò et al., 2001).

Despite the extensive amount of research on mitochondria within neurodegeneration models, the exact role of mitochondria is still debated. It remains to be established whether mitochondria play a protective or destructive role within degeneration (Figure 1.2). In other words, axonal demise could arise from the loss of a survival role or from the acquisition of a toxic role. Compromised mitochondria may be unable to protect the cell and support axonal maintenance. In this case, a decrease in energy or calcium buffering could lead cells down a path of gradual destruction. Alternatively, mitochondria may play an active and toxic role in neurodegeneration through the release of reactive oxygen

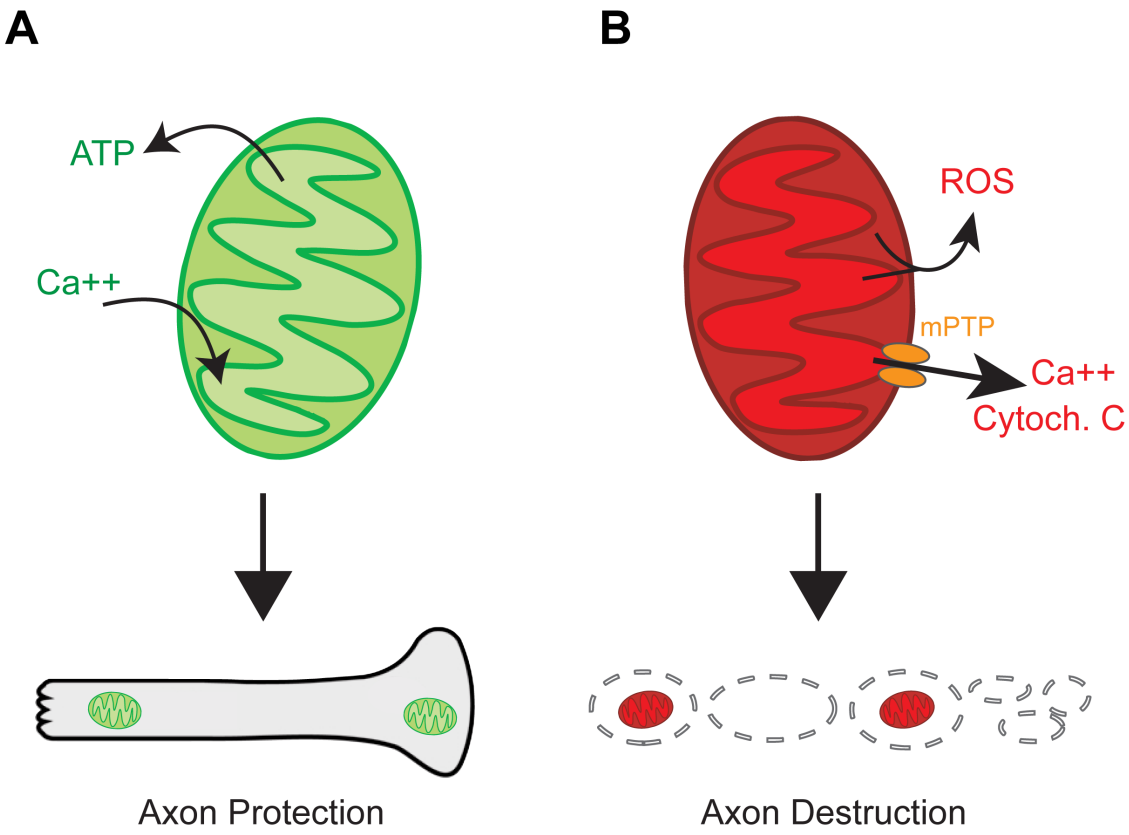

Figure 1.2. The potential roles for mitochondria in protecting and destroying axons. (A) Mitochondria can protect axons by supplying energy (ATP) and buffering cytosolic calcium, which might otherwise initiate degeneration signaling. (B) Mitochondria are known to participate in the destruction of cells through the production of reactive oxygen species (ROS) and the opening of the mitochondrial permeability transition pore (mPTP, orange), which releases calcium and apoptosis factors into the cytosol. Mitochondria may be playing a similar role in the destruction of severed axons.

species (ROS) and apoptotic factors.

Energy supply

Oxidative phosphorylation, or the supply of ATP, is a critical function for mitochondria. The nervous system consumes a disproportionately large amount of energy in the human body. Much of this energy consumption is dedicated to reversing ion fluctuations following an action potential in order to restore the resting membrane potential (Harris et al., 2012). Insufficient ATP levels are likely to result in the failure of Na^+/K^+ pumps, which will lead in an accumulation of Na^+ within the neuron. High Na^+ levels will in turn reverse the direction of the Na^+/Ca^{2+} exchanger, resulting in a detrimental influx of calcium into the cell (Mandolesi et al., 2004; Stys et al., 1992). A more recent study demonstrates that the greatest ATP sink in neurons is synaptic vesicle recycling (Rangaraju et al., 2014). Thus, preventing neuronal activity should enhance ATP levels by removing the need for energy expenditure on synaptic vesicle recycling and membrane potential maintenence. If ATP levels are critical for axon survival, inhibiting neuronal activity should be neuroprotective. However, the data are conflicting; inhibition of neuronal activity is neuroprotective in some cases (Garthwaite et al., 2002; Kapoor et al., 2003; Wolf et al., 2001; Zhai et al., 2006) and ineffective in others (George et al., 1998; Press and Milbrandt, 2008). Considering that oxidative phosphorylation is not important for maintaining resting levels of ATP (Rangaraju et al., 2014), it seems unlikely that ATP supply from mitochondria is critical for axon maintenance.

Calcium buffering

Calcium is important in cell signaling and is tightly regulated by the cell. A role for excess calcium in promoting degeneration has been repeatedly demonstrated (reviewed in Wang et al., 2012; Zündorf and Reiser, 2011). For example, calcium channel blockers and calcium chelators can impede axon degeneration (Barrientos et al., 2011; George et al., 1998; Knöferle et al., 2010). Although mitochondria have not directly been shown to buffer calcium following an injury, indirect evidence suggests that they do. The calcium rise in injured Wld^S axons is significantly reduced, and isolated Wld^S mitochondria are able to load significantly greater amounts of calcium in vitro (Avery et al., 2012). The role of mitochondria in buffering calcium is discussed further in Chapter 4.

Reactive oxygen species

Evidence suggests that mitochondria are also involved in the destruction of axons. Elevated levels of ROS have been shown to induce degeneration (Alvarez et al., 2008; Koeberle and Ball, 1999; Lucius and Sievers, 1996) and mitochondria are the primary source of ROS (Shigenaga et al., 1994). The amounts of detectable ROS are enhanced in models of multiple neurodegenerative diseases (Alam et al., 1997; Bogdanov et al., 2001; Browne et al., 1997; Ferrante et al., 1997; Krebiehl et al., 2010; Manczak, 2006; Wang et al., 2005b). Furthermore, antioxidant treatments can ameliorate disease states (reviewed by Bastianetto and Quirion, 2004). For example, treatment of neurons with rotenone, an electron transport chain inhibitor, dramatically increases ROS

levels and induces degeneration, but application of the antioxidant Vitamin E robustly protected the axons from degeneration (Press and Milbrandt, 2008). Thus, ROS generation by dysfunctional mitochondria may be an important regulator of neurodegeneration.

Apoptosis and the mPTP

Other studies have shown that mitochondria are active in the process of degeneration through the mitochondria permeability transition pore (mPTP) and apoptosis pathway. The mPTP is thought to open after mitochondria are overloaded with calcium. Opening of the mPTP releases both calcium and the apoptotic factor cytochrome C into the cytosol (Correia et al., 2010). Hallmarks of mPTP, such as mitochondrial swelling and decreased membrane potential, are frequently observed in disease models (Casley, 2002; Cassarino et al., 1999; Choo, 2004; Hsu et al., 2000; Moreira et al., 2001, 2002; Song et al., 2004). Blocking or eliminating a key component of the mPTP, cyclophilin D, can ameliorate disease conditions (Borlongan et al., 1996; Cassarino et al., 1999; Choo, 2004; Du et al., 2008; Kim et al., 2002; Matsuura et al., 1996; Okonkwo and Povlishock, 1999). A recent study by Barrientos *et al*. has shown that the mPTP is likely required for axon degeneration (Barrientos et al., 2011).

Several apoptosis pathway members have been shown to participate in the process of degrading axons (Keller et al., 2011; Kuo et al., 2006; Schoenmann et al., 2010; Williams et al., 2006). The role of apoptosis components in axon degeneration is discussed further in Chapter 3.

Are mitochondria required for axon degeneration?

Recent studies demonstrate that mitochondria are actively participating in axon degeneration. Mitochondria may have a role in initiating degeneration. The degeneration of motor neuron axons following a crush injury was significantly delayed in milton knockouts that lack mitochondria in axons (Kitay et al., 2013). Eight hrs after the crush injury, over 60% of wild-type axons were fragmented, whereas only ~20% of the milton knockout axons were fragmented. By 16 hrs, they were both fully fragmented. Thus, the milton knockout axons were not protected from degeneration but had a delayed onset, suggesting that mitochondria normally play a role in initiating axon degeneration.

Other studies suggest that mitochondria are more strictly required for the execution of axon degeneration. Severed axons cultured in the presence of an mPTP inhibitor were protected from axon degeneration, arguing that mitochondria are acting locally in the destruction of axons (Barrientos et al., 2011). Additionally, the loss of mitochondria was protective in an alpha-spectrin disease model (Keller et al., 2011). Knockdown of alpha-spectrin leads to the degeneration of neuromuscular junctions. Mutating the mitochondrial transport gene *miro* reduced the number of mitochondria in axons and suppressed neuromuscular junction degeneration. In other words, removing mitochondria from the axon abates degeneration, suggesting that mitochondria are required for this process to occur.

Dissertation Outline

In this dissertation, I will characterize axon degeneration in *C. elegans* and demonstrate the critical role for mitochondria in axon survival. The nematode has not previously been used for the study of axon degeneration following an injury. In addition to establishing the utility of this model system, I also tested several controversial mediators of axon degeneration. In Chapter 2, I demonstrate that the decision for an axon to degenerate or remain stable is dependent upon the localization of mitochondria. These experiments reveal that mitochondria potently protect axons and are not required for the execution of axon degeneration. Chapter 2 also contains the characterization of *ric-7*, a novel regulator of mitochondrial transport. In Chapter 3, I investigate the role of the apoptosis pathway in both injury-induced axon degeneration and in a beta-spectrin neurodegeneration model. The caspase *ced-3* is likely involved in the fragmentation of degenerating axons and the engulfment genes *ced-1* and *ced-6* are required for the removal of fragmented axons. The engulfment gene *ced-7* was only required in the beta-spectrin mutants, suggesting that *ced-7* may be uniquely regulated depending on the type of axon degeneration. In Chapter 4, I discuss preliminary and future experiments that will elucidate the mechanisms of mitochondria-mediated axon protection and RIC-7 function.

References

Alam, Z.I., Jenner, A., Daniel, S.E., Lees, A.J., Cairns, N., Marsden, C.D., Jenner, P., and Halliwell, B. (1997). Oxidative DNA damage in the parkinsonian brain: an apparent selective increase in 8-hydroxyguanine levels in substantia nigra. J. Neurochem. *69*, 1196–1203.

Alexander, C., Votruba, M., Pesch, U.E., Thiselton, D.L., Mayer, S., Moore, A., Rodriguez, M., Kellner, U., Leo-Kottler, B., Auburger, G., et al. (2000). OPA1, encoding a dynamin-related GTPase, is mutated in autosomal dominant optic atrophy linked to chromosome 3q28. Nat Genet *26*, 211–215.

Alvarez, S., Moldovan, M., and Krarup, C. (2008). Acute energy restriction triggers Wallerian degeneration in mouse. Exp. Neurol. *212*, 166–178.

Araki, T., Sasaki, Y., and Milbrandt, J. (2004). Increased nuclear NAD biosynthesis and SIRT1 activation prevent axonal degeneration. Sci. N. Y. NY *305*, 1010–1013.

Avery, M.A., Sheehan, A.E., Kerr, K.S., Wang, J., and Freeman, M.R. (2009). Wld S requires Nmnat1 enzymatic activity and N16-VCP interactions to suppress Wallerian degeneration. J. Cell Biol. *184*, 501–513.

Avery, M.A., Rooney, T.M., Pandya, J.D., Wishart, T.M., Gillingwater, T.H., Geddes, J.W., Sullivan, P.G., and Freeman, M.R. (2012). WldS prevents axon degeneration through increased mitochondrial flux and enhanced mitochondrial Ca2+ buffering. Curr. Biol. 1–5.

Awasaki, T., Tatsumi, R., Takahashi, K., Arai, K., Nakanishi, Y., Ueda, R., and Ito, K. (2006). Essential role of the apoptotic cell engulfment genes draper and ced-6 in programmed axon pruning during Drosophila metamorphosis. Neuron *50*, 855–867.

Babetto, E., Beirowski, B., Janeckova, L., Brown, R., Gilley, J., Thomson, D., Ribchester, R.R., and Coleman, M.P. (2010). Targeting NMNAT1 to axons and synapses transforms its neuroprotective potency in vivo. J. Neurosci. *30*, 13291–13304.

Barrientos, S.A., Martinez, N.W., Yoo, S., Jara, J.S., Zamorano, S., Hetz, C., Twiss, J.L., Alvarez, J., and Court, F.A. (2011). Axonal degeneration is mediated by the mitochondrial permeability transition pore. J. Neurosci. *31*, 966–978.

Bastianetto, S., and Quirion, R. (2004). Natural antioxidants and neurodegenerative diseases. Front Biosci *9*, 3447–3452.

Beirowski, B., Berek, L., Adalbert, R., Wagner, D., Grumme, D.S., Addicks, K., Ribchester, R.R., and Coleman, M.P. (2004). Quantitative and qualitative analysis of Wallerian degeneration using restricted axonal labelling in YFP-H mice. J. Neurosci. Methods *134*, 23–35.

Beirowski, B., Adalbert, R., Wagner, D., Grumme, D.S., Addicks, K., Ribchester, R.R., and Coleman, M.P. (2005). The progressive nature of Wallerian degeneration in wild-type and slow Wallerian degeneration (WldS) nerves. BMC Neurosci. *6*, 6.

Beirowski, B., Babetto, E., Gilley, J., Mazzola, F., Conforti, L., Janeckova, L., Magni, G., Ribchester, R.R., and Coleman, M.P. (2009). Non-nuclear WldS determines its neuroprotective efficacy for axons and synapses in vivo. J. Neurosci. *29*, 653–668.

Berger, F., Lau, C., Dahlmann, M., and Ziegler, M. (2005). Subcellular compartmentation and differential catalytic properties of the three human nicotinamide mononucleotide adenylyltransferase isoforms. J. Biol. Chem. *280*, 36334–36341.

Bogdanov, M.B., Andreassen, O.A., Dedeoglu, A., Ferrante, R.J., and Beal, M.F. (2001). Increased oxidative damage to DNA in a transgenic mouse model of Huntington's disease. J. Neurochem. *79*, 1246–1249.

Borlongan, C.V., Freeman, T.B., Hauser, R.A., Cahill, D.W., and Sanberg, P.R. (1996). Cyclosporine-A increases locomotor activity in rats with 6-hydroxydopamine-induced hemiparkinsonism: relevance to neural transplantation. Surg Neurol *46*, 384–388.

Browne, S.E., Bowling, A.C., MacGarvey, U., Baik, M.J., Berger, S.C., Muqit, M.M., Bird, E.D., and Beal, M.F. (1997). Oxidative damage and metabolic dysfunction in Huntington's disease: selective vulnerability of the basal ganglia. Ann Neurol *41*, 646–653.

Casley, C. (2002). β-Amyloid Fragment 25–35 Causes Mitochondrial Dysfunction in Primary Cortical Neurons. Neurobiol Dis *10*, 258–267.

Cassarino, D.S., Parks, J.K., Parker, W.D., and Bennett, J.P. (1999). The parkinsonian neurotoxin MPP+ opens the mitochondrial permeability transition pore and releases cytochrome c in isolated mitochondria via an oxidative mechanism. Biochim Biophys Acta *1453*, 49–62.

Choo, Y.S. (2004). Mutant huntingtin directly increases susceptibility of mitochondria to the calcium-induced permeability transition and cytochrome c release. Hum. Mol. Genet. *13*, 1407–1420.

Chung, S., Gumienny, T.L., Hengartner, M.O., and Driscoll, M. (2000). A common set of engulfment genes mediates removal of both apoptotic and necrotic cell corpses in C. elegans. Nat. Cell Biol. *2*, 931–937.

Coleman, M.P., and Freeman, M.R. (2010). Wallerian degeneration, wld(s), and nmnat. Annu. Rev. Neurosci. *33*, 245–267.

Coleman, M.P., Conforti, L., Buckmaster, E.A., Tarlton, A., Ewing, R.M., Brown, M.C., Lyon, M.F., and Perry, V.H. (1998). An 85-kb tandem triplication in the slow Wallerian degeneration (Wlds) mouse. Proc. Natl. Acad. Sci. U. S. A. *95*, 9985–9990.

Conforti, L., Fang, G., Beirowski, B., Wang, M.S., Sorci, L., Asress, S., Adalbert, R., Silva, A., Bridge, K., Huang, X.P., et al. (2007). NAD(+) and axon degeneration revisited: Nmnat1 cannot substitute for Wld(S) to delay Wallerian degeneration. Cell Death Differ. *14*, 116–127.

Correia, S.C., Santos, R.X., Perry, G., Zhu, X., Moreira, P.I., and Smith, M.A. (2010). Mitochondria: the missing link between preconditioning and neuroprotection. J. Alzheimers Dis. JAD *20 Suppl 2*, S475–85.

Dadon-Nachum, M., Melamed, E., and Offen, D. (2011). The “dying-back” phenomenon of motor neurons in ALS. J. Mol. Neurosci. MN *43*, 470–477.

Delettre, C., Lenaers, G., Griffoin, J.M., Gigarel, N., Lorenzo, C., Belenguer, P., Pelloquin, L., Grosgeorge, J., Turc-Carel, C., Perret, E., et al. (2000). Nuclear gene OPA1, encoding a mitochondrial dynamin-related protein, is mutated in dominant optic atrophy. Nat Genet *26*, 207–210.

Du, H., Guo, L., Fang, F., Chen, D., Sosunov, A.A., Mckhann, G.M., Yan, Y., Wang, C., Zhang, H., Molkentin, J.D., et al. (2008). Cyclophilin D deficiency attenuates mitochondrial and neuronal perturbation and ameliorates learning and memory in Alzheimer’s disease. Nat Med *14*, 1097–1105.

Fang, Y., Soares, L., Teng, X., Geary, M., and Bonini, N.M. (2012). A novel drosophila model of nerve injury reveals an essential role of Nmnat in maintaining axonal integrity. Curr. Biol. 1–6.

Ferrante, R.J., Browne, S.E., Shinobu, L.A., Bowling, A.C., Baik, M.J., MacGarvey, U., Kowall, N.W., Brown, R.H., and Beal, M.F. (1997). Evidence of increased oxidative damage in both sporadic and familial amyotrophic lateral sclerosis. J. Neurochem. *69*, 2064–2074.

Ferri, A., Sanes, J.R., Coleman, M.P., Cunningham, J.M., and Kato, A.C. (2003). Inhibiting axon degeneration and synapse loss attenuates apoptosis and disease progression in a mouse model of motoneuron disease. Curr. Biol. CB *13*, 669–673.

Garthwaite, G., Goodwin, D.A., Batchelor, A.M., Leeming, K., and Garthwaite, J. (2002). Nitric oxide toxicity in CNS white matter: an in vitro study using rat optic nerve. Neuroscience *109*, 145–155.

George, E.B., Glass, J.D., and Griffin, J.W. (1998). Axotomy-induced axonal degeneration is mediated by calcium influx through ion-specific channels. J. Neurosci. Off. J. Soc. Neurosci. *15*, 6445–6452.

Gilley, J., and Coleman, M.P. (2010). Endogenous Nmnat2 is an essential survival factor for maintenance of healthy axons. PLoS Biol. *8*, e1000300.

Han, I., You, Y., Kordower, J.H., Brady, S.T., and Morfini, G.A. (2010).

Differential vulnerability of neurons in Huntington's disease: the role of cell type-specific features. J. Neurochem. *113*, 1073–1091.

Harris, J.J., Jolivet, R., and Attwell, D. (2012). Synaptic energy use and supply. Neuron *75*, 762–777.

Hoopfer, E., Mclaughlin, T., Watts, R., Schuldiner, O., Oleary, D., and Luo, L. (2006). Wlds protection distinguishes axon degeneration following injury from naturally occurring developmental pruning. Neuron *50*, 883–895.

Hosmane, S., Tegenge, M.A., Rajbhandari, L., Uapinyoying, P., Kumar, N.G., Thakor, N., and Venkatesan, A. (2012). Toll/Interleukin-1 receptor domain-containing adapter inducing Interferon-β mediates microglial phagocytosis of degenerating axons. J. Neurosci. *32*, 7745–7757.

Howell, G.R., Libby, R.T., Jakobs, T.C., Smith, R.S., Phalan, F.C., Barter, J.W., Barbay, J.M., Marchant, J.K., Mahesh, N., Porciatti, V., et al. (2007). Axons of retinal ganglion cells are insulted in the optic nerve early in DBA/2J glaucoma. J. Cell Biol. *179*, 1523–1537.

Hsu, L.J., Sagara, Y., Arroyo, A., Rockenstein, E., Sisk, A., Mallory, M., Wong, J., Takenouchi, T., Hashimoto, M., and Masliah, E. (2000). alpha-synuclein promotes mitochondrial deficit and oxidative stress. Am J Pathol *157*, 401–410.

Jia, H., Yan, T., Feng, Y., Zeng, C., Shi, X., and Zhai, Q. (2007). Identification of a critical site in Wld(s): essential for Nmnat enzyme activity and axon-protective function. Neurosci. Lett. *413*, 46–51.

Kanaan, N.M., Pigino, G.F., Brady, S.T., Lazarov, O., Binder, L.I., and Morfini, G.A. (2013). Axonal degeneration in Alzheimer's disease: when signaling abnormalities meet the axonal transport system. Exp. Neurol. *246*, 44–53.

Kapoor, R., Davies, M., Blaker, P.A., Hall, S.M., and Smith, K.J. (2003). Blockers of sodium and calcium entry protect axons from nitric oxide-mediated degeneration. Ann. Neurol. *53*, 174–180.

Kariya, S., Mauricio, R., Dai, Y., and Monani, U.R. (2009). The neuroprotective factor Wlds fails to mitigate distal axonal and neuromuscular junction (NMJ) defects in mouse models of spinal muscular atrophy. Neurosci. Lett. *449*, 246–251.

Keller, L.C., Cheng, L., Locke, C.J., Müller, M., Fetter, R.D., and Davis, G.W. (2011). Glial-derived prodegenerative signaling in the drosophila neuromuscular system. Neuron *72*, 760–775.

Kim, H.-S., Lee, J.-H., Lee, J.-P., Kim, E.-M., Chang, K.-A., Park, C.H., Jeong, S.-J., Wittendorp, M.C., Seo, J.-H., Choi, S.-H., et al. (2002). Amyloid beta peptide induces cytochrome C release from isolated mitochondria. Neuroreport

13, 1989–1993.

Kitay, B.M., Mccormack, R., Wang, Y., Tsoulfas, P., and Zhai, R.G. (2013). Mislocalization of neuronal mitochondria reveals regulation of Wallerian degeneration and NMNAT/WLDS-mediated axon protection independent of axonal mitochondria. Hum. Mol. Genet. 1–14.

Knöferle, J., Koch, J.C., Ostendorf, T., Michel, U., Planchamp, V., Vutova, P., Tönges, L., Stadelmann, C., Brück, W., Bähr, M., et al. (2010). Mechanisms of acute axonal degeneration in the optic nerve in vivo. Proc. Natl. Acad. Sci. *107*, 6064–6069.

Koeberle, P.D., and Ball, A.K. (1999). Nitric oxide synthase inhibition delays axonal degeneration and promotes the survival of axotomized retinal ganglion cells. Exp. Neurol. *158*, 366–381.

Krebiehl, G., Ruckerbauer, S., Burbulla, L.F., Kieper, N., Maurer, B., Waak, J., Wolburg, H., Gizatullina, Z., Gellerich, F.N., Woitalla, D., et al. (2010). Reduced basal autophagy and impaired mitochondrial dynamics due to loss of Parkinson's disease-associated protein DJ-1. PLoS ONE *5*, e9367.

Kuo, C., Zhu, S., Younger, S., Jan, L., and Jan, Y. (2006). Identification of E2/E3 ubiquitinating enzymes and caspase activity regulating drosophila sensory neuron dendrite pruning. Neuron *51*, 283–290.

Lucius, R., and Sievers, J. (1996). Postnatal retinal ganglion cells in vitro: protection against reactive oxygen species (ROS)-induced axonal degeneration by cocultured astrocytes. Brain Res *743*, 56–62.

Lunn, E.R., Perry, V.H., Brown, M.C., Rosen, H., and Gordon, S. (1989). Absence of wallerian degeneration does not hinder regeneration in peripheral nerve. Eur. J. Neurosci. *1*, 27–33.

Luo, L., and O'Leary, D.D.M. (2005). Axon retraction and degeneration in development and disease. Annu. Rev. Neurosci. *28*, 127–156.

Macdonald, J., Beach, M., Porpiglia, E., Sheehan, A., Watts, R., and Freeman, M. (2006). The Drosophila cell corpse engulfment receptor draper mediates glial clearance of severed axons. Neuron *50*, 869–881.

Mack, T.G., Reiner, M., Beirowski, B., Mi, W., Emanuelli, M., Wagner, D., Thomson, D., Gillingwater, T., Court, F., Conforti, L., et al. (2001). Wallerian degeneration of injured axons and synapses is delayed by a Ube4b/Nmnat chimeric gene. Nat. Neurosci. *4*, 1199–1206.

Manczak, M. (2006). Mitochondria are a direct site of A accumulation in Alzheimer's disease neurons: implications for free radical generation and oxidative damage in disease progression. Hum. Mol. Genet. *15*, 1437–1449.

Mandolesi, G., Madeddu, F., Bozzi, Y., Maffei, L., and Ratto, G.M. (2004). Acute physiological response of mammalian central neurons to axotomy: ionic regulation and electrical activity. FASEB J. *18*, 1934–1936.

Matsuura, K., Kabuto, H., Makino, H., and Ogawa, N. (1996). Cyclosporin A attenuates degeneration of dopaminergic neurons induced by 6-hydroxydopamine in the mouse brain. Brain Res *733*, 101–104.

Milde, S., Gilley, J., and Coleman, M.P. (2013). Subcellular localization determines the stability and axon protective capacity of axon survival factor Nmnat2. PLoS Biol. *11*, e1001539.

Moreira, P.I., Santos, M.S., Moreno, A., and Oliveira, C. (2001). Amyloid beta-peptide promotes permeability transition pore in brain mitochondria. Biosci Rep *21*, 789–800.

Moreira, P.I., Santos, M.S., Moreno, A., Rego, A.C., and Oliveira, C. (2002). Effect of amyloid beta-peptide on permeability transition pore: A comparative study. J Neurosci Res *69*, 257–267.

Nikolaev, A., Mclaughlin, T., O'leary, D.D.M., and Tessier-Lavigne, M. (2009). APP binds DR6 to trigger axon pruning and neuron death via distinct caspases. Nature *457*, 981–989.

Nunomura, A., Perry, G., Aliev, G., Hirai, K., Takeda, A., Balraj, E.K., Jones, P.K., Ghanbari, H., Wataya, T., Shimohama, S., et al. (2001). Oxidative damage is the earliest event in Alzheimer disease. J Neuropathol Exp Neurol *60*, 759–767.

O'Donnell, K.C., Vargas, M.E., and Sagasti, A. (2013). WldS and PGC-1 regulate mitochondrial transport and oxidation state after axonal injury. J. Neurosci. *33*, 14778–14790.

Okonkwo, D.O., and Povlishock, J.T. (1999). An intrathecal bolus of cyclosporin A before injury preserves mitochondrial integrity and attenuates axonal disruption in traumatic brain injury. J Cereb Blood Flow Metab *19*, 443–451.

Praticò, D., Uryu, K., Leight, S., Trojanoswki, J.Q., and Lee, V.M. (2001). Increased lipid peroxidation precedes amyloid plaque formation in an animal model of Alzheimer amyloidosis. J Neurosci *21*, 4183–4187.

Press, C., and Milbrandt, J. (2008). Nmnat delays axonal degeneration caused by mitochondrial and oxidative stress. J. Neurosci. Off. J. Soc. Neurosci. *28*, 4861–4871.

Rangaraju, V., Calloway, N., and Ryan, T.A. (2014). Activity-driven local ATP synthesis is required for synaptic function. Cell *156*, 825–835.

Rose Jr., F.F., Meehan, P.W., Coady, T.H., Garcia, V.B., Garcia, M.L., and Lorson, C.L. (2008). The Wallerian degeneration slow (Wlds) gene does not attenuate disease in a mouse model of spinal muscular atrophy. Biochem. Biophys. Res. Commun. *375*, 119–123.

Sasaki, Y., Araki, T., and Milbrandt, J. (2006). Stimulation of nicotinamide adenine dinucleotide biosynthetic pathways delays axonal degeneration after axotomy. J. Neurosci. Off. J. Soc. Neurosci. *26*, 8484–8491.

Sasaki, Y., Vohra, B.P.S., Baloh, R.H., and Milbrandt, J. (2009a). Transgenic mice expressing the Nmnat1 protein manifest robust delay in axonal degeneration in vivo. J. Neurosci. *29*, 6526–6534.

Sasaki, Y., Vohra, B.P.S., Lund, F.E., and Milbrandt, J. (2009b). Nicotinamide mononucleotide adenylyl transferase-mediated axonal protection requires enzymatic activity but not increased levels of neuronal nicotinamide adenine dinucleotide. J. Neurosci. Off. J. Soc. Neurosci. *29*, 5525–5535.

Schoenmann, Z., Assa-Kunik, E., Tiomny, S., Minis, A., Haklai-Topper, L., Arama, E., and Yaron, A. (2010). Axonal degeneration is regulated by the apoptotic machinery or a NAD+-sensitive pathway in insects and mammals. J. Neurosci. *30*, 6375–6386.

Shigenaga, M.K., Hagen, T.M., and Ames, B.N. (1994). Oxidative damage and mitochondrial decay in aging. Proc Natl Acad Sci USA *91*, 10771–10778.

Song, D.D., Shults, C.W., Sisk, A., Rockenstein, E., and Masliah, E. (2004). Enhanced substantia nigra mitochondrial pathology in human alpha-synuclein transgenic mice after treatment with MPTP. Exp. Neurol. *186*, 158–172.

Stys, P.K., Waxman, S.G., and Ransom, B.R. (1992). Ionic mechanisms of anoxic injury in mammalian CNS white matter: role of Na+ channels and Na(+)-Ca2+ exchanger. J. Neurosci. *12*, 430–439.

Tanaka, T., Ueno, M., and Yamashita, T. (2009). Engulfment of axon debris by microglia requires p38 MAPK activity. J. Biol. Chem. *284*, 21626–21636.

Tao, J., and Rolls, M.M. (2011). Dendrites have a rapid program of injury-induced degeneration that is molecularly distinct from developmental pruning. J. Neurosci. *31*, 5398–5405.

Velde, C.V., Garcia, M.L., Yin, X., Trapp, B.D., and Cleveland, D.W. (2004). The neuroprotective factor Wlds does not attenuate mutant SOD1-mediated motor neuron disease. NeuroMolecular Med. *5*, 193–203.

Waller, A. (1850). Experiments on the section of the glossopharyngeal and hypoglossal nerves of the frog, and observations of the alterations produced thereby in the structure of their primitive fibres. R. Soc. Lond. Philos. Trans. Ser. I

140, 423–429.

Wang, J., Zhai, Q., Chen, Y., Lin, E., Gu, W., McBurney, M.W., and He, Z. (2005a). A local mechanism mediates NAD-dependent protection of axon degeneration. J. Cell Biol. *170*, 349–355.

Wang, J., Xiong, S., Xie, C., Markesbery, W.R., and Lovell, M.A. (2005b). Increased oxidative damage in nuclear and mitochondrial DNA in Alzheimer's disease. J. Neurochem. *93*, 953–962.

Wang, J.T., Medress, Z.A., and Barres, B.A. (2012). Axon degeneration: molecular mechanisms of a self-destruction pathway. J. Cell Biol. *196*, 7–18.

Williams, D.W., Kondo, S., Krzyzanowska, A., Hiromi, Y., and Truman, J.W. (2006). Local caspase activity directs engulfment of dendrites during pruning. Nat Neurosci *9*, 1234–1236.

Wolf, J.A., Stys, P.K., Lusardi, T., Meaney, D., and Smith, D.H. (2001). Traumatic axonal injury induces calcium influx modulated by tetrodotoxin-sensitive sodium channels. J. Neurosci. Off. J. Soc. Neurosci. *21*, 1923–1930.

Yan, T., Feng, Y., Zheng, J., Ge, X., Zhang, Y., Wu, D., Zhao, J., and Zhai, Q. (2010). Nmnat2 delays axon degeneration in superior cervical ganglia dependent on its NAD synthesis activity. Neurochem. Int. *56*, 101–106.

Zang, S., Ali, Y.O., Ruan, K., and Zhai, R.G. (2012). Nicotinamide mononucleotide adenylyltransferase maintains active zone structure by stabilizing Bruchpilot. EMBO Rep. *14*, 87–94.

Zhai, R.G., Cao, Y., Hiesinger, P.R., Zhou, Y., Mehta, S.Q., Schulze, K.L., Verstreken, P., and Bellen, H.J. (2006). Drosophila NMNAT maintains neural integrity independent of its NAD synthesis activity. PLoS Biol. *4*, e416.

Züchner, S., Mersiyanova, I.V., Muglia, M., Bissar-Tadmouri, N., Rochelle, J., Dadali, E.L., Zappia, M., Nelis, E., Patitucci, A., Senderek, J., et al. (2004). Mutations in the mitochondrial GTPase mitofusin 2 cause Charcot-Marie-Tooth neuropathy type 2A. Nat Genet *36*, 449–451.

Zündorf, G., and Reiser, G. (2011). Calcium dysregulation and homeostasis of neural calcium in the molecular mechanisms of neurodegenerative diseases provide multiple targets for neuroprotection. Antioxid. Redox Signal. *14*, 1275–1288.

CHAPTER 2

AXONS DEGENERATE IN THE ABSENCE OF MITOCHONDRIA IN *C. ELEGANS*

Summary

Many neurodegenerative disorders are associated with mitochondrial defects (Chang et al., 2006; Patten et al., 2010; Schon and Przedborski, 2011). Mitochondria can play an active role in degeneration by releasing reactive oxygen species and apoptotic factors (Alvarez et al., 2008; Koeberle and Ball, 1999; Lucius and Sievers, 1996; Shigenaga et al., 1994). Alternatively, mitochondria can protect axons from stress and insults, for example by buffering calcium (Avery et al., 2012). Recent studies manipulating mitochondria lend support to both of these models (Barrientos et al., 2011; Fang et al., 2012; Iijima-Ando et al., 2012; Keller et al., 2011; Kitay et al., 2013). Here, we identify a *C. elegans* mutant, *ric-7*, in which mitochondria are unable to exit the neuron cell bodies, similar to the kinesin-1/*unc-116* mutant. When axons lacking mitochondria are cut with a laser, they rapidly degenerate. Some neurons even spontaneously degenerate in *ric-7* mutants. Degeneration can be suppressed by forcing mitochondria into the axons of the mutants. The protective effect of mitochondria is also observed in the wild type: a majority of axon fragments

containing a mitochondrion survive axotomy, whereas those lacking mitochondria degenerate. Thus, mitochondria are not required for axon degeneration and serve a protective role in *C. elegans* axons.

Highlights

- *ric-7* and kinesin-1 are required for localization of mitochondria to axons.
- Axons lacking mitochondria rapidly degenerate after axotomy.
- In wild-type worms, mitochondria prevent axon degeneration.
- Forcibly pulling mitochondria into *ric-7* mutant axons suppresses axon degeneration.

Results

ric-7 mutants have impaired neurotransmission

We identified a novel gene *ric-7* (resistant to inhibitors of cholinesterase) that is essential for mitochondrial localization in axons. Alleles were isolated in unrelated genetic screens either for mutants with neurotransmission defects or for mutants with abnormal axon morphology. The *ric-7* locus was identified by positional cloning and was also described by Hao *et al.* (Hao et al., 2012). Microinjection of cosmid F58E10 rescued *ric-7* mutants, and microinjection of PCR fragments localized the rescuing activity to an 18 kilobase sequence predicted to contain two open reading frames, F58E10.1 and F58E10.7 (Figure 2.1A). To determine which open reading frame represents the *ric-7* locus, we

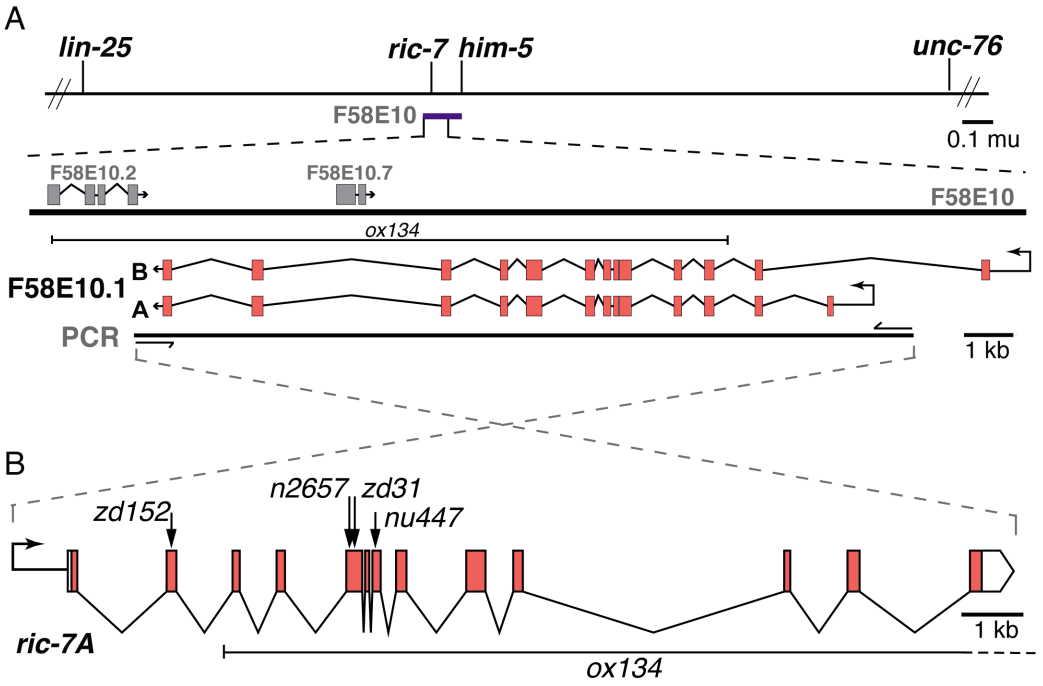

Figure 2.1. Cloning of *ric-7*. (A) The mutation *n2657* was mapped to the interval on chromosome V between *lin-25* and *unc-76*. Cosmid F58E10 (purple bar) spans 41 kilobases in this interval and rescued *ric-7* mutants as a transgene. Further experiments using PCR fragments indicated that rescuing activity was contained in an 18 kilobase (kb) fragment that contains two hypothetical genes, F58E10.1 and F58E10.7. (B) All five *ric-7* alleles contain alterations in F58E10.1 exons (see Table 2S.1). Arrows mark the locations of premature stops. *ox134* is a large deletion affecting three genes.

identified the molecular lesions associated with the three *ric-7* alleles. All alleles contain mutations in predicted exons of F58E10.1 (Figure 2.1B, Table 2S.1). The potential functions of RIC-7 were not obvious from the sequence; the RIC-7 protein lacks conserved domains and has rapidly diverged even among nematodes (Figure 2S.1A).

Both acetylcholine and GABA neurotransmission are impaired in *ric-7* mutants. Wild-type animals become paralyzed and die upon exposure to an acetylcholinesterase inhibitor Aldicarb. Paralysis is due to a build up of

acetylcholine in the synaptic cleft; thus, animals with impaired acetylcholine release are slower to respond to the drug. *ric-7* mutants are resistant to the effects of Aldicarb (Hao et al., 2012) (Figure 2S.1B). GABA neurotransmission is also disrupted in *ric-7* mutants. In *C. elegans,* defecation is a programmed behavior that requires GABA release onto the enteric muscles (Liu and Thomas, 1994; McIntire et al., 1993a). *ric-7(n2657)* animals are constipated due to the absence of enteric muscle contractions (Hao et al., 2012) (Figure 2S.1C). Restoring *ric-7* exclusively to GABA neurons using the *unc-47* promoter rescues the mutant defecation phenotype ('RIC-7(+)'), demonstrating that RIC-7 acts cell autonomously. These results demonstrate that mutations in *ric-7* disrupt both GABA and acetylcholine neurotransmission, suggesting that *ric-7* is generally required for synaptic transmission in *C. elegans*.

In spite of defects in neurotransmission, *ric-7* mutants have normal presynaptic structures. The active zone protein RIM (UNC-10), the synaptic vesicle protein vGAT (UNC-47), and the dense core vesicle protein FLP-3 are normally distributed along axons (Figure 2S.1G-I). Wild-type and mutant animals have a similar density of synaptic puncta in GABA motor neurons (Figure 2S.1D,E). *ric-7* synapses also appear normal at the ultrastructural level; specifically, there is no alteration in synaptic vesicle number (Figure 2S.1F,J). Consistent with the normal appearance of synapses, *ric-7* mutants exhibit normal synaptic activity as measured by electrophysiology (Hao et al., 2012).

Mitochondria are absent in axons of *ric-7* mutants

A transcriptional reporter construct indicates that the *ric-7* gene is expressed in most neurons and head muscles (Figure 2S.1K). A translational reporter construct (Figure 2S.2A) suggests that RIC-7 can associate with mitochondria. N-terminally tagged RIC-7 (RFP::RIC-7) can rescue *ric-7* mutants when expressed on extrachromosomal arrays, and fluorescence colocalizes with the mitochondrial marker Tom20::GFP, 'mito::GFP' (Figure 2.2A). Single copy insertions were dim or not visible (Fig 2S.2B).

To determine whether mitochondria are altered in *ric-7* mutants, we examined the distribution of GFP-tagged mitochondria in wild-type and mutant animals. In the wild type, mitochondria are distributed along the entire axon. However, in *ric-7* mutants, mitochondria are located almost exclusively in the cell bodies (Figure 2.2B,C). Occasionally, one or two mitochondria can be seen in proximal axons on the ventral side, typically near the cell body, whereas the distal axons in the dorsal nerve cord are completely void of mitochondria in *ric-7* mutants (Figure 2S.2C). This suggests that in the few cases where mitochondria are able to exit the cell body, they cannot make it far in the absence of RIC-7. This mitochondrial distribution closely resembles that of the strong hypomorphic allele of kinesin-1, *unc-116(rh24sb79)*. The other predominant kinesin in *C. elegans* motor neurons, kinesin-3/*unc-104*, is not required for trafficking of mitochondria out of the cell bodies (Figure 2.2B,D). Expressing N-terminally tagged RIC-7 (RFP::RIC-7) in *ric-7* mutants rescues the mitochondrial distribution in GABA neurons (Figure 2.2C, 'RIC-7 (+)').

Figure 2.2. RIC-7 colocalizes with mitochondria and is required for mitochondrial distribution in axons. (A) Tagged RIC-7 expressed in GABA neurons (P*unc-47:RFP::RIC-7, oxEx1598*) rescues *ric-7* mutants and colocalizes with mitochrondria tagged with Tom20::GFP ('mito::GFP'). Worms were imaged with the dorsal nerve cord facing the objective. See also Figure 2S.2A,B. (B) Mitochondria tagged with Tom20::GFP are trapped in the cell body and absent from axons in *ric-7* and kinesin-1/*unc-116* mutants but not kinesin-3/*unc-104* mutants. Arrowheads indicate cell bodies, and arrows point to axonal mitochondria. Asterisks indicate gut autofluorescence. See also Figure 2S.2C,D. Worms were imaged with the ventral nerve cord facing the objective. All scale bars are 10 μm. (C) Average number of mitochondria per 50 μm in the ventral nerve cord of GABA motor neuron axons +/- SEM. Mitochondrial distribution is rescued cell autonomously in axons when RFP::RIC-7 is expressed from an array ('RIC-7(+)', *oxEx1598*). $p < 0.0001$ Kruskal-Wallis test with Dunn's multiple comparisons to the wild type (black) and to *ric-7(n2657)* (red) *** $p<0.001$, * $p<0.05$. The number of animals is displayed below.

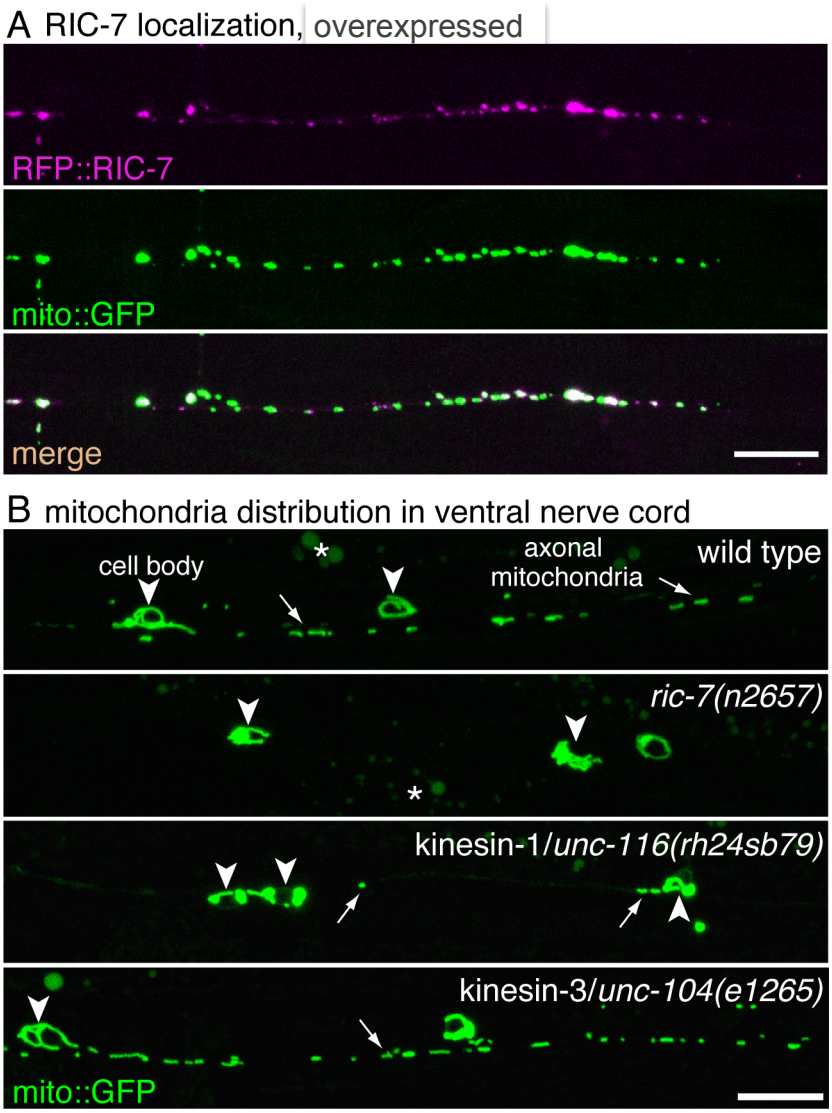
A RIC-7 localization, overexpressed
RFP::RIC-7
mito::GFP
merge
B mitochondria distribution in ventral nerve cord
cell body
axonal mitochondria
wild type
ric-7(n2657)
kinesin-1/unc-116(rh24sb79)
kinesin-3/unc-104(e1265)
mito::GFP
C mitochondria number in ventral nerve cord
mitochondria/ 50 µm
18
16
14
12
10
8
6
4
2
0
***
***
*
***
wild type
ric-7 (n2657)
ric-7 (ox134)
unc-116
unc-104
n2657; RIC-7(+)
N=
18
16
11
10
10
10

Mitochondrial distribution within other cell types, including muscle and hypodermis, is normal in *ric-7* mutants, indicating that *ric-7* does not have a general role in mitochondrial localization (Figure 2S.2D,E). Other organelles such as synaptic vesicles and dense core vesicles are normally distributed in *ric-7* mutant axons (Figure 2S.1H,I). These data suggest that *ric-7* is specifically required for the localization of mitochondria in neurons.

Axon degeneration is enhanced in *ric-7* mutants

Axons from two neurons, PVQ and HSN, spontaneously degenerate in the absence of mitochondria. Mutations in *ric-7* were identified in an axon morphology screen because they had truncated PVQ axons in adult worms. However, the truncation is not due to an outgrowth defect; PVQ axons in *ric-7* mutants extend normally during embryogenesis and remain largely intact during the first three larval stages (Figure 2.3A,B). However, at the beginning of the fourth larval stage, the axons begin to swell and degenerate (Figure 2.3C). By adulthood, most PVQ axons are truncated, typically near the vulva (Figure 2.3D). The proximal axon and cell body remain intact for the remaining life of the worm. The HSN axons, which grow out during early larval stages, degenerate in a similar fashion during early adulthood in *ric-7* mutants (Figure 2S.3B-E).

Remarkably, the majority of axons in *ric-7* mutants remain stable throughout the life of the worm. Thus, *ric-7* mutants provide a tool to address whether mitochondria are required for axonal degeneration. Severing the axon in a *ric-7* mutant provides an axonal environment that is now completely removed

Figure 2.3. Axon degeneration is enhanced in the absence of mitochondria. (A) PVQ axons spontaneously degenerate in *ric-7* mutants. The degenerating axons proceed through the following morpholigies; swollen, beaded, and finally truncated. The percentage of axons with a given morphology is depicted for each life stage of *ric-7(zd152)*. The number of worms assayed is indicated. (B) In the first larval stage, PVQ axons are intact in *ric-7(zd152)* mutants. GFP is expressed in PVQ and head neurons (ASH, ASI) under the *sra-6* promoter. The two PVQ cell bodies are in the tail; each extends an axon along the ventral nerve cord to the head. (C) During the fourth larval stage, the distal portion of the axon degenerates, beginning with swellings. (D) PVQ axons are typically truncated, frequently near the vulva, by the end of the fourth larval stage. The proximal half of the axons and the cell bodies remain intact. Scale bar = 100 μm. See also Figure 2S.3A-E. (E) GABA motor neuron axons degenerate following laser axotomy. Arrowheads point to the cut sites in the image taken immediately after axotomy. There are three severed axons (numbered). (F) After 24 hrs of recovery, worms were reimaged and the presence or absence of severed axons was scored. The wild-type panel is the same worm from panel E. Two of the three axons exhibit swellings but are still present. Severed motor neuron axons completely degenerate in *ric-7* and kinesin-1/*unc-116* mutants. Scale bar = 25 μm. (G) The average percent of axons that are still present 24 hrs after axotomy +/- SEM. More axons degenerate in mutants lacking mitochondria compared to the wild type. The kinesin-3/*unc-104* mutant, which has mitochondria throughout their axons, degenerates at wild-type levels. $p < 0.0001$ Kruskal-Wallis test with Dunn's multiple comparisons to the wild type, *** $p<0.001$, **$p<0.01$. See also Figure 2S.3F-K.

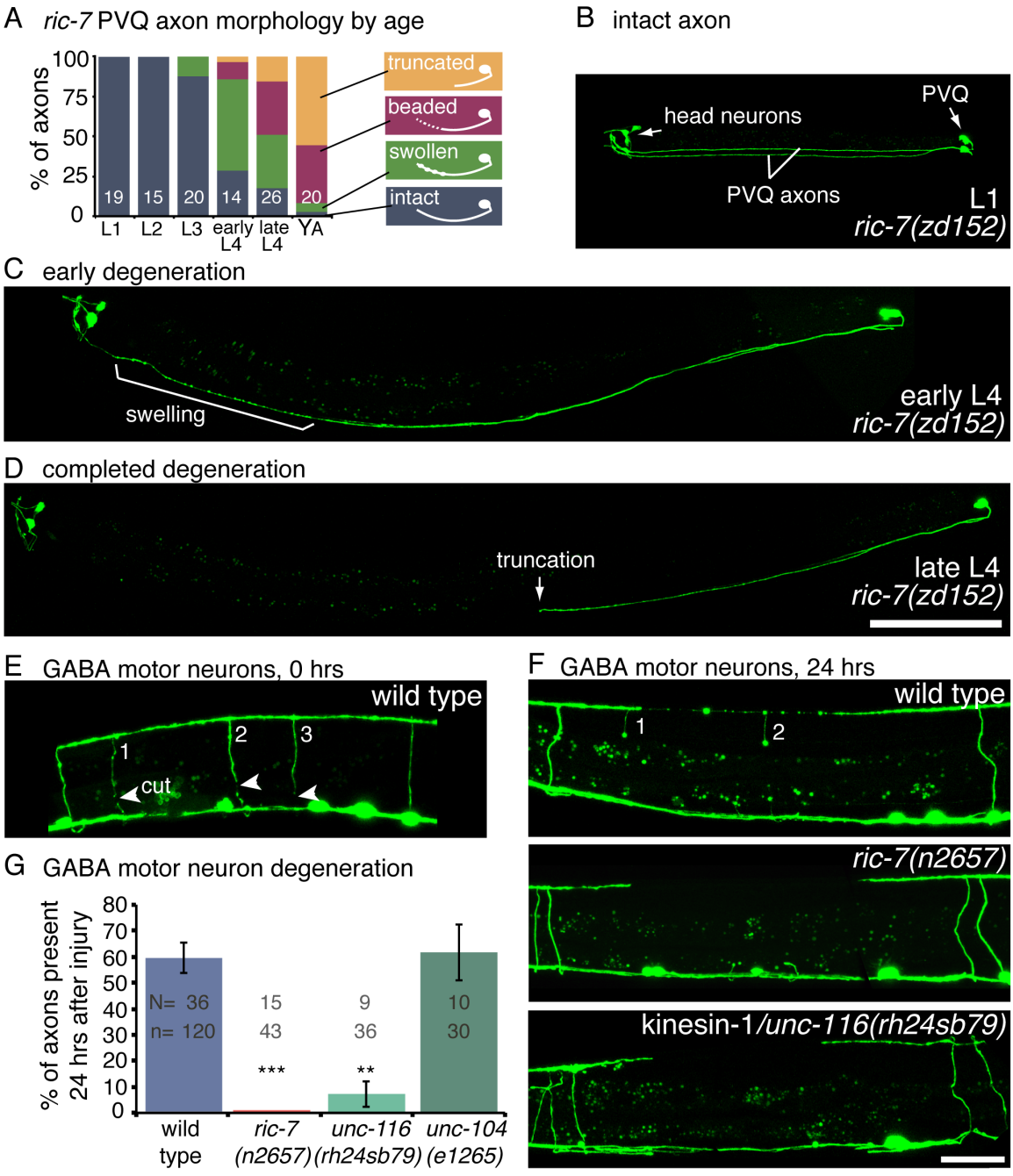
A ric-7 PVQ axon morphology by age
% of axons
100
75
50
25
0
19
15
20
14
26
20
L1
L2
L3
early L4
late L4
YA
truncated
beaded
swollen
intact
B intact axon
head neurons
PVQ
PVQ axons
L1
ric-7(zd152)
C early degeneration
swelling
early L4
ric-7(zd152)
D completed degeneration
truncation
late L4
ric-7(zd152)
E GABA motor neurons, 0 hrs
wild type
1
2
3
cut
F GABA motor neurons, 24 hrs
wild type
1
2
ric-7(n2657)
kinesin-1/unc-116(rh24sb79)
G GABA motor neuron degeneration
% of axons present 24 hrs after injury
80
70
60
50
40
30
20
10
0
N= 36
n= 120
15
43
***
9
36
**
10
30
wild type
ric-7 (n2657)
unc-116 (rh24sb79)
unc-104 (e1265)

from the influence of mitochondria. To determine the role of mitochondria in axonal degeneration, GABA motor neuron axons were cut using a laser in *ric-7* mutants and wild-type animals. Motor neuron axons cross from the ventral to the dorsal cord in single axon commissures. The axons were visualized by expressing a soluble GFP under the *unc-47* (vGAT) promoter. Four to five commissures were severed in the posterior of L2 worms, typically 3 VD and 1-2 DD axons. The cell bodies were subsequently killed with the laser to prevent the regeneration of new axons, which would obscure the degenerating distal axons. After 24 hrs of recovery, the worms were reimaged and the presence of commissures was scored. In wild-type worms, 58% of the GABA axons are present after 24 hrs, whereas no axons remain in *ric-7* mutants (Figure 2.3F,G).

To determine whether additional cell types are hypersensitive to degeneration in *ric-7* mutants, we also performed axotomy on acetylcholine motor neurons and the ALA neuron. We expressed membrane-bound GFP under the *acr-5* promoter, which expresses in the acetylcholine DB motor neurons, ALA, and neurons in the head and tail ganglia. Two DB commissures were severed in each worm and then scored after 24 hrs for their presence or absence. Only 11% of *ric-7* acetylcholine motor neuron axons remained after 24 hrs, whereas 84% of wild-type axons were still present (Figure 2S.3F). The ALA axon also displayed robust degeneration after injury in *ric-7* mutants. The ALA neuron sends out two axons that run from the head to the tail on each side of the worm. Severed ALA axons are still present 24 hrs after axotomy in the wild type; however, in *ric-7* mutants, severed axons completely degenerate (Figure

2S.3G,H). Interestingly, injured axons are quite stable in wild-type *C. elegans,* which has been previously noted within regeneration studies (Pinan-Lucarre et al., 2012; Wu et al., 2007). In all three cell types tested, *ric-7* mutants exhibited robust levels of axon degeneration.

Mitochondrial localization mutants have enhanced degeneration

If the enhanced degeneration in *ric-7* mutants is due to the loss of mitochondria, then other mutants with abberrantly localized mitochondria should also have increased levels of axon degeneration. To test this, we performed laser axotomy on kinesin-1 mutants, which also have a severe loss of mitochondria in their GABA motor neuron axons (Figure 2.2B,C). Similar to *ric-7*, the vast majority of injured axons degenerate in kinesin-1 mutants (Figure 2.3F,G). Kinesin-1 mutants could have increased degeneration due to their severe health impairments or to a general disruption in axonal transport. However, mutants for kinesin-3/*unc-104,* which are equally unhealthy and deficient for key axon components such as synaptic vesicles (Hall and Hedgecock, 1991), have wild-type levels of degeneration (Figure 2.3F,G).

We additionally tested worms overexpressing a dominant negative form of DRP-1 (dynamin-related protein) in GABA neurons. DRP-1 is required for mitochondrial fission (Otsuga et al., 1998; Smirnova et al., 1998), and neurons overexpressing a dominant-negative version DRP-1(K40S) have long tubular mitochondria extending from the cell body into the proximal axons, but

mitochondria numbers are reduced in the distal axons. When these axons lacking mitochondria are cut, they rapidly degenerate; only 23% of the axons remain after 24 hrs (compared to 58% in the wild type, Figure 2S.3I-K). Of these surviving axons, 70% contained visible escapee mitochondria when inspected. Thus, absence of mitochondria leads to an enhancement in axon degeneration in a variety of mutants.

Mitochondria prevent axon degeneration in wild-type animals

To determine whether mitochondria mediate axon survival in healthy animals as well, we performed experiments on wild-type ALA axons. The ALA axon is long and has a naturally sparse distribution of mitochondria, approximately 1 mitochondrion per 100 μm (0.47 ± 0.05 mitochondria per 50 μm, n= 17 L2 worms). To isolate axon segments that were void of mitochondria, the ALA axon was cut into multiple pieces. Because these axon segments recieve a calcium influx through two lesion sites, they may be especially sensitive to the calcium buffering capacity of mitochondria. Each worm was imaged immediately following axotomy; roughly half of the fragments contained mitochondria (61%). 24 hrs later, axon segments were scored for survival. 72% of axon segments containing mitochondria survived, whereas only 26% of segments lacking visible mitochondria survived (Figure 2.4A-C). Thus, the absence of mitochondria promotes degeneration in both mutant and wild-type axons.

Axons lacking mitochondria may be hypersensitive to degeneration due to

Figure 2.4. Mitochondria mediate axon protection. (A) The presence of mitochondria protects axons from degeneration in a wild-type background. ALA axons are labeled by expressing membrane-bound GFP under the *acr-5* promoter ('axon::GFP') and mitochondria are labelled by expressing mito:RFP under the *ida-1* promoter. ALA axons were cut by laser axotomy into multiple segments in wild-type worms that either contained (A) or lacked (B) mitochondria. 24 hrs after axotomy, the axon segment with a mitochondrion was still intact (below), whereas the segment without a mitochondrion had degenerated. The mito::RFP images have been inverted and the contrast has been enhanced to increase the visibilty of the mitochondria (arrows). Asterisks indicate gut autofluorescence. Scale bar = 10 μm. (C) 72% of the axon fragments containing a mitochondrion were still present 24 hrs later, whereas only 26% of axon fragments without mitochondria perdured. Error bars represent the 95% confidence interval (n = 13 worms and 48 axon fragments, p= 0.0028, two-tailed Fisher's Exact Test). (D) A transport chimera construct was created by fusing the cDNA for *unc-116* (kinesin-1) to the *tomm-7* gene, which encodes for the outer mitochondrial membrane protein Tom7. GFP flanked by linkers was inserted between the motor and the mitochondrial protein. The construct was expressed in GABA neurons under the *unc-47* promoter. Below is a conceptual cartoon of the transport chimera protein. (E) Expression of the transport chimera 'Kinesin::Tom7' restores mitochondria in *ric-7* mutant axons. See also Figure 2S.4B. (F) The transport chimera suppresses the GABA neurotransmission defects in *ric-7* mutants. In *C. elegans,* GABA release is required for enteric muscle contractions (emc) following posterior body muscle contractions (pboc). In *ric-7* mutants, only 16% of pbocs are followed by an emc. This defect was rescued by expressing RIC-7(+) (*oxEx1598*[RFP::RIC-7]), or the transport chimera 'Kinesin::Tom7' in GABA neurons. (G) Restoring mitochondria to *ric-7* mutant axons (magenta bar) also suppressed degeneration of GABA motor neuron axons following injury. The transport chimera has no effect in a wild-type background (purple bar). See also Figure 2S.4C. The wild-type and *ric-7* data are the same as in Figure 2.3G. For E-G, $p < 0.0001$ Kruskal-Wallis test with Dunn's multiple comparisons to the wild type (black) and to *ric-7(n2657)* (red), *** $p<0.001$, **$p<0.01$.

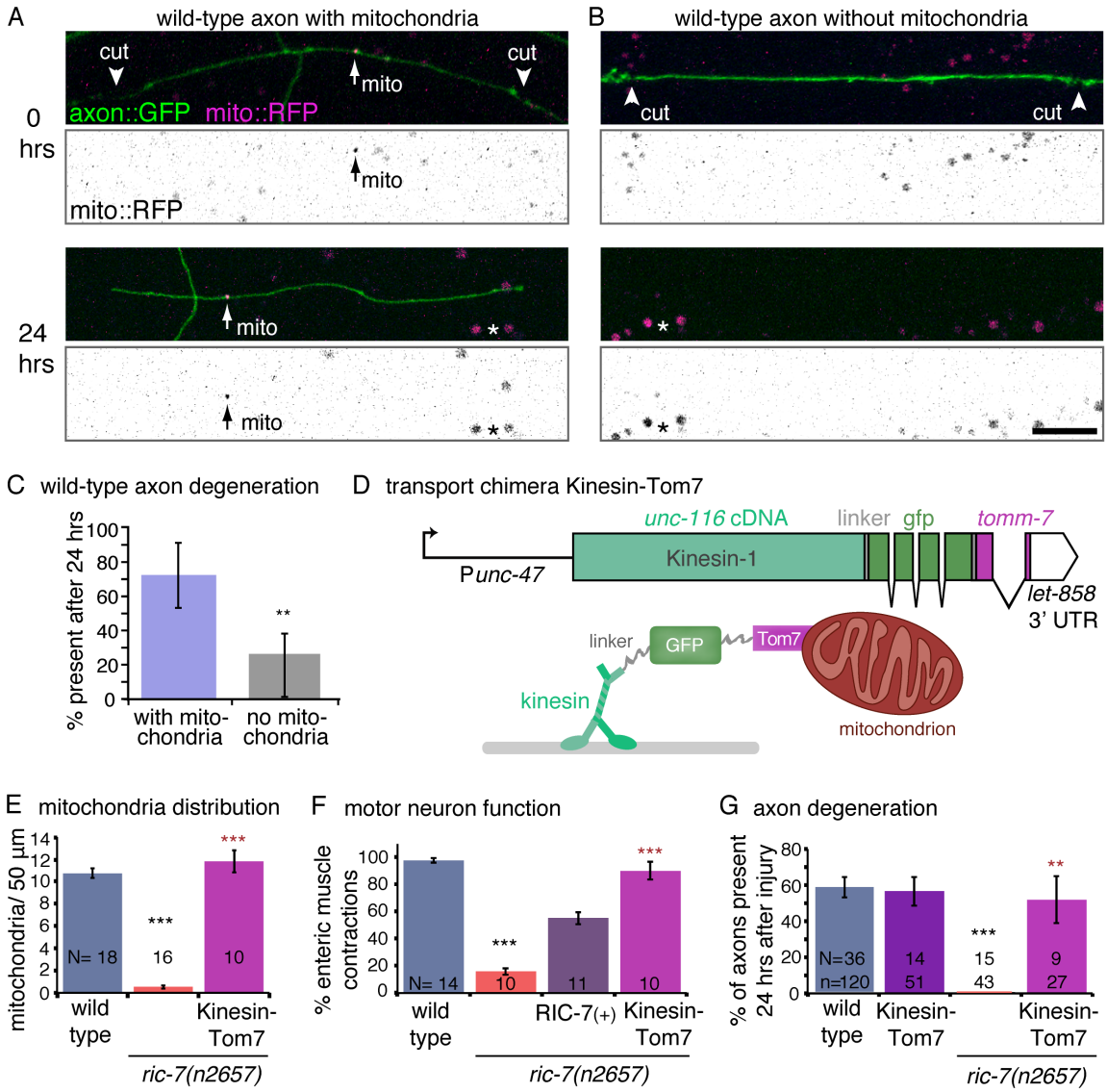
A
wild-type axon with mitochondria
cut
mito
cut
axon::GFP mito::RFP
0 hrs
mito::RFP
mito
24 hrs
mito
mito
B
wild-type axon without mitochondria
cut
cut
C wild-type axon degeneration
% present after 24 hrs
with mito-chondria
no mito-chondria
D transport chimera Kinesin-Tom7
unc-116 cDNA
linker
gfp
tomm-7
Punc-47
Kinesin-1
let-858 3' UTR
linker
GFP
Tom7
kinesin
mitochondrion
E mitochondria distribution
mitochondria/ 50 µm
N= 18
16
10
wild type
Kinesin-Tom7
ric-7(n2657)
F motor neuron function
% enteric muscle contractions
N= 14
10
11
10
wild type
RIC-7(+)
Kinesin-Tom7
ric-7(n2657)
G axon degeneration
% of axons present 24 hrs after injury
N=36 n=120
14 51
15 43
9 27
wild type
Kinesin-Tom7
Kinesin-Tom7
ric-7(n2657)

a loss of metabolic support. To test whether mitochondrial metabolism is key for axon survival, mutants with electron transport chain defects were assayed for degeneration following axotomy. *nuo-1* encodes for a subunit of Complex I and homozygous mutants arrest at the third larval stage (Tsang, 2001). Mutants lacking MEV-1, a subunit of Complex II, are viable as homozygotes but are uncoordinated, slow-growing, and have a shortened life-span (Ishii et al., 1998). In spite of their mitochondrial dysfunction and health defects, these worms do not show an increase in axon degeneration following axotomy; instead, there are slightly more axons remaining compared to the wild type (73% and 71%, respectively, of axons remain after 24 hrs, Figure 2S.4A). The electron transport chain mutants indicate that, (i) mitochondrial dysfunction is insufficient to induce axon degeneration on its own and (ii) energy levels are not likely to be the rate-limiting factor for axon preservation in *C. elegans*. In humans, nonlethal mutations affecting oxidative phosphorylation are rarely associated with neurodegeneration, suggesting that impaired mitochondrial bioenergetics do not reliably initiate degeneration (Schon and Przedborski, 2011). Additionally, some studies suggest that the glycolytic activity of a cell can promote survival during impaired oxidative phosphorylation (Calupca et al., 1999; Fünfschilling et al., 2013; Misko et al., 2012; Tekk k et al., 2003; Winkler et al., 2000).

Restoring mitochondria in *ric-7* mutant axons suppresses degeneration

Even though mutant and wild-type axons lacking mitochondria have

enhanced degeneration, it still remains possible that axon degeneration in *ric-7* mutants is caused by another defect, not noticed in our assays. If mitochondrial loss is responsible for the enhanced degeneration, then restoring mitochondria into *ric-7* deficient axons should suppress axon degeneration. To rescue mitochondria localization in *ric-7* mutants, we constructed a chimeric transport protein that fuses Kinesin-1 (UNC-116) to the outer mitochondrial membrane protein Tom7 (encoded by *tomm-7*) (Kinesin::Tom7, Figure 2.4D). The proteins are separated by linkers and GFP. When the chimeric transport protein is expressed in GABA neurons, mitochondria are transported into the axons of *ric-7* mutants (Figure 2.4E, 2S.4B). It is also notable that expression of the transport chimera also rescues GABA motor neuron function (Figure 2.4F). Restoring mitochondria to axons in *ric-7* mutants also fully suppresses the degeneration phenotype. Axon survival after axotomy is 52% in *ric-7* animals in which the Kinesin::Tom7 construct is expressed (compared to 58% in the wild type and 0% in *ric-7,* Figure 2.4G, S4C). Expression of the transport chimera does not influence degeneration in the wild type. Rescue by forced transport of mitochondria in the *ric-7* mutant demonstrates that the relevant cause of rapid axon degeneration and defective neurotransmission is the absence of mitochondria.

Discussion

Recent studies suggest contradictory roles for mitochondria in axon degeneration. In some cases, mitochondria seem to *prevent* axon degeneration.

For example, loss of mitochondria caused by knockdown of the kinesin adaptor milton lead to degeneration of axons in the fly wing (Fang et al., 2012). Similarly, disease-associated alleles of mitofusin-2 in cultured dorsal root ganglia neurons disrupted the regular distribution of mitochondria in axons and was associated with degeneration (Misko et al., 2012).

In other cases, mitochondria seem to *promote* axon degeneration. For example, degeneration of neuromuscular junctions is caused by mutations in alpha spectrin in flies, and this degeneration is suppressed by mutations in the mitochondria transport adaptor miro (Keller et al., 2011). In another example, the degeneration of severed axons was prevented by blocking the mitochondrial permeability transition pore with the drug cyclosporin A (Barrientos et al., 2011). Severed sciatic nerves were cultured in the absence of their neuronal cell bodies, thus the drug is acting on mitochondria within the axon to prevent degeneration. These studies indicate that mitochondria promote axonal degeneration in both a disease model and an injury-based model.

Our data demonstrate that mitochondria are not a necessary component of the degeneration process but rather are required for the protection of axons in *C. elegans*. In *ric-7* mutants, mitochondria never migrate into the axons. Some axons lacking mitochondria spontaneously degenerate in *ric-7* mutants and axons that are intact rapidly degenerate after an injury. Other strains with disrupted mitochondrial localization, such as animals defective for mitochondrial transport (kinesin-1) or mitochondrial division (DRP-1(K40S)), also exhibit rapid degeneration after axotomy. Importantly, the absence of mitochondria in wild-

type axons also causes degeneration, demonstrating that neurodegeneration is not due to secondary defects of the mutations, but rather is due to the absence of mitochondria. The protective role of mitochondria is underscored by their ability to rescue degeneration when they are forced into axons. Hauling mitochondria out of cell bodies in *ric-7* mutants using a chimeric transport protein (Kinesin::Tom7) rescues both neurotransmission and axon degeneration in *ric-7* mutants.

Perhaps a more nuanced view of mitochondria is warranted; they are neither solely protective or destructive but rather seem to play both Jekyll and Hyde roles in neurodegeneration. Previous data have demonstrated that mitochondria can promote or accelerate degeneration in certain disease states (Keller et al., 2011; reviewed in Schon and Przedborski, 2011). Here we show that mitochondria are required for axon stability in *C. elegans*. The absence of mitochondria causes rapid degeneration of cut axons in both wild-type and mutant axons. These observations suggest two further conclusions: First, mitochondria are not required for degeneration. In other words, the swelling, beading, and engulfment processes are not directed by mitochondria but must lie within the molecular pathways of the axon itself and the surrounding cells. Second, mitochondria provide an active, protective role, somehow blocking the initiation of these processes.

Acknowledgments

The work in this chapter is a manuscript in press at Current Biology and has been a collaborative effort. Lung Yam and Scott Clark identified and characterized the spontaneous degeneration of the PVQ and HSN neurons. Robby Weimer cloned *ric-7* and collected most of the data in Figures 1.1 and 2S.1. Eric Bend performed much of the molecular biology. *ric-7* was originally isolated in the lab of H. Robert Horvitz and Erika Hartwieg conducted the electron microscopy experiments.

We thank Jamie White, Marc Hammarlund, and Holly Holman for critical review of the manuscript. We thank Mike Bastiani and Paola Nix for the use of their laser axotomy system. We are grateful to Villu Maricq and Dane Maxfield for the use of their Nikon spinning disc confocal. We thank the following people for providing reagents; Kim Schuske, Rob Hobson, Andrew Jones, Marc Hammarlund, Shaili Johri, Fred Horndli, Jean Louis Bessereau, and Gunther Hollopeter. The FLP-3::Venus strain was a gift from Ken Miller. The *unc-116*(*rh24sb79*) strain was a gift from Frank McNally. Some strains were provided by the CGC (NIH P40 OD010440). The *nu447* allele was a gift from Josh Kaplan, and we appreciate discussions before publication. This work was supported by NIH NS39397 to SGC and NIH NS034307 and NSF IOS-0920069 to EMJ. None of the authors of this work has a financial interest related to this work.

Supplemental Materials

Figure 2S.1. Characterization of *ric-7*. (A) The phylogenetic tree of RIC-7B orthologs shows rapid divergence among nematodes. The RIC-7A isoform is present only in the Rhabditina clade. RIC-7 from *C. elegans* and *B. malayi* only share 23% identity; other mitochondrial proteins such as MIRO share 58% identity in these species. Orthologs of the RIC-7 isoforms were identified by performing BLAST searches of other nematode sequence data and were hand-assembled from multiple EST and genomic sequences. Sequence identity was determined by pairwise BLASTp alignment. (B) *ric-7* mutants are defective for acetylcholine neurotransmission. Animals become paralyzed when exposed to the acetylcholinesterase inhibitor Aldicarb due to accumulation of acetylcholine in the synaptic cleft. Paralysis in response to Aldicarb was assayed after 8 hrs. *ric-7* mutants are resistant to Aldicarb, indicating impaired acetylcholine release (n= 10-20 worms per data point). Similar results have been reported by Hao *et al.* (Hao et al., 2012). (C) In *C. elegans,* GABA stimulates contraction of the enteric muscles (Liu and Thomas, 1994; McIntire et al., 1993a). *ric-7* mutants display reduced enteric muscle contractions following posterior body muscle contractions, and this defect was rescued by expressing RIC-7 (*oxEx233*) in the GABA neurons, 'RIC-7(+)'. n-values shown in each bar, $p<0.01$. (D) The active zone protein RIM (UNC-10) is normally distributed in the dorsal cord of *ric-7(n2657)* mutants. RFP is fused to the PDZ and C2A domains of RIM, which are sufficient for proper localization (Otsuga et al., 1998). The number of RIM puncta is similar between the wild type and *ric-7(n2657)* mutants (avg # of RIM puncta per 50 µm +/- SEM, 30 and 31 images, respectively, $p=0.53$ two-tailed t-test). (E) A synaptic vesicle marker, the vesicular GABA transporter (vGAT/UNC-47), is normally localized in *ric-7* mutants. vGAT was tagged with GFP and inserted as a single copy. The number of vGAT::GFP puncta is normal in *ric-7* mutants (avg # of vGAT puncta per 50 µm +/-SEM, 12 and 9 images, respectively, $p=0.46$ Mann-Whitney Test). (F) Electron micrographs of neuromuscular junctions in the adult ventral nerve cord revealed that *ric-7(n2657)* has normal numbers of vesicles per synapse profile (wild type: 16 synapses, 75 profiles, *ric-7(n2657)*: 15 synapses, 68 profiles). (G) The active zone protein RIM (UNC-10) is normally distributed in the dorsal cord of *ric-7(n2657)* mutants. (H) A synaptic vesicle marker, the vesicular GABA transporter (vGAT/UNC-47), is normally localized in *ric-7* mutants. (I) Dense core vesicles are distributed evenly throughout the axons of *ric-7* mutants, shown here using the neuropeptide marker FLP-3::Venus. Scale bar = 10 µm. (J) Electron micrographs of neuromuscular junctions show synaptic vesicles (arrowheads) surrounding the dense projection (*) for the wild type and *ric-7(n2657)*. Scale bar = 250 nm. (K) *ric-7* is expressed in neurons and head muscles. DNA 5 kb upstream of the *ric-7a* start codon through the second exon was fused to a nuclear localization signal (NLS) and GFP (left). Fluorescence was observed in most neurons in the head, as well as in the head muscles (middle), and motor neurons (right); examples of each are labeled. An asterisk marks autofluorescent gut granules. Anterior is to the left.

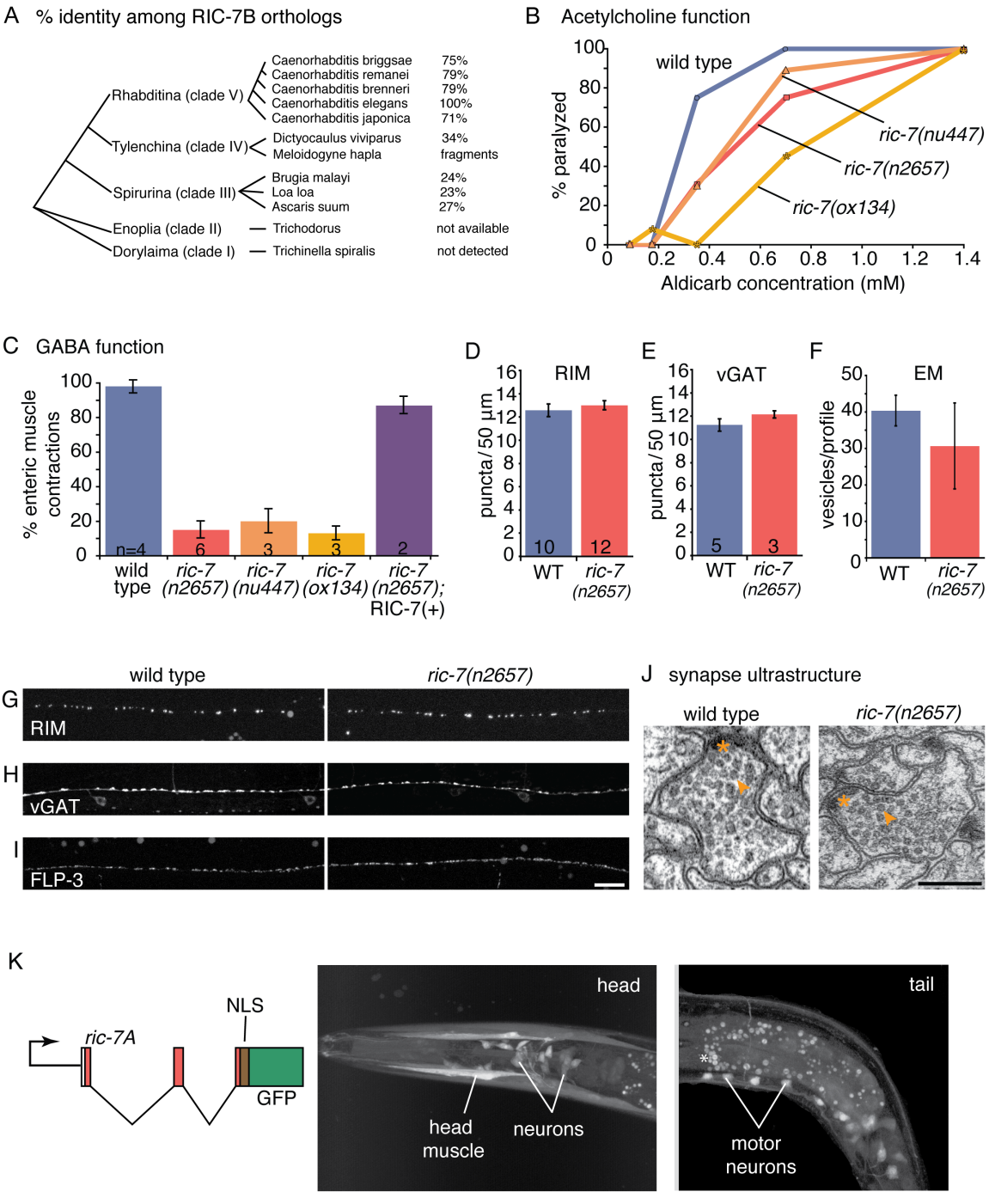
A % identity among RIC-7B orthologs
Rhabditina (clade V)
Caenorhabditis briggsae 75%
Caenorhabditis remanei 79%
Caenorhabditis brenneri 79%
Caenorhabditis elegans 100%
Caenorhabditis japonica 71%
Tylenchina (clade IV)
Dictyocaulus viviparus 34%
Meloidogyne hapla fragments
Spirurina (clade III)
Brugia malayi 24%
Loa loa 23%
Ascaris suum 27%
Enoplia (clade II) Trichodorus not available
Dorylaima (clade I) Trichinella spiralis not detected
B Acetylcholine function
% paralyzed
Aldicarb concentration (mM)
wild type
ric-7(nu447)
ric-7(n2657)
ric-7(ox134)
C GABA function
% enteric muscle contractions
wild type
ric-7 (n2657)
ric-7 (nu447)
ric-7 (ox134)
ric-7 (n2657); RIC-7(+)
D RIM
puncta/50 µm
WT
ric-7 (n2657)
E vGAT
puncta/50 µm
F EM
vesicles/profile
G RIM
H vGAT
I FLP-3
wild type
ric-7(n2657)
J synapse ultrastructure
K
ric-7A
NLS
GFP
head
head muscle
neurons
tail
motor neurons

Figure 2S.2. RIC-7 and mitochondria localization. (A) Tagged RIC-7 (RFP::RIC-7) was made by combining the cDNA for exons 1-10 with the genomic sequence for exons 11 through the 3'UTR. The 10th intron was shortened in order to remove the coding region for F58E10.7. RFP flanked by linker sequences was inserted at the N-terminus. The construct was expressed in GABA neurons using the *unc-47* promoter. (B) When inserted as a single-copy transgene, RFP::RIC-7 is distributed diffusely in the GABA motor neuron cell body (arrowhead) and axons. Scale bar = 10 μm. (C) Mitochondria are absent in axons of the dorsal nerve cord in *ric-7(n2657)* mutants. GABA motor neuron axons are labeled with soluble RFP and mitochondria in the GABA neurons are labelled with mito::GFP. Scale bar = 10 μm. (D) Mito::citrine was expressed in the hypodermis under the *dpy-7* promoter. Similar structures were observed in the wild type and *ric-7* mutants. (E) Mito::citrine was expressed in the body wall muscles under the *myo-3* promoter. Muscle mitochondria form a similar network in *ric-7* mutants and the wild type. Scale bar = 5 μm.

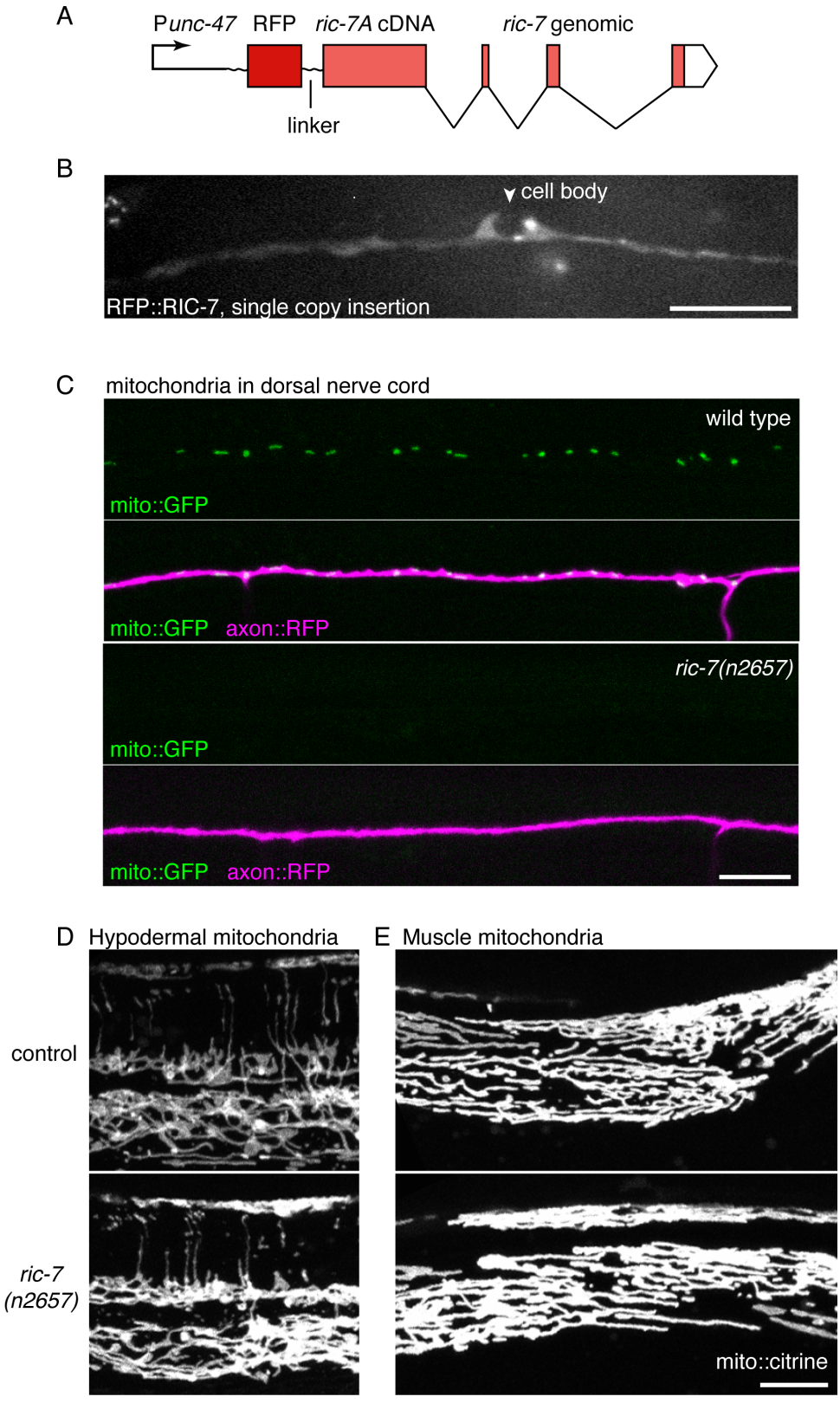
A
P*unc-47* RFP *ric-7A* cDNA *ric-7* genomic
linker
B
cell body
RFP::RIC-7, single copy insertion
C
mitochondria in dorsal nerve cord
wild type
mito::GFP
mito::GFP axon::RFP
ric-7(n2657)
mito::GFP
mito::GFP axon::RFP
D Hypodermal mitochondria
E Muscle mitochondria
control
ric-7 (n2657)
mito::citrine

Figure 2S.3. Axon degeneration is enhanced in the absence of mitochondria. (A) The PVQ axon remains intact in the wild type. Scale bar = 100 µm. (B) HSN axons spontaneously degenerate in *ric-7* mutants. Schematic of the HSN axon in the wild type and *ric-7(zd31)* mutants. The HSN cell bodies extend a single axonal process to the nerve ring during larval development. (C) In a wild-type animal, the HSN axon is continuous and reaches into the nerve ring. (D) HSN axons were unaffected in *ric-7* young adults, yet degeneration was evident in older animals (E). Swelling and distal degeneration was similar to that of PVQ. (F) Severed acetylcholine motor neuron axons degenerate in *ric-7* mutants but not wild-type worms. Two acetylcholine (DB) axons were cut per animal and reimaged 24 hrs later. The presence or absence of severed axons was scored. ***p<0.0001 two-tailed Fisher's Exact Test. (G) Severed ALA axons persist in the wild type but degenerate in *ric-7* mutants. Lengths of intact ('sham') and severed ('axotomy') ALA axons 24 hrs after axotomy in wild-type worms and *ric-7* mutants. Worms with sham axotomies were mounted for surgery but the axons were not cut. (p< 0.0001, Kruskal-Wallis Test with Dunn's multiple comparisons ***p<0.001 and **p<0.01 compared to the wild type). (H) ALA axons were cut once near the head by laser axotomy in L2 animals and reimaged 24 hrs later. ALA axons were labelled using the P*acr-5:GAP-43::GFP* transgene. In these images, the right side was cut in the wild type and the left in the *ric-7* worm. Arrows mark the ends of the severed axon in the wild type. Arrowheads mark the approximate location of the lesion site from the previous day. The cell bodies were killed to prevent regeneration, and an asterisk marks the former location of the cell body. Scale bar = 100 µm. (I) Overexpression of dominant negative DRP-1(K40S) reduces mitochondria in the distal axon and increases degeneration of GABA motor neurons. Three axons are visible immediately after axotomy. Arrowheads mark the cut sites and arrows indicate some mitochondria that have escaped into the distal axon. The worm was moving slightly after the surgery. To increase visibility these images were scaled 215% relative to the 24 hr images, both scale bars are 10 µm. (J) After 24 hrs, only the axon with escapee mitochondria is still present. Axon 1 has completely degenerated and only two small pieces of debris remain for axon 3. Arrows indicate the location of mitochondria in Axon 2. (K) Axons were scored for their presence or absence 24 hrs after axotomy. In worms overexpressing a dominant negative form of DRP-1(K40S), only 23% of axons are still present. Of these axons, 70% contain visible mitochondria (Average % of axons present 24 hrs after axotomy +/- SEM). p = 0.0002 two-tailed t-test with Welch correction for unequal variances. The wild-type data is the same as in Figure 2.3G.

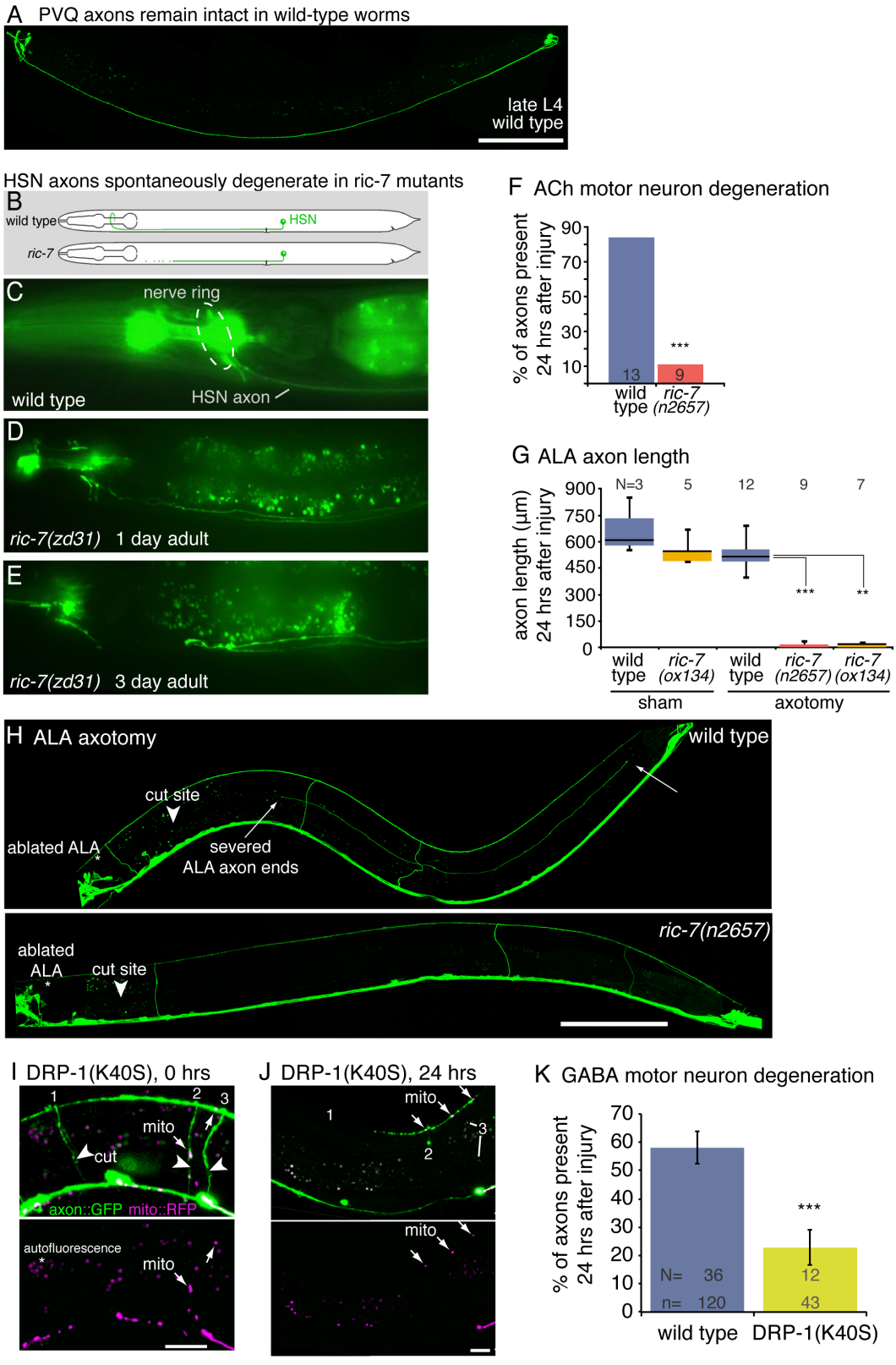
A PVQ axons remain intact in wild-type worms
late L4
wild type
HSN axons spontaneously degenerate in ric-7 mutants
B
wild type
HSN
ric-7
C
nerve ring
wild type
HSN axon
D
ric-7(zd31) 1 day adult
E
ric-7(zd31) 3 day adult
F ACh motor neuron degeneration
% of axons present 24 hrs after injury
90
70
50
30
10
13
9
***
wild type
ric-7 (n2657)
G ALA axon length
axon length (µm) 24 hrs after injury
900
750
600
450
300
150
0
N=3
5
12
9
7
***
**
wild type
ric-7 (ox134)
wild type
ric-7 (n2657)
ric-7 (ox134)
sham
axotomy
H ALA axotomy
wild type
cut site
ablated ALA
severed ALA axon ends
ric-7(n2657)
ablated ALA
cut site
I DRP-1(K40S), 0 hrs
1
2
3
mito
cut
axon::GFP mito::RFP
autofluorescence
mito
J DRP-1(K40S), 24 hrs
mito
1
3
2
mito
K GABA motor neuron degeneration
% of axons present 24 hrs after injury
70
60
50
40
30
20
10
0
***
N= 36
n= 120
12
43
wild type
DRP-1(K40S)

Figure 2S.4. The transport chimera restores mitochondria to *ric-7* axons and suppresses degeneration. (A) Impaired mitochondrial function does not promote axon degeneration. The electron transport chain mutants *mev-1(kn1) and nuo-1(ua1)* do not have enhanced axon degeneration in spite of their mitochondrial dysfunction and impaired health. p = 0.38 one-way ANOVA. The wild-type data is the same as in Figure 2.3G. (B) Overexpression of the chimeric transport protein Kinesin-Tom7 restores mitochondria out into the axons of *ric-7* mutants. Scale bar = 10 μm. (C) Axons can survive axotomy in *ric-7* mutants that are expressing Kinesin-Tom7. Two surviving axons can be seen and mitochondria are visible in the dorsal nerve cord. In the RFP-only image, a mask was created over the gut autofluorescence (grey outline) so that the actual mito::RFP signal from the ventral and dorsal cords is discernable. Scale bar = 25 μm.

A mitochondria dysfunction

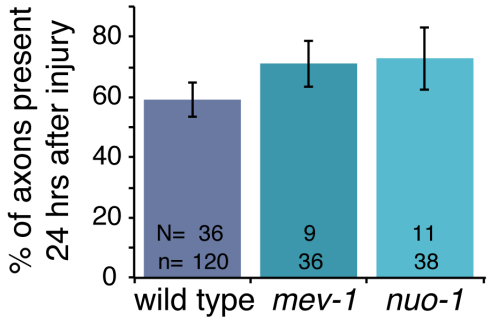

B transport chimera rescues mitochondria distribution

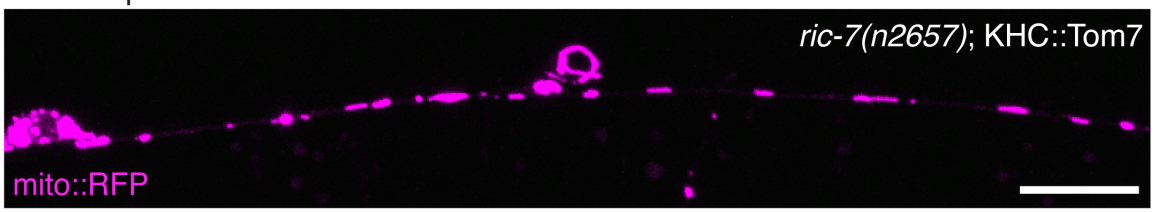

C transport chimera suppresses degeneration

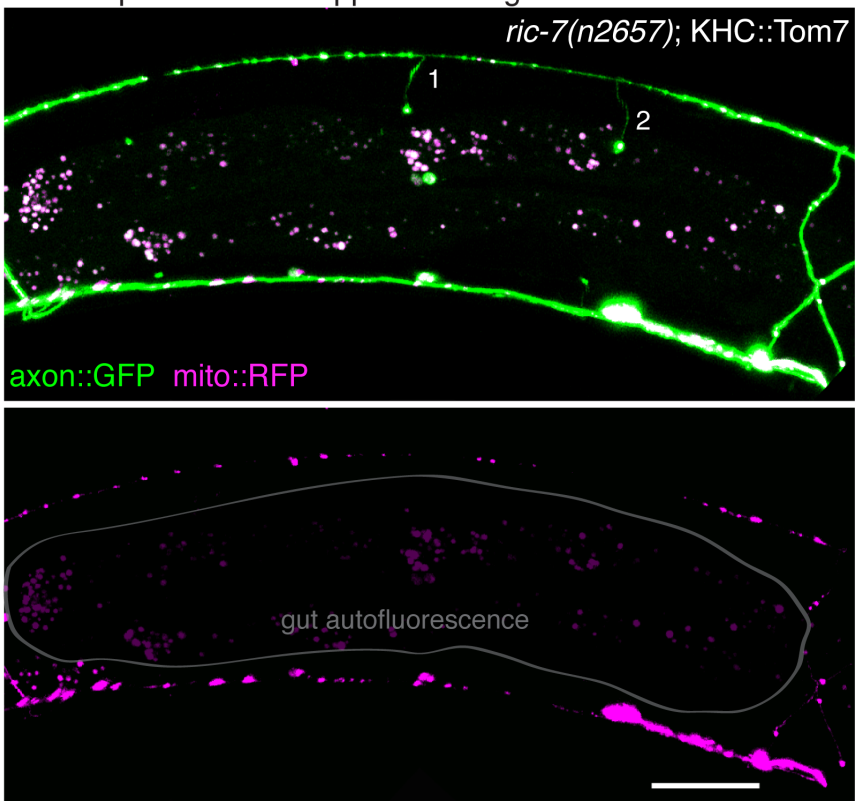

Table 2S.1. *ric-7* mutations.

Allele	**DNA mutation** (relative to *ric-7a* cDNA)	**Protein modification** (relative to RIC-7A)	**Mutagen**
ox134	14.6 kb deletion beginning in the 2nd intron	only amino acids 1-84 would remain	ENU
zd152	c148t	R50stop	ENU
n2657	g576a	W192stop	EMS
zd31	c634t	Q212stop	EMS
nu447	c785t, + 32 base pair deletion (nt 865-896)	A262V, + out of frame after C288 and an early stop codon at position 291	EMS

Supplemental Experimental Procedures

Strains

Animals were maintained on *E. coli* OP50-seeded NGM plates according to standard methods. See Table 2S.1 for a complete list of strains. See Table 2S.2 for a complete list of worm strains.

Cloning of *ric-7*

Three *ric-7* alleles were isolated from three behavioral screens for neurotransmission defective mutants: defecation defective, aldicarb resistance (Hao et al., 2012), and shrinker behavior, *n2657*, *nu447,* and *ox134*, respectively. The *ric-7* reference allele *n2657* was isolated in a screen for excitatory GABA neurotransmission defective mutants. Wild-type hermaphrodites were treated

Table 2S.2. Worm strains

	Strain	Genotype	Transgenes
n2657	MT6924	*ric-7(n2657) V*	
ox134	EG2355	*ric-7(ox134) V*	
nu447	KP7048	*ric-7(nu447) V*	
zd31	SK31	*ric-7/wly-1(zd31) V*	
zd152	SK152	*ric-7/wly-1(zd152) V*	
Pric-7:GFP	EG1702	*lin-15(n765ts) X; oxEx174*	P*ric-7a::NLS:GFP, lin-15(+)*
RIC-7::GFP	EG1474	*ric-7(n2657) V; lin-15(n765ts) X; oxEx233*	P*unc-47::RIC-7::GFP, lin-15(+)*
PCR rescue	EG2298	*ric-7(n2657) V; lin-15(n765ts) X*	18kb PCR product, *lin-15(+)*
RIM wild type	EG7001	*lin-15(n765ts) V; oxEx1637*	P*unc-47:RIM_C2APDZ::RFP*, P*myo-2:GFP*, lin-15(+)
RIM *n2657*	EG7000	*ric-7(n2657) V; lin-15(n765ts) X; oxEx1636*	P*unc-47:RIM_C2APDZ::RFP*, P*myo-2:GFP*, *lin-15(+)*
vGAT wild type	EG5717	*unc-119(ed3) III; oxSi36 IV*	P*unc-47:unc-47+GFP(E144), CB unc-119(+)*
vGAT *n2657*	EG5787	*oxSi36 IV; ric-7(n2657) V*	P*unc-47:unc-47+GFP(E144), CB unc-119(+)*
FLP-3 wild type	KG1645	*ceIs61 II*	P*unc-129:flp-3::Venus*, P*unc-129:mCherry::snb-1*, P*ttx-3:mCherry*
FLP-3 *n2657*	EG6336	*ric-7(n2657) V; ceIs61 II*	P*unc-129:flp-3::Venus*, P*unc-129:mCherry::snb-1*, P*ttx-3:mCherry*
RFP::RIC-7	EG6793	*ric-7(n2657) V; lin-15(n765ts) X; oxEx1598*	P*unc-47:RFP_ric-7AcDNA_3'minigene*, P*unc-47:Tom20::GFP*, *lin-15(+)*
mito::GFP wild type	EG5043	*lin-15(n765ts) X; oxEx1182*	P*unc-47:Tom20::GFP*, P*myo-2:GFP*, *lin-15(+)*
mito::GFP *n2657*	EG6496	*ric-7(n2657) V; lin-15(n765ts) X; oxEx1182*	Punc-47:Tom20::GFP, Pmyo-2:GFP, lin-15(+)
mito::GFP *ox134*	EG7308	*ric-7(ox134) V; lin-15(n765ts) X; oxEx1772*	P*unc-47:Tom20::GFP,* P*myo-2:GFP*, *lin-15(+)*
Axon::RFP mito::GFP	EG6531	*oxIs608; oxEx1182*	P*unc-47:mCherry*; P*unc-47:Tom20::GFP*, P*myo-2:GFP*
Axon::RFP mito::GFP	EG7161	*ric-7(n2657) V; lin-15(n765ts) X; oxEx1720*	P*unc-47:mCherry*, P*unc-47:Tom20::GFP*, *lin-15(+)*
PVQ axon wild type	PY1058	*oyIs14 V*	P*sra-6::GFP*
PVQ axon *zd152*	SK5175	*ric-7/wly-1(zd152) oyIs14 V*	P*sra-6::GFP*
ALA:GFP wild type	EG1399	*lin-15(n765ts) X; oxEx81*	P*acr-5:GAP43::GFP, lin-15(+)*
ALA:GFP *n2657*	EG1968	*ric-7(n2657) V; lin-15(n765ts) X; oxEx81*	P*acr-5:GAP43::GFP, lin-15(+)*
ALA:GFP *ox134*	EG1967	*ric-7(ox134) V; lin-15(n765ts) X; oxEx81*	P*acr-5:GAP43::GFP, lin-15(+)*
ALA:GFP mito::RFP	EG6863	*oxIs609; oxEx1606*	P*acr-5:GAP43::GFP, lin-15(+)*; P*ida-1:Tom20::RFP*
GABA cuts wild type	EG1285	*lin-15(n765ts) oxIs12 X*	P*unc-47::GFP, lin-15(+)*
GABA cuts *n2657*	EG1960	*ric-7(n2657) V; lin-15(n765ts) oxIs12 X*	P*unc-47::GFP, lin-15(+)*
RFP::RIC-7 single copy	EG6753	*unc-119(ed3) III; oxSi451 II*	P*unc-47:RFP::ric-7AcDNA_ 3'minigene*, *Cb-unc-119(+)*
Hypodermis mito WT	EG6463	*lin-15(n765ts) X; oxEx1541*	P*dpy-7:Tom20::citrine, lin-15(+)*
Hypodermis mito *n2657*	EG6611	*ric-7(n2657) V; lin-15(n765ts) X; oxEx1541*	P*dpy-7:Tom20::citrine, lin-15(+)*
Muscle mito wild type	EG5515	*lin-15(n765ts) X; oxEx1329*	P*myo-3:Tom20::citrine, lin-15(+)*
Muscle mito *n2657*	EG6859	*ric-7(n2657) V; lin-15(n765ts) X; oxEx1329*	P*myo-3:Tom20::citrine, lin-15(+)*
HSN *ric-7(zd31)*	SK5249	*zdIs13 IV; ric-7/wly-1(zd31) V*	*tph-1::gfp*

Table 2S.2. continued

	Strain	Genotype	Transgenes
kinesin-1 mito::GFP	EG6615	*unc-116(rh24sb79) III; oxEx1182*	P*unc-47:Tom20::GFP*, P*myo-2:GFP*, *lin-15(+)*
kinesin-3 mito::GFP	EG8300	*unc-104(e1265) II; oxEx1182*	P*unc-47:Tom20::GFP*, P*myo-2:GFP*, *lin-15(+)*
kinesin-1 axotomy	MJB1280	*unc-116(rh24sb79) III; oxIs12 X*	P*unc-47::GFP, lin-15(+)*
kinesin-3 axotomy	MJB1281	*unc-104(e1265) II; oxIs12 X*	P*unc-47::GFP, lin-15(+)*
DRP-1(K40S)	EG8125	*oxIs12 X; oxEx1974*	P*unc-47:DRP-1(K40S)*, P*unc-47:Tom20::mCherry*, P*myo-2::mCherry*, *lin-15(+)*
Kinesin::Tom7	EG8301	*oxIs12 X; oxEx1973*	P*unc-47::unc-116_GFP::tomm-7*, P*unc-47::Tom20::mCherry*, P*myo-2::mCherry, lin-15(+)*
Kinesin::Tom7 *ric-7(n2657)*	EG8124	*ric-7(n2657) V; lin-15(n765ts) oxIs12 X; oxEx1973*	P*unc-47::unc-116_GFP::tomm-7*, P*unc-47::Tom20::mCherry*, P*myo-2::mCherry, lin-15(+)*
mev-1	EG8302	*mev-1(kn1) III; oxIs12 X*	P*unc-47::GFP, lin-15(+)*
nuo-1	EG8303	*nuo-1(ua1)/mIn1[dpy-10(e128) mIs14] II; oxIs12 X*	P*unc-47::GFP, lin-15(+)*

with ethyl methanesulfonate (EMS), and F2 progeny were screened for animals exhibiting a constipated phenotype. Two alleles (*zd31, zd152*) were recovered from a screen for mutants with defects in growth or morphology of the PVQ axons (see Clark and Chiu, 2003 for details). In brief, *sra-6::gfp(oyIs14)* animals were treated with EMS or N-ethyl-N-nitrosourea (ENU), and F2 progeny that exhibited behavioral defects were picked. F3 progeny were then examined using epifluorescence microscopy to find mutants with PVQ axonal defects. The alleles *zd31* and *zd152* exhibited discontinuous blebbing and truncation of the PVQ axons and the gene was named *wly-1* (wallerian-like decay). *wly-1* and *ric-7* were independently cloned and later established to be the same gene. Because the gene name *ric-7* is published, we use the name *ric-7* as well.

The reference allele *n2657* was mapped between *lin-25* and *unc-76* on chromosome V. Three-factor mapping placed *ric-7* to the left of *him-5* (Figure 2.1A). Cosmid F58E10 rescued the Aldicarb-resistance phenotype of *ric-7* mutants by germline transformation. F58E10 contains 11 predicted genes. Using PCR and germline rescue experiments, we localized the rescuing activity of F58E10 to an 18 kilobase fragment that contains two hypothetical genes, F58E10.1 and F58E10.7 (Figure 2.1A). A similar series of mapping and rescue experiments identified F58E10.1 as the gene *wly-1*. To ascertain which of the two candidate genes represents *ric-7/wly-1*, we identified the molecular lesions associated with the five mutant alleles. All alleles contain mutations in F58E10.1 exons (Figure 2.1B). Mutations are summarized in Table 2S.1.

Gene structure and protein. The *ric-7* coding region is contained in 13

exons dispersed over 15 kb (WBGene00010259, www.wormbase.org). We sequenced the full-length *ric-7* cDNA clone yk14h10 (gift from Yuji Kohara, Japan) to confirm the predicted gene structure. The *ric-7* cDNA contains 2085 bases of coding sequence, 86 bp of 5' UTR and 378 bp of 3' UTR. Analysis of *ric-7* cDNAs indicates that *ric-7* encodes two splice forms that differ in their first exon: RIC-7A (694 aa) and RIC-7B (709 aa).

To investigate the function of RIC-7, we sought possible homologous sequences. Blast searches of the full-length protein with sequence databases failed to identify homologs in species outside of nematodes. Even within nematodes, RIC-7 sequences appear to have diverged rapidly (Figure 2S.1A). The RIC-7 amino acid sequence does not contain any obvious protein domains.

Gene expression analysis indicates that *ric-7a* is expressed primarily in neurons and a few muscles. We generated a reporter containing genomic sequence from 5 kb upstream of the *ric-7*a ATG through to the second exon fused to a nuclear localization signal (NLS) and GFP. GFP was detected primarily in neurons as well as in the head muscle cells (Figure 2S.3A). Despite the presence of an NLS, GFP expression appears to be cytosolic.

Molecular biology

Most plasmids were made using the Invitrogen multisite Gateway cloning technique. We created the mitochondrial marker by fusing GFP to the mitochondrial targeting sequence (first 54 amino acids) of the translocase of outer mitochondrial membrane (Tom20, encoded by *tomm-20*) (Watanabe et al.,

2011). RIM localization was determined by fusing RFP to the C2A and PDZ domains of UNC-10. These two domains are sufficient to localize the RIM fragment to the dense projection (Deken, 2005). The synaptic vesicle marker was constructed by inserting GFP between E144 and N145 of UNC-47. The construct was inserted into the worm genome as a single copy using the MosSCI technique (Frøkjær-Jensen et al., 2008). The ALA:GFP transgene (*oxEx81*) encodes a membrane-bound GFP (40 aa myristoylation sequence of GAP43::GFP) and is expressed under the *acr-5* promoter (Knobel et al., 2001). *oxIs609* was generated by X-ray integration of *oxEx81*.

The constructs for tagging RIC-7 with RFP were made by combining the cDNA for exons 1-10 (Gateway [1-2] vector) with the genomic sequence for exons 11 through the 3'UTR (Gateway [2-3] vector). The third recombination site attB2 is embedded within the 10th intron, which was shortened to remove the coding region for F58E10.7. This hybrid construct expressed under the *unc-47* promoter rescued mitochondrial distribution in the GABA motor neurons. RFP flanked by linker sequences was inserted into the base constructs at five different locations; N-terminus, C-terminus, H104, E332, and Q440. All three internal tags yielded modest to poor rescue of mitochondrial distribution. The N-terminal tag was the only transgene that was visible when integrated at single copy. The A splice form was used because it provided better rescue of the mitochondrial localization defect than the B form did (data not shown).

The mitochondria transport chimera construct (Kinesin-Tom7) contains the following elements in order from 5' to 3': the *unc-47* promoter (1,254 bp), the

cDNA for *unc-116* (2,448 bp), linker sequence (36 bp), GFP with syntrons (864 bp), att recombination site + 2nd linker (63 bp), the genomic sequence of *tomm-7* (437 bp), and the *let-858* 3' UTR (439 bp). The *unc-116* cDNA through GFP are in a [1-2] Gateway vector and the second linker through the 3'UTR are in a [2-3] Gateway vector.

Behavioral assays

In *C. elegans,* defecation is a programmed behavior that occurs every 45-50 seconds. The defecation cycle is initiated by a posterior body wall muscle contraction (pBoc) and completed with an enteric muscle contraction (Emc). The Emc requires nervous system function and the excitatory action of the neurotransmitter GABA (Liu and Thomas, 1994; McIntire et al., 1993a, 1993b). The defecation cycle of young adults from each strain were scored as described previously (Thomas, 2002). Briefly, the number of pBocs followed by an Emc were quantified. For Figure 2.4F, each worm was assayed for at least 6 cycles.

Aldicarb sensitivity was assayed as previously described (Nguyen et al., 1995). Unless otherwise stated, Aldicarb was added to NGM plates at the final concentrations: 0.01, 0.02, 0.04, 0.09, 0.18, 0.35, 0.70, 1.4 mM. Ten to 20 young adults from each strain were placed on a plate at each Aldicarb concentration, incubated at 20°C for 8 hrs, and then scored.

Electron microscopy

Adult nematodes were prepared for transmission electron microscopy as previously described (Jorgensen et al., 1995). Specimens were fixed in 0.8% glutaraldehyde, 0.7% osmium tetroxide in 0.1 M cacodylate for 2 hrs and then washed in buffer. Next, the animals' heads and tails were removed, the tissue postfixed in 2% osmium tetroxide in 0.1 M cacodylate overnight at 4°C, then washed extensively in water. 117 specimens were then stained *en bloc* in 1% uranyl acetate, dehydrated with ethanol, passed through propylene oxide, and embedded in epoxy resin. Ribbons of ultrathin (~33 nm) sections were imaged.

Imaging

Worms were immobilized in either 10 mM muscimol or 25 mM sodium azide on 3% agarose pads. Images were acquired on a Pascal LSM5 confocal microscope (Zeiss) with a 63x 1.4NA oil objective. Dorsal and ventral cord images were taken with the cord facing toward the objective. Three Z-stacks were acquired from each worm, 16.81 µm by 96.84 µm with a 1.5 zoom factor. The total number of fluorescent puncta was quantified from maximum intensity projections using the Cell Counter ImageJ plugin. Images were blinded by assigning each a random 5-digit number generated in Excel. The data are presented as the average number of puncta per 50 µm.

Images of the RFP::RIC-7 single copy insert (Figure 2S.2B) were acquired using a Nikon spinning disc confocal with a Photometrics Cascade II EMCCD camera, generously made available by the laboratory of V. Maricq. A single focal

plane was imaged with a 300 ms exposure time. The signal is very dim, so 20 frames were averaged to enhance the signal-to-noise ratio.

Laser axotomy

L2 worms were immobilized as described above. Axons containing GFP were cut using 1) a pulsing 810 nm light from a Ti:Sapphire laser (Mira900, Coherent) assembled on a LSM510 Meta confocal microscope (Zeiss) and focused through a 63x 1.4NA objective or 2) a pulsing 355 nm laser (FTSS355-Q3, CryLaS GmbH, Germany) assembled on a Nikon D-Eclipse C1, 90i confocal microscope with a Nikon 40x 1.3NA objective. The ALA neuron has a single cell body in the head of the worm (dorsal to the posterior bulb of the pharynx) and extends two axons along the length of the worm at the right and left midline. In all experiments, either the right or left axon was cut and the same side of the worm was imaged on the following day. After the axons were cut, the laser was used to kill the cell bodies, which would otherwise regenerate new axons that obscure the degeneration analysis. Images were acquired immediately after cutting. Worms were then recovered from the agarose pad and placed on bacterial NGM plates for 24 +/- 4 hrs. Images were acquired on the Pascal confocal (Zeiss) on the following day. For the *ric-7* experiments (Figure 2.5A,B), the ALA axon was cut once in the anterior of the worm behind the head, and then the cell body was killed. Images from the following day were analyzed in ImageJ by tracing the axon segment to measure its length.

For the wild-type experiments (Figure 2.5D-F), the ALA axon was cut into

multiple pieces proceeding anterior to posterior, and then the cell body was killed. The most anterior and posterior axon pieces were not included in the analysis, since the head and tail ganglia make it impossible to determine the presence or absence of mitochondria in these segments. On average, there were four axon segments per worm, and 61% of segments contained at least one mitochondrion. For each worm, the images from both days were compared side-by-side to determine which segments were still present. Each segment was also scored for the presence or absence of mitochondria at both time points.

The GABA and acetylcholine motor neuron commissures were cut once just below the midline of the worm. The cell bodies were then killed to prevent regeneration. Four to five VD/DD or two DB commissures were cut per worm; the transgenes *oxIs12* and *oxEx81* were used, respectively. The worms were imaged again 24 hrs later and the number of commissures still present was quantified. The GFP in the GABA motor neuron experiments is soluble and on occasion would leak out of the commissures immediately following the injury. Images were acquired postaxotomy and only commissures that were still visible were included in the 24 hr analysis.

Statistics

In most cases, nonparametric tests were used; the Kruskal-Wallis for multiple comparisons and the Fisher's Exact test for two-sample data sets. The data sets did not meet the requirements for parametric tests for the following reasons. The mitochondria distribution and enteric muscle contraction data sets

did not pass the equal variance test. The degeneration data sets are not normally distributed because the *ric-7* data are consistently at zero. All statistics were performed with the GraphPad InStat software.

References

Alvarez, S., Moldovan, M., and Krarup, C. (2008). Acute energy restriction triggers Wallerian degeneration in mouse. Exp. Neurol. *212*, 166–178.

Avery, M.A., Rooney, T.M., Pandya, J.D., Wishart, T.M., Gillingwater, T.H., Geddes, J.W., Sullivan, P.G., and Freeman, M.R. (2012). WldS prevents axon degeneration through increased mitochondrial flux and enhanced mitochondrial Ca2+ buffering. Curr. Biol. 1–5.

Barrientos, S.A., Martinez, N.W., Yoo, S., Jara, J.S., Zamorano, S., Hetz, C., Twiss, J.L., Alvarez, J., and Court, F.A. (2011). Axonal degeneration is mediated by the mitochondrial permeability transition pore. J. Neurosci. *31*, 966–978.

Calupca, M.A.M., Hendricks, G.M.G., Hardwick, J.C.J., and Parsons, R.L.R. (1999). Role of mitochondrial dysfunction in the Ca2+-induced decline of transmitter release at K+-depolarized motor neuron terminals. J. Neurophysiol. *81*, 498–506.

Chang, D.T.W., Rintoul, G.L., Pandipati, S., and Reynolds, I.J. (2006). Mutant huntingtin aggregates impair mitochondrial movement and trafficking in cortical neurons. Neurobiol. Dis. *22*, 388–400.

Clark, S.G., and Chiu, C. (2003). C. elegans ZAG-1, a Zn-finger-homeodomain protein, regulates axonal development and neuronal differentiation. Dev. Camb. Engl. *130*, 3781–3794.

Deken, S.L. (2005). Redundant localization mechanisms of RIM and ELKS in Caenorhabditis elegans. J. Neurosci. *25*, 5975–5983.

Fang, Y., Soares, L., Teng, X., Geary, M., and Bonini, N.M. (2012). A novel drosophila model of nerve injury reveals an essential role of Nmnat in maintaining axonal integrity. Curr. Biol. 1–6.

Frøkjær-Jensen, C., Davis, M.W., Hopkins, C.E., Newman, B.J., Thummel, J.M., Olesen, S.-P., Grunnet, M., and Jorgensen, E.M. (2008). Single-copy insertion of transgenes in Caenorhabditis elegans. Nat. Genet. *40*, 1375–1383.

Fünfschilling, U., Supplie, L.M., Mahad, D., Boretius, S., Saab, A.S., Edgar, J., Brinkmann, B.G., Kassmann, C.M., Tzvetanova, I.D., Möbius, W., et al. (2013).

Glycolytic oligodendrocytes maintain myelin and long-term axonal integrity. Nature *485*, 517–521.

Hall, D.H., and Hedgecock, E.M. (1991). Kinesin-related gene unc-104 is required for axonal transport of synaptic vesicles in C. elegans. Cell *65*, 837–847.

Hao, Y., Hu, Z., Sieburth, D., and Kaplan, J.M. (2012). RIC-7 promotes neuropeptide secretion. PLoS Genet. *8*, e1002464.

Iijima-Ando, K., Sekiya, M., Maruko-Otake, A., Ohtake, Y., Suzuki, E., Lu, B., and Iijima, K.M. (2012). Loss of axonal mitochondria promotes tau-mediated neurodegeneration and Alzheimer's disease–related tau phosphorylation via PAR-1. PLoS Genet. *8*, e1002918.

Ishii, N., Fujii, M., Hartman, P.S., Tsuda, M., Yasuda, K., Senoo-Matsuda, N., Yanase, S., Ayusawa, D., and Suzuki, K. (1998). A mutation in succinate dehydrogenase cytochrome b causes oxidative stress and ageing in nematodes. Nature *394*, 694–697.

Jorgensen, E.M., Hartwieg, E., Schuske, K., Nonet, M.L., Jin, Y., and Horvitz, H.R. (1995). Defective recycling of synaptic vesicles in synaptotagmin mutants of Caenorhabditis elegans. Nature *378*, 196–199.

Keller, L.C., Cheng, L., Locke, C.J., Müller, M., Fetter, R.D., and Davis, G.W. (2011). Glial-derived prodegenerative signaling in the Drosophila neuromuscular system. Neuron *72*, 760–775.

Kitay, B.M., Mccormack, R., Wang, Y., Tsoulfas, P., and Zhai, R.G. (2013). Mislocalization of neuronal mitochondria reveals regulation of Wallerian degeneration and NMNAT/WLDS-mediated axon protection independent of axonal mitochondria. Hum. Mol. Genet. 1–14.

Knobel, K.M., Davis, W.S., Jorgensen, E.M., and Bastiani, M.J. (2001). UNC-119 suppresses axon branching in C. elegans. Development *128*, 4079–4092.

Koeberle, P.D., and Ball, A.K. (1999). Nitric oxide synthase inhibition delays axonal degeneration and promotes the survival of axotomized retinal ganglion cells. Exp. Neurol. *158*, 366–381.

Liu, D.W., and Thomas, J.H. (1994). Regulation of a periodic motor program in C. elegans. J. Neurosci. Off. J. Soc. Neurosci. *14*, 1953–1962.

Lucius, R., and Sievers, J. (1996). Postnatal retinal ganglion cells in vitro: protection against reactive oxygen species (ROS)-induced axonal degeneration by cocultured astrocytes. Brain Res. *743*, 56–62.

McIntire, S.L., Jorgensen, E., Kaplan, J., and Horvitz, H.R. (1993a). The GABAergic nervous system of Caenorhabditis elegans. Nature *364*, 337–341.

McIntire, S.L., Jorgensen, E., and Horvitz, H.R. (1993b). Genes required for GABA function in Caenorhabditis elegans. Nature *364*, 334–337.

Misko, A.L., Sasaki, Y., Tuck, E., Milbrandt, J., and Baloh, R.H. (2012). Mitofusin2 mutations disrupt axonal mitochondrial positioning and promote axon degeneration. J. Neurosci. Off. J. Soc. Neurosci. *32*, 4145–4155.

Nguyen, M., Alfonso, A., Johnson, C.D., and Rand, J.B. (1995). Caenorhabditis elegans mutants resistant to inhibitors of acetylcholinesterase. Genetics *140*, 527–535.

Otsuga, D., Keegan, B.R., Brisch, E., Thatcher, J.W., Hermann, G.J., Bleazard, W., and Shaw, J.M. (1998). The Dynamin-related GTPase, Dnm1p, controls mitochondrial morphology in yeast. J. Cell Biol. *143*, 333–349.

Patten, D.A., Germain, M., Kelly, M.A., and Slack, R.S. (2010). Reactive oxygen species: stuck in the middle of neurodegeneration. J. Alzheimers Dis. JAD *20 Suppl 2*, S357–67.

Pinan-Lucarre, B., Gabel, C.V., Reina, C.P., Hulme, S.E., Shevkoplyas, S.S., Slone, R.D., Xue, J., Qiao, Y., Weisberg, S., Roodhouse, K., et al. (2012). The core apoptotic executioner proteins CED-3 and CED-4 promote initiation of neuronal regeneration in Caenorhabditis elegans. PLoS Biol *10*, e1001331.

Schon, E.A., and Przedborski, S. (2011). Mitochondria: the next (neurode) generation. Neuron *70*, 1033–1053.

Shigenaga, M.K., Hagen, T.M., and Ames, B.N. (1994). Oxidative damage and mitochondrial decay in aging. Proc. Natl. Acad. Sci. U. S. A. *91*, 10771–10778.

Smirnova, E., Shurland, D.-L., Ryazantsev, S.N., and Bliek, A.M. van der (1998). A human Dynamin-related protein controls the distribution of mitochondria. J. Cell Biol. *143*, 351–358.

Tekk k, S.B., Brown, A.M., and Ransom, B.R. (2003). Axon function persists during anoxia in mammalian white matter. J. Cereb. Blood Flow Metab. 1340–1347.

Thomas, J.H. (2002). Genetic analysis of defecation in Caenorhabditis elegans. Genetics *124*, 855–872.

Tsang, W.Y. (2001). Mitochondrial respiratory chain deficiency in Caenorhabditis elegans results in developmental arrest and increased life span. J. Biol. Chem. *276*, 32240–32246.

Watanabe, S., Punge, A., Hollopeter, G., Willig, K.I., Hobson, R.J., Davis, M.W., Hell, S.W., and Jorgensen, E.M. (2011). Protein localization in electron micrographs using fluorescence nanoscopy. Nat. Methods *8*, 80–84.

Winkler, B.S., Arnold, M.J., Brassell, M.A., and Puro, D.G. (2000). Energy metabolism in human retinal Müller cells. Invest. Ophthalmol. Vis. Sci. *41*, 3183–3190.

Wu, Ghosh-Roy, Yanik, Zhang, Jin, Y., and Chisholm (2007). Caenorhabditis elegans neuronal regeneration is influenced by life stage, ephrin signaling, and synaptic branching. Proc Natl Acad Sci U A.

CHAPTER 3

ENGULFMENT OF AXONAL DEBRIS BY EPITHELIAL CELLS REQUIRES CED-1 AND CED-6 BUT NOT THE RAC1 PATHWAY

Abstract

Axon degeneration occurs in response to disease and injury. After an axon is detached from the cell body, it fragments into small pieces, which are then engulfed by other cells. We are studying axon degeneration using a genetic neurodegeneration model, as well as laser axotomy of wild-type axons. In beta-spectrin/*unc-70* mutants, axons break spontaneously and the portion of the axon distal to the break degenerates. We have examined the role of apoptosis genes in the break down and removal of degenerating axons in *C. elegans*. Two parallel engulfment pathways act to remove cell corpses after apoptosis: *ced-1, -6, -7* and *ced-2, -5, -12*. Both *ced-1* and *ced-6* are required for the engulfment of axonal debris in *C. elegans*. However, *ced-7* was only involved in removing debris during neurodegeneration in beta-spectrin mutants. None of the members of the *ced-2, -5, -12* pathway nor *ced-10* are required for axonal debris removal. Thus, the engulfment of axonal debris in *C. elegans* requires only one of the two pathways that function in apoptotic cell corpse removal.

Introduction

Axon degeneration occurs in neurodegenerative diseases, in response to injury, and during developmental pruning (Luo and O'Leary, 2005). While generally considered deleterious, degeneration can actually play beneficial roles in neuronal health. Developmental pruning is essential for an optimally functioning nervous system (Luo and O'Leary, 2005), and the removal of damaged axons is advantageous for recovery (Hosmane et al., 2012; Tanaka et al., 2009).

In recent years, multiple studies have identified roles for the apoptosis pathway in breaking down and clearing axons. The apoptosis pathway was originally identified in *C. elegans* for its role in programmed cell death and subsequent cell corpse removal during embryogenesis (Ellis and Horvitz, 1986; Hedgecock et al., 1983). The apoptosis pathway consists of multiple phases, including the killing phase and the engulfment phase. During the killing phase, CED-4 is released from CED-9 and activates the caspase CED-3, which then initiates the process of destroying the cell (Conradt, 2009; Conradt and Horvitz, 1998; Ellis and Horvitz, 1986). Once the cell has died, the corpse is cleared away by other cells through engulfment. There are two parallel pathways involved in cell corpse engulfment; the CED-1, -6, -7 pathway and the CED-2, -5, -12 pathway (Mangahas and Zhou, 2005; Reddien and Horvitz, 2004).

The CED-1, -6, -7 pathway is involved in cell corpse recognition. The ABC transporter CED-7 is required in both the corpse and the engulfing cell and is responsible for displaying the phosphatidylserine (PS) 'eat me' signal on the surface of the cell corpse (Hamon et al., 2000; Mapes et al., 2012; Wu and Horvitz, 1998a). CED-1 is a phagocytic receptor located on the surface of the engulfing cell. CED-1 recognizes

the ‘eat me’ signal and recruits the engulfing cell to the surface of the cell corpse (Zhou et al., 2001a). CED-6/GULP is a PTB domain protein that interacts with the intracellular portion of CED-1 and is believed to transduce the phagocytosis signal from the cell membrane to cytoplasmic machinery (Liu and Hengartner, 1998; Su et al., 2002).

The CED-2, -5, -12 engulfment pathway is involved in regulating the cytoskeleton within the engulfing cell. CED-2/CrkII, CED-5/DOCK180, and CED-12/ELMO form a complex that serves as a guanine exchange factor (GEF) to activate the Rac GTPase CED-10 (Brugnera et al., 2002; Gumienny et al., 2001; Reddien and Horvitz, 2000; Wu et al., 2001; Zhou et al., 2001b). Rac is then responsible for rearranging the cytoskeleton to engulf the corpse (Mangahas and Zhou, 2005; Zhou et al., 2001b).

Components of both the killing and engulfment pathways have been implicated in the breakdown of axons and dendrites. *Drosophila* studies on axon pruning and injury-induced dendritic degeneration did not find a role for caspases in neurite destruction (Awasaki et al., 2006; Tao and Rolls, 2011). However, multiple other studies have suggested that caspases and their up- and down-stream regulators are involved in the pruning of dendrites. Dronc is an apoptotic Nedd-2-like initiator caspase that interacts with the fly homolog of CED-4, Dark (Dorstyn et al., 1999; Quinn et al., 2000). Dronc has been shown to mediate dendritic pruning of the ddaC and Cd4a sensory neurons (Kuo et al., 2006; Schoenmann et al., 2010; Tao and Rolls, 2011; Williams et al., 2006). Effector caspases of Dronc have also been implicated in dendritic pruning via experiments with effector caspase inhibitors and cleavage products (Williams et al., 2006).

Caspases and other members of the killing pathway are also active during axon

degeneration. One Dronc effector caspase candidate is Dcp1/caspase-6. Caspase-6 has been shown to mediate axon degeneration in mammalian cells along with Bax (Nikolaev et al., 2009; Schoenmann et al., 2010), and more recently, Dcp1 has been shown to promote the degeneration of neuromuscular junctions in fly *ankyrin2* mutants, along with Dark/CED-4 and the Bcl2-homolog Debcl (Keller et al., 2011).

Studies in *Drosophila* have additionally shown that the apoptosis engulfment pathways are involved in the removal of degenerating axons. CED-1/Draper and CED-6 are required for axon engulfment following both axotomy and developmental pruning (Awasaki et al., 2006; Macdonald et al., 2006; Williams et al., 2006). More recently, the CED-2, -5, -12 pathway has also been shown to mediate the engulfment of degenerating axons following axotomy (Ziegenfuss et al., 2012). Ziegenfuss *et al.* demonstrate that CED-1/Draper is essential for the recruitment of glia to injured neurons and that the CED-2, -5, -12 pathway is required for their internalization.

Here we examine the role of the engulfment pathways in both genetically- and injury-induced axon degeneration in *C. elegans*. Mutations in spectrin result in neurodegeneration in animal models and spastic paraplegia in humans (Ikeda et al., 2006; Massaro et al., 2009; Parkinson et al., 2001). In *C. elegans* beta-spectrin/*unc-70* mutants, axons break due to movement (Hammarlund et al., 2007). The distal, detached portion of the axon undergoes degeneration while the proximal axon will generate a growth cone and extend a new axon. The new axons are eventually broken and the cycle repeats itself, resulting in animals that are continually undergoing axon degeneration. We examined the role of caspases and the engulfment pathways in axon degeneration using beta-spectrin mutants and laser axotomy of wild-type animals.

Results

The *ced-1, -6, -7* pathway is required for engulfment of axonal debris in *unc-70*

In beta-spectrin null mutants, *unc-70*(*s1502*), axons spontaneously break and are continually undergoing axon degeneration and regeneration (Hammarlund et al., 2007). This is an ideal model in which to study the process of axon degeneration; degeneration can be observed at any time point without the need for invasive experimental procedures. Animals are expressing soluble GFP in the GABA neurons under the *unc-47*/vGAT promoter, *oxIs12*[P*unc-47*::GFP]. The degenerating GABA motor neuron axons in beta-spectrin mutants undergo morphological changes similar to those described by Augustus Waller, known as Wallerian degeneration. After a break occurs, the axon first blebs, turning into a string of beads, the beads eventually become isolated particles of debris that are then cleared away by neighboring cells (Hammarlund et al., 2007).

Beta-spectrin animals examined at the fourth larval stage (L4) display large detached segments of axons (average of 2.3 +/- 0.3, N=46; 0 in wild-type worms) as well as considerable amounts of axon debris particles (on average 16.4 debris particles per worm +/- 1.4, N=56, compared to 2.3 +/- 0.5, N=10 in the wild type). Mutations in genes required for clearing away dead cells are predicted to result in an increase in axonal debris in beta-spectrin mutants. Mutations for engulfment pathway members *ced-1(e1735)*, *ced-6(n1813)*, and *ced-7(n1996)* were crossed into the beta-spectrin mutants. All three of these alleles displayed a significant increase in the amount of axonal debris (Figure 3.1., $p < 0.0001$ Kruskal Wallis test). Both *ced-1(e1735)* and *ced-*

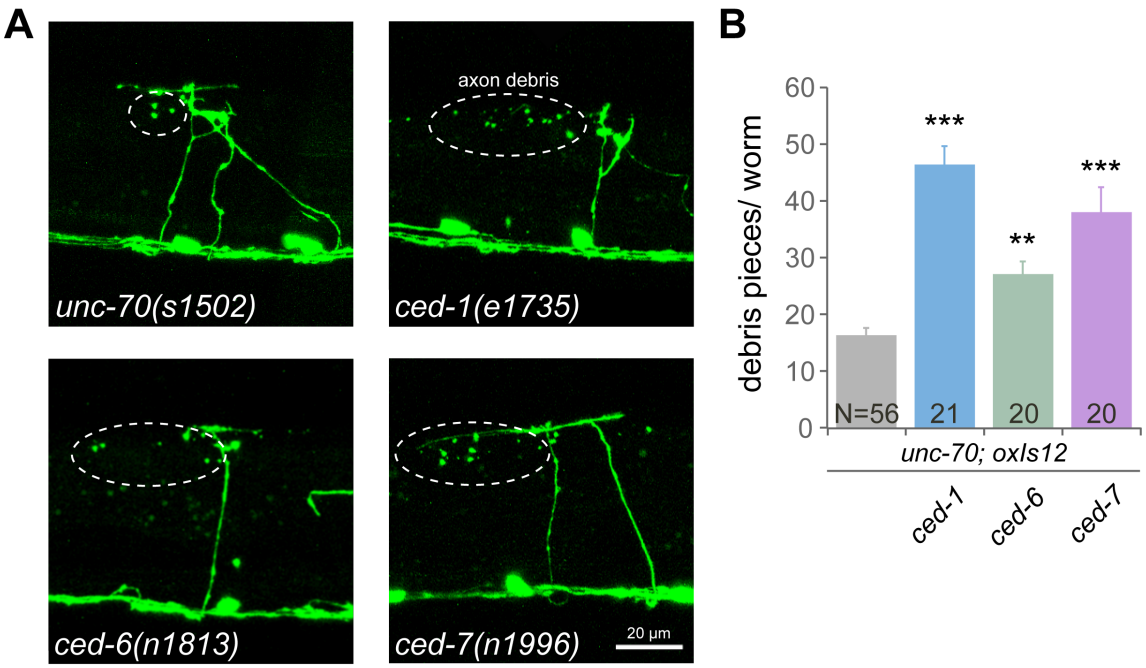

Figure 3.1. *ced-1*, *ced-6*, and *ced-7* are required for the clearance of axonal debris in beta-spectrin mutants. (A) The GABA motor neuron axons in beta-spectrin/*unc-70* mutants break during movement and are undergoing a continuous cycle of regeneration and degeneration. Broken axons undergo fragmentation and clearance. In L4 beta-spectrin null mutants, pieces of axonal debris can be seen (dashed circle). Axonal debris is accumulated in worms that are also carrying mutations for *ced-1*, *ced-6*, or *ced-7*. All worms are *unc-70(s1502)* and expressing soluble GFP in the GABA motor neurons under the *unc-47* promoter (*oxIs12*). (B) The average number of debris pieces per worm + SEM. N= total number of worms. $p < 0.0001$ Kruskal-Wallis test with Dunn's multiple comparisons, *** $p < 0.001$, **$p < 0.01$ compared to *unc-70* alone (gray bar).

7(n1996) are null alleles. *ced-6(n1813)* is a loss-of-function allele and had the smallest increase in axonal debris of the three alleles.

The *ced-2, -5, -12* pathway is not required for engulfment of axonal debris in beta-spectrin mutants

Engulfment of cell corpses is carried out by two parallel pathways. To determine whether the second engulfment pathway is also involved in clearing axonal debris, we crossed null mutations for *ced-2(e1752)*, *ced-5(n1812)*, and *ced-12(k149)* into beta-spectrin mutants. Unlike the *ced-1* pathway, these mutations did not result in an increase in axonal debris. Alleles for all three mutations contained an amount of axonal debris similar to that of *unc-70* alone (average debris pieces per worm are 20.5, 20.1, and 15.4, respectively. n.s., p = 0.38 One-way ANOVA).

It is possible that the *ced-2* engulfment pathway is contributing a minor role to the engulfment of axon debris that cannot be easily revealed in beta-spectrin mutants. To ensure that this pathway is not contributing to engulfment, we tested whether there is an additive effect for removing *ced-5* in a *ced-1* background. In cell corpse removal, mutations in the *ced-2, -5, -12* engulfment pathway can enhance the impairment seen in *ced-1* mutants, as is typical for mutations in parallel pathways. However, *ced-5* did not enhance the amount of axon debris observed in *ced-1*; *unc-70* animals (49.3 vs. 46.4 average debris pieces per worm, respectively. Figure 3.2 C,D). This further demonstrates that the *ced-2*, *-5*, *-12* pathway is not functioning in the clearance of degenerating axons in *C. elegans*.

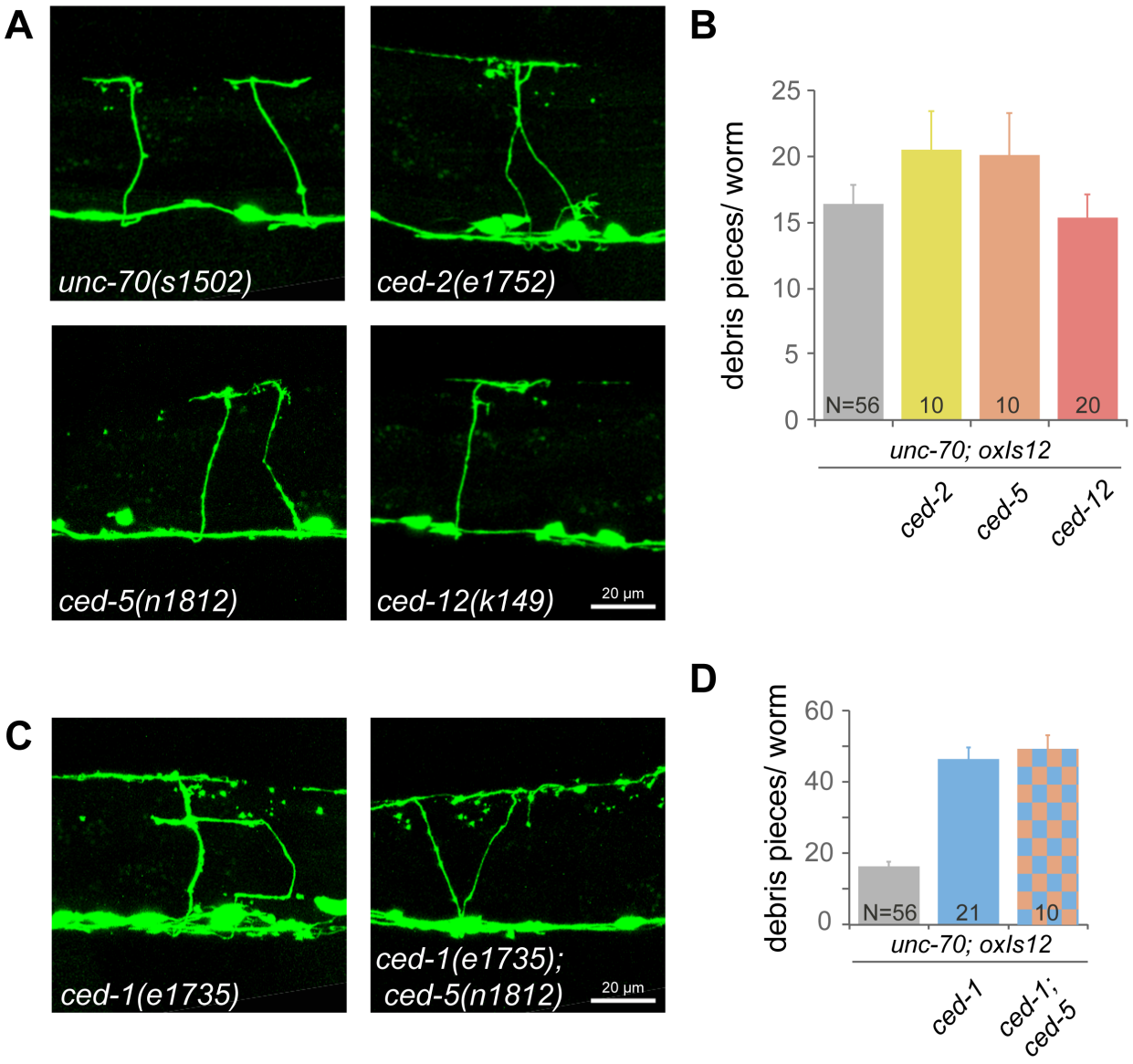

Figure 3.2. The *ced-2*, *-5*, *-12* engulfment pathway is not required for the clearance of degenerating axons in *C. elegans*. (A) Axonal debris pieces are not accumulated in beta-spectrin/*unc-70* mutants that are carrying mutations for *ced-2*, *ced-5*, or *ced-12*. (B) Average number of debris pieces per worm + SEM. n.s., p = 0.38 One-way ANOVA. N= total number of worms. The beta-spectrin data (gray bar) are the same as in Figure 3.1B. (C) *ced-5* does not have an additive effect on *ced-1* for the clearance of degenerating axons. (D) The average number of debris pieces per worm is unchanged between *ced-1* and *ced-1*; *ced-5* double mutants. The beta-spectrin data (gray bar) and the *ced-1* data (blue bar) are the same as in Figure 3.1B. N= total number of worms. All worms are in a *unc-70(s1502)*; *oxIs12* background.

The core apoptosis pathway is modestly involved

in axonal degeneration

We questioned whether the killing phase of the cell death pathway is involved in fragmenting broken axons. To investigate this possibility, null beta-spectrin mutants were crossed into strong-loss-of-function mutations for *ced-3(n717)* and *ced-4(n1162),* and a gain of function mutation in *ced-9(n1950dm)*, which has an antiapoptotic function. To assay fragmentation in beta-spectrin mutants, we measured the portion of the dorsal side of the worm that is covered with continuous sections of axons. In a wild-type worm, the coverage is close to 100%, whereas only around 40% of the dorsal nerve cord is present in a beta-spectrin mutant. If removing the apoptotic caspase pathway decreases degeneration, there should be an increase in the dorsal cord coverage as broken axons should perdure and accumulate. However, mutations in the core apoptotic pathway did not alter dorsal cord coverage, suggesting degeneration was unaffected (Figure 3S.1A,B). It is possible that engulfment may be able to override the fragmentation process. In other words, axon pieces may be engulfed and cleared away even in the absence of efficient fragmentation. To impair engulfment, *ced-1(e1735)* was crossed into each strain. In *ced-1*, apoptosis double mutants, we observed a significant increase in the amount of dorsal nerve cord coverage compared to *ced-1* alone (Figure 3.3, $p= 0.0016$ one-way ANOVA). *ced-1*; *ced-3* double mutants had the greatest amount of axon preservation (57% dorsal cord coverage compared to 30% for *ced-1*, $p< 0.001$ Tukey-Kramer Multiple comparisons), whereas *ced-1*; *ced-4* and *ced-1*; *ced-9* double mutants only had a modest increase in dorsal nerve cord coverage (Figure 3.3B). This suggests that the caspase *ced-3* is involved in axon fragmentation in beta-spectrin

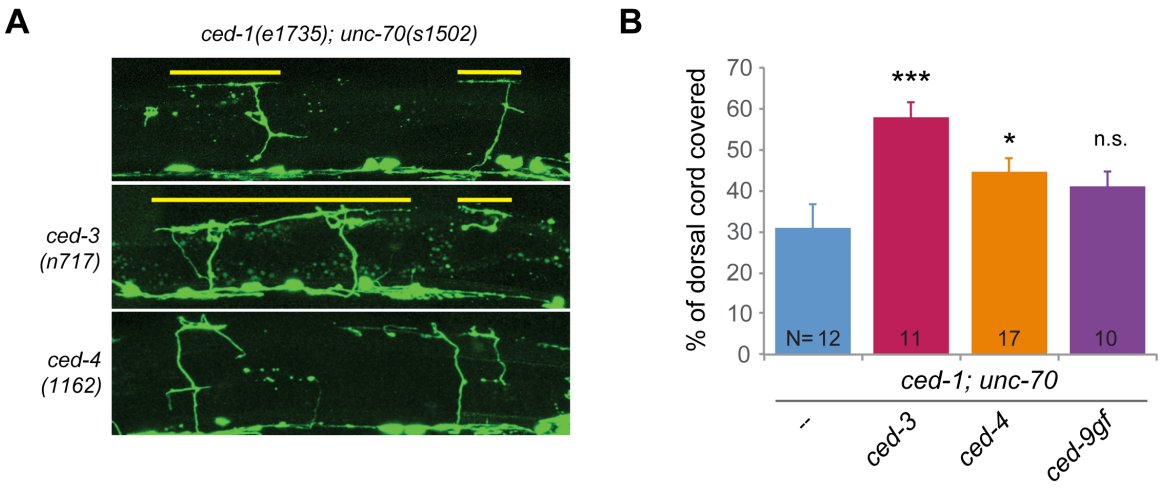

Figure 3.3. The caspase *ced-3* is required for axon degeneration in beta-spectrin mutants. (A) In wild-type animals, nearly 100% of the dorsal cord contains GABA motor neuron axons. In beta-spectrin/*unc-70* mutants, only 42% of the dorsal cord is covered in axons and 30% is covered in *ced-1(e1735); unc-70(s1502)* mutants. Crossing in mutants for the killing phase of the apoptosis pathway augments the dorsal nerve cord coverage, suggesting that there is greater axon preservation. The yellow lines illustrate the sections of the dorsal cord that are covered with axons. (B) For each worm, the distances of axon coverage were measured, summed, and divided by the length of the worm. The average % of dorsal cord + SEM are shown. *ced-4(n1162)* and the gain-of-function (gf) mutation *ced-9(n1950dm)* modestly increased dorsal cord coverage. The loss of function mutation in the caspase *ced-3(n717)* significantly increased the dorsal cord coverage in *ced-1; unc-70* worms (p= 0.0002 One-way ANOVA with Dunnett's multiple comparisons to *ced-1*; *** p<0.001, *p<0.05). N= total number of worms.

mutants.

There are several points of caution to this result. Firstly, as mentioned above, the caspase pathway does not alter the dorsal cord coverage in the absence of the *ced-1(e1735)* mutation (Figure 3S.1A,B). However, cooperativity between the engulfment and the cell killing pathways has been repeatedly demonstrated (Galvin et al., 2008; Hoeppner et al., 2001; Li and Baker, 2007; Neher et al., 2011; Neukomm et al., 2011; Reddien et al., 2001). Thus, a functioning *ced-1* pathway could be promoting fragmentation even in the absence of *ced-3*. Secondly, if the caspase pathway is

required for fragmentation, then the amount of large axon segments should increase while the amount of debris should diminish. There is no change in the number of large axon segments (Figure 3S.1C) and only *ced-9(gf)* has significantly less debris, although *ced-3* also shows a decrease (Figure 3S.1D). Lastly, the increase in the dorsal nerve cord coverage could be due to an enhancement in regeneration, which might explain the significantly greater number of commissures in the *ced-1*; *ced-3* double mutants (Figure 3S.1E). This, however, is unlikely to be the case as the Driscoll lab has recently shown that *ced-3* and *ced-4* are required for regeneration (Pinan-Lucarre et al., 2012). An impairment in regeneration could explain why there is not a stronger result for this pathway during degeneration. The degeneration assay is dependent upon robust regeneration to continually provide degenerating axons. If these mutants have decreased regeneration, it may be challenging to detect an accumulation of intact but broken axons.

In wild-type worms, ced-1 and ced-6 are required

for engulfment of axonal debris

To determine whether the engulfment pathways are involved in axon degeneration independent of the beta-spectrin mutation, we performed laser axotomy on wild-type worms and *ced* mutants. Axon degeneration is limited in wild-type *C. elegans* (Chapter 2; Pinan-Lucarre et al., 2012; Wu et al., 2007). Axons cut in larval stage 4 (L4) worms do not degenerate and can persist for at least 8 days (data not shown). However, if axons are cut in young worms, larval stage 2 (L2), degeneration is observed. Axon regeneration in *C. elegans* is also age-dependent (Hammarlund et al.,

2009; Nix et al., 2011; Wu et al., 2007). We performed axotomy on the ALA neuron in L2 worms expressing membrane-bound GFP under the *acr-5* promoter, *oxEx81*[P*acr-5*::GAP43$_{40aa}$::GFP] (Figure 3.4). After axotomy, the worms are recovered to standard worm maintenance conditions for 24 hrs, reimaged, and assayed for degeneration. The ALA axon originates in the head and projects to the tail of the worm along the lateral midline (Figure 3.4A). When this long axon is cut into multiple pieces, nearly half of the pieces (45% +/- 4.3%, N=26) will degenerate in a wild-type worm (Figure 3.4B, C).

In wild-type worms, ALA axon degeneration is complete within 24 hrs and axonal debris is rarely present. By contrast, axonal debris is accumulated in both *ced-1* and *ced-6* mutants (Figure 3.5, $p < 0.0001$ Kruskal-Wallis Test). Two loss of function alleles were tested for *ced-6*. While *ced-1(e1735)* has 23-fold greater debris than the wild type, *ced-6(n2095)* and *ced-6(n1813)* have 12-fold and nearly 5-fold greater amounts of debris, respectively. The data are expressed as the average amount of debris per 100 µm in order to control for any variability in worm size. Because only some of the axon pieces degenerate, the axon debris tends to be clustered (dashed circles, Figure 3.5A) rather than evenly distributed across the worm. The number of large axon pieces was not increased in any of the mutants (Figure 3S.2A). Surprisingly, we did not observe an involvement for *ced-7* in axon debris clearance after injury of healthy axons. Neither of the null mutations *ced-7(1996)* or *ced-7(n1892)* lead to an accumulation of axonal debris following axotomy of the ALA axon (Figure 3.5B,C).

We additionally tested *ced-1* mutants for engulfment after axotomy of the GABA motor neurons (Figure 3S.2B,C). After 48 hrs, *ced-1(e1735)* mutants had significantly

Figure 3.4. Axon degeneration following laser axotomy of the ALA axon. (A) Schematic of the laser axotomy procedure for ALA axons. The ALA neuron is in the dorsal head of the worm and extends an axon along the lateral midline of the worm. The axon is first severed at the anterior of the worm. Second, multiple cuts are made along the axon moving anterior to posterior. Third, the ALA cell body is killed with the laser to prevent axon regeneration from occurring and obscuring the degenerating axons. (B) Images of an L2 worm immediately preceding and following laser axotomy. Worms are expressing P*acr-5*::GAP4340aa::GFP (*oxEx81*), which is a membrane-bound GFP expressing in the ALA neuron, head and tail ganglia neurons, and the DB motor neurons. The ALA axon was severed into 6 pieces (excluding the most anterior and posterior segments which are largely concealed by the head and tail ganglia). The location of the cut sites are marked with arrows and the axon segments are numbered. (C) After a 24 hr recovery period, the worm was imaged again. There are three axon segments remaining (arrowheads) and the rest of the axon has degenerated. On average 45% (+/- 4.3%, N= 26 worms) of the axons segments degenerated. In a wild-type worm, the degenerating axons are completely cleared away within 24 hrs and debris remnants of axons are rarely seen. (D) The ALA axon runs down the midsection of an uninjured L4 worm. The dotted yellow line marks where the dorsal nerve cord is out of the focal plane. (E) A magnified view of the region outlined by a red box in panel C. Two of the axon segments that did not degenerate are marked with arrowheads. The asterisk indicates autofluorescence from the gut. (F) An expanded view of the region within the red box in panel D. The uninjured ALA axon can be seen at the midpoint between the dorsal and ventral nerve cords.

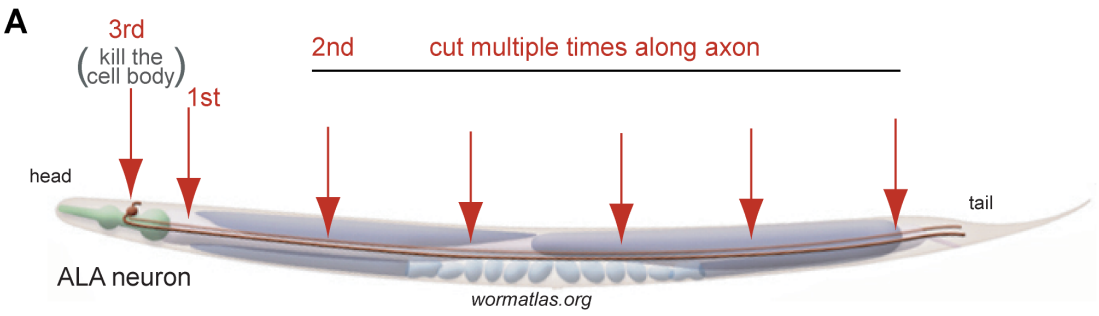
A
3rd
(kill the cell body)
1st
2nd
cut multiple times along axon
head
tail
ALA neuron
wormatlas.org

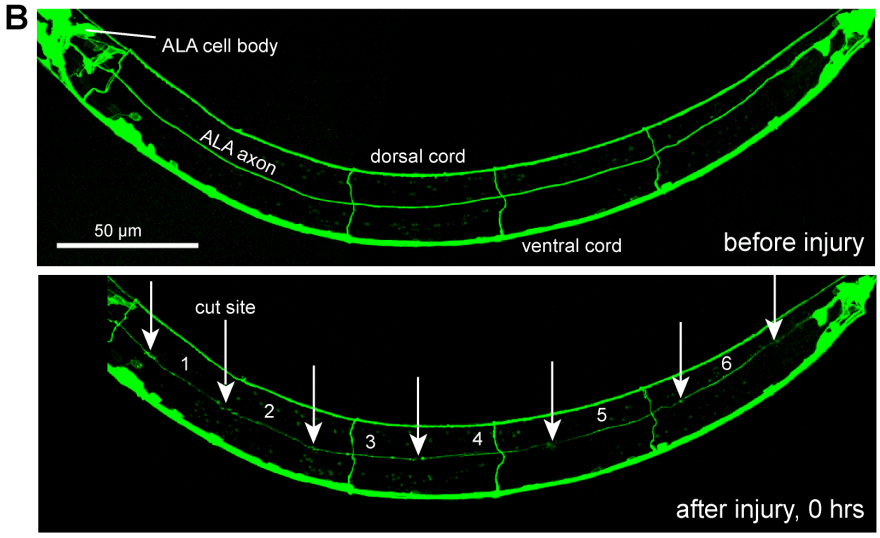
B
ALA cell body
ALA axon
dorsal cord
50 µm
ventral cord
before injury
cut site
1
2
3
4
5
6
after injury, 0 hrs

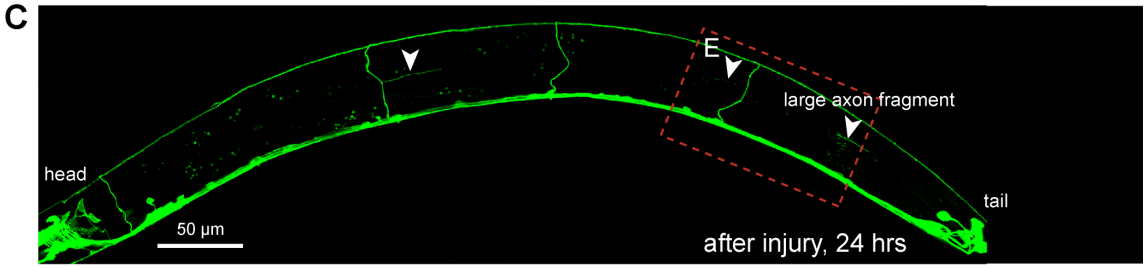
C
E
large axon fragment
head
tail
50 µm
after injury, 24 hrs

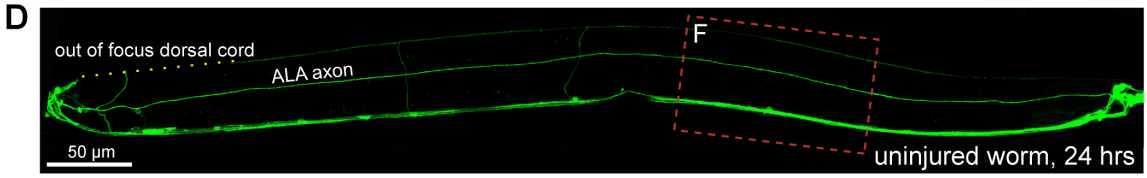
D
out of focus dorsal cord
ALA axon
F
50 µm
uninjured worm, 24 hrs

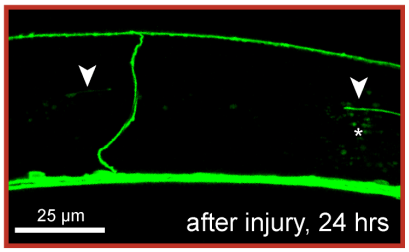
E
25 µm
after injury, 24 hrs


F
dorsal cord
intact ALA axon
ventral cord
uninjured worm, 24 hrs

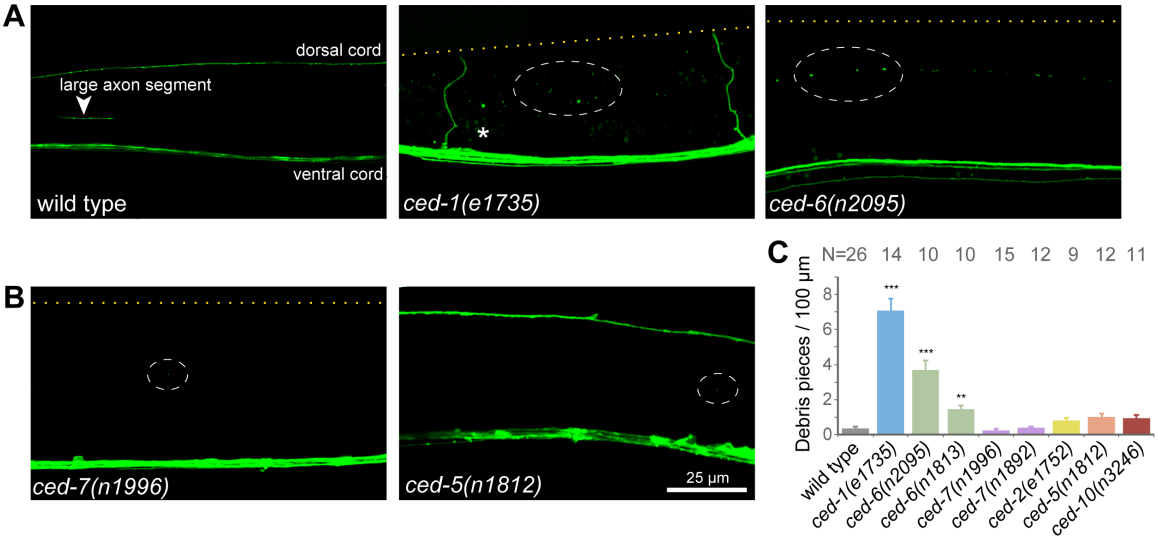

Figure 3.5. *ced-1* and *ced-6* are required for engulfing axonal debris after injury. (A) In wild-type worms, axonal debris is rarely observed 24 hrs after axotomy of the ALA axon. However, in *ced-1* and *ced-6* mutants, axonal debris remains uncleared after one day. The dashed white circles highlight clusters of perduring axonal debris. The dotted yellow line marks where the out of focus dorsal nerve cord would be. The asterisk indicates autofluorescence from the gut, which is dimmer and more uniform in size compared to the axonal debris. (B) *ced-7* and *ced-5* are not required for the engulfment of degenerating ALA axons after axotomy. Pieces of axonal debris are only rarely observed (dashed circles). (C) *ced-1* and two alleles of *ced-6* have significantly greater amounts of axonal debris compared to the wild type (average # of debris pieces per 100 µm + SEM, p< 0.0001 Kruskal-Wallis Test, *** p<0.001, **p<0.01 Dunn's multiple comparisons test compared to the wild type). Contrary to the beta-spectrin mutant results, *ced-7* is not required for clearing away severed axons in a wild-type background. *ced-2*, *ced-5*, and *ced-10* are not involved in clearing axonal debris in *C. elegans*. N= total number of worms

greater amounts of debris from severed commissures compared to the wild type (3.5 +/- 0.9 vs. 0.4 +/- 0.3, p= 0.0036 two-tailed Mann-Whitney test). Thus, *ced-1* and *ced-6* are required for the engulfment of axonal debris in response to both a neurodegenerative disorder and an injury.

Similar to the beta-spectrin data, there was no increase in axonal debris in *ced-2* or *ced-5* mutants following axotomy of the ALA axon. This further demonstrates that

only one of the engulfment pathways is involved in the removal of axonal debris in *C. elegans*. Classically, the Rac GTPase *ced-10* is thought to be downstream of the *ced-2*, *-5*, *-12* pathway. However, recent work has shown that the two engulfment pathways can converge onto *ced-10* (Kinchen et al., 2005; Ziegenfuss et al., 2012). If this is true, we would expect to see an involvement of *ced-10* in axon debris removal in *C. elegans* even though the *ced-2*, *-5*, *-12* pathway is not active. Null alleles of *ced-10* are lethal so we performed laser axotomy of ALA in the strong hypomorphic allele *ced-10(n3246)*. The *n3246* allele has a mutated GTP binding site and has been shown to have significant impairments in cell corpse engulfment in developing embryos (Kinchen et al., 2005; Reddien and Horvitz, 2000). However, this mutation did not exhibit any impairments in axonal debris clearance, indicating that in *C. elegans* axon degeneration, *ced-10* is not acting downstream of the *ced-1* engulfment pathway (Figure 3.5C).

Hypodermal cells engulf axon debris in *C. elegans*

To determine which cell type is engulfing axon debris in *C. elegans,* we conducted cell-specific rescue experiments for *ced-1*. In vertebrates, the engulfing cell is typically macrophages or glial cells (Sokolowski and Mandell, 2011). However, the *C. elegans* glial sheath cells are only found in the head and tail of the worm. Instead, axons are in close proximity to the hypodermis and neighboring neurons. *ced-1* cDNA was expressed in neurons (P*rab-3*), the hypodermis (P*dpy-7*), or all cells (P*eft-3*) and inserted into the genome as a single copy using the mosSCI technique (Frøkjær-Jensen et al., 2008). Each of the transgenes was crossed into the *ced-1(e1735)*; *oxEx81* strain.

Rescue of developmental cell corpse engulfment was assessed to confirm that the *ced-1* construct was functional. *C. elegans* embryos have an accumulation of apoptotic cell corpses in *ced-1* mutants, which can be rescued by expressing *ced-1* under its endogenous promoter (Zhou et al., 2001a). Both the ubiquitous- and hypodermis-expressing constructs rescued the perdurance of apoptotic cell corpses in *ced-1* null embryos, confirming the *ced-1* construct is functional (Figure 3S.3A).

The ALA axon was cut into multiple sections, as described above. After 24 hrs, the worms were reimaged and the amount of axonal debris was quantified. Both the *ced-1(e1735); oxEx81* parent strain and the neuronal rescue strain had perduring axonal debris (4.1 +/- 0.5 debris pieces/100 μm and 3.6 +/- 0.5, respectively), whereas the hypodermis and ubiquitous *ced-1* expressing strains were rescued for the engulfment of axonal debris (Figure 3.6. $p < 0.0001$ Kruskal-Wallis test). The hypodermal rescue of *ced-1* reduced the amount of axonal debris by 85% (0.6 +/- 0.2), indicating that the hypodermis is responsible for engulfing the vast majority of debris following neuronal injury. The ubiquitous rescue of *ced-1* dropped the amount of debris by an additional 12% (0.13 +/- 0.04), suggesting that some other cell types may contribute to the engulfment of injured axons as well.

Discussion

There are several main conclusions from our data. First, both *ced-1* and *ced-6* are consistently required for the engulfment of debris during axon degeneration in *C. elegans*. Second, *ced-7* is only involved in engulfment during genetically-induced neurodegeneration, but not in response to an injury. Third, the *ced-2*, *-5*, *-12* engulfment

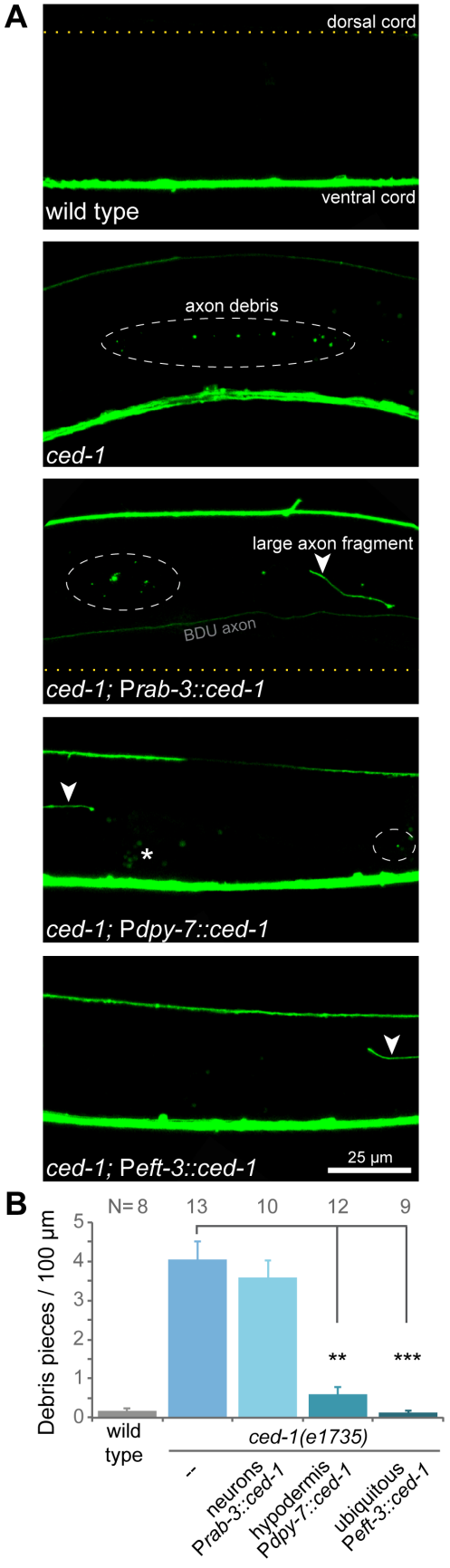

Figure 3.6. Hypodermal cells engulf degenerating axons. (A) ALA axons were cut into multiple pieces in L2 worms. After 24 hrs, the worms were imaged and the amount of axonal debris was quantified. A single copy insert of *ced-1* cDNA in a null mutant background rescues axonal debris clearance if expressed ubiquitously (P*eft-3*) or in the hypodermis (P*dpy-7*) but not when expressed in neurons (P*rab-3*). Examples of persisting axonal debris are indicated by dashed circles and arrowheads mark examples of large axon pieces that have not degenerated. The dotted yellow line indicates where the out of focus dorsal or ventral nerve cord would be. Asterisk indicates gut autofluorescence. All worms are expressing *oxEx81* [P*acr-5*::GAP4340aa::GFP]. (B) Wild-type worms have very few pieces of axon debris 24 hrs after axotomy. *ced-1(e1735)* mutants have an accumulation of axonal debris, which was not rescued by the neuronal expression of *ced-1*. Both the hypodermal and ubiquitous rescuing transgenes significantly reduced the amount of debris in *ced-1* mutants ($p < 0.0001$ Kruskal-Wallis test with Dunn's multiple comparisons, *** $p<0.001$ and ** $p<0.01$ compared to *ced-1(e1735)*).

pathway does not play a role in clearing degenerating axons in *C. elegans,* suggesting that epithelial cells are uniquely regulated during degeneration compared to macrophages and glial cells. To our knowledge, this is the first time the Rac1 pathway has been found not to play a role in engulfment. Four, caspases may be involved in fragmenting broken axons during neurodegenerative disease. Lastly, hypodermal cells engulf degenerating axon debris in *C. elegans*. The hypodermal cells of the worm are analogous to epithelial cells, which have been shown to engulf pruned and injured dendrites (Han et al., 2014) and ovary germline cells in *Drosophila* (Etchegaray et al., 2012).

The variable involvement of *ced-7* in axon degeneration is particularly intriguing. *ced-7* was only required for the engulfment of axon debris in beta-spectrin mutants but not axotomized axons in otherwise healthy animals. There are several possible explanations for this discrepancy. 1) *ced-7* may be uniquely involved in forms of neurodegeneration but not neuronal injury. In support of this notion, the engulfment of necrotic neurons also requires *ced-7* function (Chung et al., 2000). 2) *ced-7* may not be expressed in ALA. *ced-7* is the only engulfment gene that is required in both the corpse and the engulfing cell (Hamon et al., 2000; Mapes et al., 2012; Wu and Horvitz, 1998b). If *ced-7* is required within the axon corpse for engulfment, but not expressed in ALA, then we would not expect to see an engulfment deficiency in its absence. 3) Other proteins may be involved in exposing phosphatidylserine (PS) to the axon surface. For example, in apoptotic germ cell engulfment, *plsc-1* but not *ced-7* was required for exposing the PS “eat-me” signal on the surface of apoptotic germ cells (Venegas and Zhou, 2007). 4) *ced-7* may be uniquely involved in beta-spectrin

mutants. These worms are very sick and much of the nervous system is undergoing degeneration. It is possible that in such an environment, cells expressing *ced-7* may become highly reactive and begin to contribute to axon debris engulfment, which they would not normally due in a healthy worm.

Unlike what has been demonstrated in *Drosophila* (Ziegenfuss et al., 2012), the *ced-2*, *-5*, *-12* pathway is not involved in axon debris removal in *C. elegans*. It is possible that these genes are no longer expressed in worms after embryogenesis. However, this is not likely to be the case. The pathway has a continued role in gonad cell corpse removal in adults (Reddien and Horvitz, 2000; Wu and Horvitz, 1998a; Wu et al., 2001) and *ced-5* expresses in the adult hypodermis (data not shown). Alternatively, *mtm-1* could be suppressing the pathway in adult worms. MTM-1 has been shown to inhibit engulfment by negatively regulating the CED-5, -12 GEF complex (Neukomm et al., 2011; Zou et al., 2009). We speculate that epithelial cells may be differentially regulated during axon degeneration compared to apoptosis.

Who is acting to rearrange the hypodermal cytoskeleton if not the CED-2, -5, -12 engulfment pathway and CED-10/Rac1? There are two other rho GTPases that could be acting within the hypodermal cells to rearrange the cytoskeleton and engulf degenerating axons; RhoA and Cdc42. While RhoA (*rho-1*) has never been shown to have a role in apoptosis in *C. elegans*, experiments with mammalian macrophages indicate a duplicitous role for RhoA in engulfment. Inhibitors of RhoA block complement receptor mediated phagocytosis (Caron and Hall, 1998; May et al., 2000) but enhance the engulfment of apoptotic cells (Leverrier and Ridley, 2001; Nakaya et al., 2006; Tosello-Trampont et al., 2003). Thus, RhoA promotes phagocytosis via the complement

receptor, but inhibits the engulfment of apoptotic cells. Cdc42 is required for phagocytosis in mammalian cells (Caron and Hall, 1998; Leverrier and Ridley, 2001; Massol et al., 1998) and for engulfment of embryonic apoptotic cells in *C. elegans* (Hsieh et al., 2012). Interestingly, *cdc-42* and its upstream mediators *pat-2* and *uig-1* are required in muscle cells and not epithelial cells. This makes them an unlikely candidate for the engulfment of axonal debris; however, it is possible that there could be a developmental switch that would allow them to be active in nonembryonic epithelial cells. Cdc-42 has been shown to function within epithelial cells during the engulfment of apoptotic cells in human cell culture lines (Fiorentini et al., 2001). Alternatively, GTPases outside of the Rho family could be involved; mutations in ARF and Rab GTPases can impair phagocytosis by macrophages (Beemiller et al., 2006; Cox et al., 2000; Zhang et al., 1998). None of the above GTPases have been shown to regulate the engulfment of degenerating axons or dendrites.

In conclusion, we show that the epithelial cells of the worm uniquely engage a single apoptosis engulfment pathway (*ced-1* and *ced-6*) for removing axonal debris during degeneration. In addition, *ced-7* may have a context-dependent role in axon degeneration. Little is known about the regulation of engulfment during the degeneration of neuronal processes. ‘Nonprofessional phagocytes’ were only recently shown to have a role in engulfing dendrites (Han et al., 2014). Here we report that they are also involved in the removal of degenerating axons. Furthermore, our data suggest that the clearance of degenerating axons is regulated in a manner that is distinct from apoptosis.

Materials and Methods

Strains

Animals were maintained on E. coli OP50-seeded NGM plates according to standard methods. Beta-spectrin mutants were cultured on HB101 or comamonas-seeded plates. A complete list of worm strains is provided in the supplemental materials.

Molecular biology

Plasmids were made using the Invitrogen multisite Gateway cloning technique. *ced-1* was amplified off of first strand cDNA. The 3,211 bp of *ced-1b* cDNA, minus the stop codon, were inserted into the [1-2] donor vector via BP reaction. The [1-2] *ced-1* cDNA was recombined with [2-3] RFP_let858 3' UTR, a mosSCI compatible donor vector (pCFJ150), and [4-1] vectors containing promoters for either *eft-3*, *dpy-7*, or *rab-3*. The expression vectors were then inserted into the worm genome at single-copy using the mosSCI technique (Frøkjær-Jensen et al., 2008). The *ced-1* transgene was crossed out of the *unc-119* background and into the ced-1(e1735); *oxEx81* strain.

The *oxEx81* transgene (P*acr-5*::GAP43::GFP) encodes a membrane-bound GFP using the 40 aa myristoylation sequence of GAP43 (Knobel et al., 2001). The *oxIs12* transgene contains soluble GFP under the vGAT promoter, P*unc-47*::GFP.

Imaging

Worms were immobilized in either 10 mM muscimol or 25 mM sodium azide on 3% agarose pads. Images were acquired on a Pascal LSM5 confocal microscope or an

LSM510 Meta with a 63x 1.4NA oil objective (Zeiss). The whole length of the worm was imaged and the maximum intensity projections were tiled together in Photoshop to generate a single image per worm. The length of each worm was measured and the total number of debris pieces were quantified using the Cell Counter ImageJ plugin. The data are presented as the average number of debris pieces per 100 μm. The beta-spectrin worms were imaged at the fourth larval stage.

Laser axotomy

L2 worms were immobilized as described above. For Figure 3.4, axons were cut using a pulsing 810 nm light from a Ti:Sapphire laser (Mira900, Coherent) assembled on a LSM510 Meta confocal microscope (Zeiss) and focused through a 63x 1.4NA objective. For Figure 3.5, axons were cut using a pulsing 355 nm laser (FTSS355-Q3, CryLaS GmbH, Germany) assembled on a Nikon D-Eclipse C1, 90i confocal microscope with a Nikon 40x 1.3NA objective.

The ALA neuron has a single cell body in the head of the worm (dorsal to the posterior bulb of the pharynx) and extends two axons along the length of the worm at the right and left midline. In all experiments, either the right or left axon was cut and the same side of the worm was imaged on the following day. The ALA axon was cut into multiple pieces proceeding anterior to posterior, and then the cell body was killed to prevent regeneration. Images were acquired immediately after cutting. Worms were then recovered from the agarose pad and placed on bacterial NGM plates for 24 +/- 4 hrs of recovery. Images were acquired on the Pascal confocal (Zeiss) or the Nikon C1 confocal on the following day. Images were analyzed in ImageJ as described above.

When counting the number of perduring large axon segments, the most anterior (attached to the cell body) and the most posterior (extending into the tail ganglia) axon pieces were not included in the analysis. Only circular fluorescent particles were counted as ‘debris’; anything with an elongated shape was classified as a ‘large axon segment’.

The GABA motor neuron commissures were cut once just below the midline of the worm. The cell bodies were then killed to prevent regeneration. Four to five VD/DD commissures were cut per worm. The worms were imaged again 24 hrs later and the number of commissures still present and the number of debris pieces were quantified. The GFP in the GABA motor neuron experiments is soluble and on occasion would leak out of the commissures immediately following the injury. Images were acquired immediately after the axotomy and only commissures that were still visible were included in the 24 hr analysis.

Statistics

Nonparametric tests were used for the following reasons. Nonparametic ANOVAs (Kruskal-Wallis Test) were performed for the *ced-1, -6, -7* data in Figure 3.1 and the *ced-1* rescue data in Figure 3.6 because the data did not pass the Bartlett’s test for equal variances. A nonparametic ANOVA (Kruskal-Wallis Test) was performed for the axotomy data in Figure 3.4 because the samples did not have equal variance and the wild-type data were not normally distributed. Dunn’s multiple comparisons tests were performed between samples in each of the examples listed above. For paramentric one-way ANOVAs, Dunnett’s multiple comparisons tests were used,

comparing the data to the control sample. For the *ced-1* GABA motor neuron axotomy data (supplemental data), a nonparametric Mann-Whitney test was used because the samples had significantly different standard deviations and the wild-type data were not normally distributed.

Acknowledgments

Marc Hammarlund initiated this project and generated many of the strains used. Mike Bastiani collected images for Figure 3S.3B and generously provided access to his axotomy system. All other data were collected and analyzed by Randi Rawson. We thank Gillian Stanfield for providing several of the strains. Some strains were provided by the CGC (P40 OD010440).

References

Awasaki, T., Tatsumi, R., Takahashi, K., Arai, K., Nakanishi, Y., Ueda, R., and Ito, K. (2006). Essential role of the apoptotic cell engulfment genes draper and ced-6 in programmed axon pruning during drosophila metamorphosis. Neuron *50*, 855–867.

Beemiller, P., Hoppe, A.D., and Swanson, J.A. (2006). A phosphatidylinositol-3-kinase-dependent signal transition regulates ARF1 and ARF6 during Fcγ receptor-mediated phagocytosis. PLoS Biol *4*, e162.

Brugnera, E., Haney, L., Grimsley, C., Lu, M., Walk, S.F., Tosello-Trampont, A.-C., Macara, I.G., Madhani, H., Fink, G.R., and Ravichandran, K.S. (2002). Unconventional Rac-GEF activity is mediated through the Dock180–ELMO complex. Nat. Cell Biol. *4*, 574–582.

Caron, E., and Hall, A. (1998). Identification of two distinct mechanisms of phagocytosis controlled by different Rho GTPases. Science *282*, 1717–1721.

Chung, S., Gumienny, T.L., Hengartner, M.O., and Driscoll, M. (2000). A common set of engulfment genes mediates removal of both apoptotic and necrotic cell corpses in C. elegans. Nat. Cell Biol. *2*, 931–937.

Conradt, B. (2009). Genetic control of programmed cell death during animal

development. Annu. Rev. Genet. *43*, 493–523.

Conradt, B., and Horvitz, H.R. (1998). The C. elegans protein EGL-1 is required for programmed cell death and interacts with the Bcl-2-like protein CED-9. Cell *93*, 519–529.

Cox, D., Lee, D.J., Dale, B.M., Calafat, J., and Greenberg, S. (2000). A Rab11-containing rapidly recycling compartment in macrophages that promotes phagocytosis. Proc. Natl. Acad. Sci. *97*, 680–685.

Dorstyn, L., Colussi, P.A., Quinn, L.M., Richardson, H., and Kumar, S. (1999). DRONC, an ecdysone-inducible Drosophila caspase. Proc. Natl. Acad. Sci. U. S. A. *96*, 4307–4312.

Ellis, H.M., and Horvitz, H.R. (1986). Genetic control of programmed cell death in the nematode C. elegans. Cell *44*, 817–829.

Etchegaray, J.I., Timmons, A.K., Klein, A.P., Pritchett, T.L., Welch, E., Meehan, T.L., Li, C., and McCall, K. (2012). Draper acts through the JNK pathway to control synchronous engulfment of dying germline cells by follicular epithelial cells. Development *139*, 4029–4039.

Fiorentini, C., Falzano, L., Fabbri, A., Stringaro, A., Logozzi, M., Travaglione, S., Contamin, S., Arancia, G., Malorni, W., and Fais, S. (2001). Activation of Rho GTPases by Cytotoxic Necrotizing Factor 1 induces macropinocytosis and scavenging activity in epithelial cells. Mol. Biol. Cell *12*, 2061–2073.

Frøkjær-Jensen, C., Davis, M.W., Hopkins, C.E., Newman, B.J., Thummel, J.M., Olesen, S.-P., Grunnet, M., and Jorgensen, E.M. (2008). Single-copy insertion of transgenes in Caenorhabditis elegans. Nat. Genet. *40*, 1375–1383.

Galvin, B.D., Kim, S., and Horvitz, H.R. (2008). Caenorhabditis elegans genes required for the engulfment of apoptotic corpses function in the cytotoxic cell deaths induced by mutations in lin-24 and lin-33. Genetics *179*, 403–417.

Gumienny, T.L., Brugnera, E., Tosello-Trampont, A.-C., Kinchen, J.M., Haney, L.B., Nishiwaki, K., Walk, S.F., Nemergut, M.E., Macara, I.G., Francis, R., et al. (2001). CED-12/ELMO, a novel member of the CrkII/Dock180/Rac pathway, is required for phagocytosis and cell migration. Cell *107*, 27–41.

Hammarlund, M., Jorgensen, E.M., and Bastiani, M.J. (2007). Axons break in animals lacking beta-spectrin. J. Cell Biol. *176*, 269–275.

Hammarlund, M., Nix, P., Hauth, L., Jorgensen, E.M., and Bastiani, M. (2009). Axon regeneration requires a conserved map kinase pathway. Sci. N. Y. NY *323*, 802–806.

Hamon, Y., Broccardo, C., Chambenoit, O., Luciani, M.-F., Toti, F., Chaslin, S., Freyssinet, J.-M., Devaux, P.F., McNeish, J., Marguet, D., et al. (2000). ABC1 promotes

engulfment of apoptotic cells and transbilayer redistribution of phosphatidylserine. Nat. Cell Biol. *2*, 399–406.

Han, C., Song, Y., Xiao, H., Wang, D., Franc, N.C., Jan, L.Y., and Jan, Y.-N. (2014). Epidermal cells are the primary phagocytes in the fragmentation and clearance of degenerating dendrites in Drosophila. Neuron *81*, 544–560.

Hedgecock, E.M., Sulston, J.E., and Thomson, J.N. (1983). Mutations affecting programmed cell deaths in the nematode Caenorhabditis elegans. Science *220*, 1277–1279.

Hoeppner, D.J., Hengartner, M.O., and Schnabel, R. (2001). Engulfment genes cooperate with ced-3 to promote cell death in Caenorhabditis elegans. Nature *412*, 202–206.

Hosmane, S., Tegenge, M.A., Rajbhandari, L., Uapinyoying, P., Kumar, N.G., Thakor, N., and Venkatesan, A. (2012). TRIF mediates microglial phagocytosis of degenerating axons. J. Neurosci. *32*, 7745–7757.

Hsieh, H.-H., Hsu, T.-Y., Jiang, H.-S., and Wu, Y.-C. (2012). Integrin α PAT-2/CDC-42 signaling is required for muscle-mediated clearance of apoptotic cells in Caenorhabditis elegans. PLoS Genet. *8*, e1002663.

Ikeda, Y., Dick, K.A., Weatherspoon, M.R., Gincel, D., Armbrust, K.R., Dalton, J.C., Stevanin, G., Dürr, A., Zühlke, C., Bürk, K., et al. (2006). Spectrin mutations cause spinocerebellar ataxia type 5. Nat. Genet. *38*, 184–190.

Keller, L.C., Cheng, L., Locke, C.J., Müller, M., Fetter, R.D., and Davis, G.W. (2011). Glial-derived prodegenerative signaling in the drosophila neuromuscular system. Neuron *72*, 760–775.

Kinchen, J.M., Cabello, J., Klingele, D., Wong, K., Feichtinger, R., Schnabel, H., Schnabel, R., and Hengartner, M.O. (2005). Two pathways converge at CED-10 to mediate actin rearrangement and corpse removal in C. elegans. Nature *434*, 93–99.

Knobel, K.M., Davis, W.S., Jorgensen, E.M., and Bastiani, M.J. (2001). UNC-119 suppresses axon branching in C. elegans. Development *128*, 4079–4092.

Kuo, C., Zhu, S., Younger, S., Jan, L., and Jan, Y. (2006). Identification of E2/E3 ubiquitinating enzymes and caspase activity regulating drosophila sensory neuron dendrite pruning. Neuron *51*, 283–290.

Leverrier, Y., and Ridley, A.J. (2001). Requirement for Rho GTPases and PI 3-kinases during apoptotic cell phagocytosis by macrophages. Curr. Biol. CB *11*, 195–199.

Li, W., and Baker, N.E. (2007). Engulfment is required for cell competition. Cell *129*, 1215–1225.

Liu, Q.A., and Hengartner, M.O. (1998). Candidate adaptor protein CED-6 promotes the engulfment of apoptotic cells in C. elegans. Cell *93*, 961–972.

Luo, L., and O'Leary, D.D.M. (2005). Axon retraction and degeneration in development and disease. Annu. Rev. Neurosci. *28*, 127–156.

Macdonald, J., Beach, M., Porpiglia, E., Sheehan, A., Watts, R., and Freeman, M. (2006). The Drosophila cell corpse engulfment receptor draper mediates glial clearance of severed axons. Neuron *50*, 869–881.

Mangahas, P.M., and Zhou, Z. (2005). Clearance of apoptotic cells in Caenorhabditis elegans. Semin. Cell Dev. Biol. *16*, 295–306.

Mapes, J., Chen, Y.-Z., Kim, A., Mitani, S., Kang, B.-H., and Xue, D. (2012). CED-1, CED-7, and TTR-52 regulate surface phosphatidylserine expression on apoptotic and phagocytic cells. Curr. Biol. CB *22*, 1267–1275.

Massaro, C.M., Pielage, J., and Davis, G.W. (2009). Molecular mechanisms that enhance synapse stability despite persistent disruption of the spectrin/ankyrin/microtubule cytoskeleton. J. Cell Biol. *187*, 101–117.

Massol, P., Montcourrier, P., Guillemot, J.-C., and Chavrier, P. (1998). Fc receptor-mediated phagocytosis requires CDC42 and Rac1. EMBO J. *17*, 6219–6229.

May, R.C., Caron, E., Hall, A., and Machesky, L.M. (2000). Involvement of the Arp2/3 complex in phagocytosis mediated by FcgammaR or CR3. Nat. Cell Biol. *2*, 246–248.

Nakaya, M., Tanaka, M., Okabe, Y., Hanayama, R., and Nagata, S. (2006). Opposite effects of Rho family GTPases on engulfment of apoptotic cells by macrophages. J. Biol. Chem. *281*, 8836–8842.

Neher, J.J., Neniskyte, U., Zhao, J.W., Bal-Price, A., Tolkovsky, A.M., and Brown, G.C. (2011). Inhibition of microglial phagocytosis is sufficient to prevent inflammatory neuronal death. J. Immunol. *186*, 4973–4983.

Neukomm, L.J., Frei, A.P., Cabello, J., Kinchen, J.M., Zaidel-Bar, R., Ma, Z., Haney, L.B., Hardin, J., Ravichandran, K.S., Moreno, S., et al. (2011). Loss of the RhoGAP SRGP-1 promotes the clearance of dead and injured cells in Caenorhabditis elegans. Nat. Cell Biol. *13*, 79–86.

Nikolaev, A., Mclaughlin, T., O'leary, D.D.M., and Tessier-Lavigne, M. (2009). APP binds DR6 to trigger axon pruning and neuron death via distinct caspases. Nature *457*, 981–989.

Nix, P., Hisamoto, N., Matsumoto, K., and Bastiani, M. (2011). Axon regeneration requires coordinate activation of p38 and JNK MAPK pathways. Proc. Natl. Acad. Sci. U. S. A. *108*, 10738–10743.

Parkinson, N.J., Olsson, C.L., Hallows, J.L., McKee-Johnson, J., Keogh, B.P., Noben-Trauth, K., Kujawa, S.G., and Tempel, B.L. (2001). Mutant beta-spectrin 4 causes auditory and motor neuropathies in quivering mice. Nat. Genet. *29*, 61–65.

Pinan-Lucarre, B., Gabel, C.V., Reina, C.P., Hulme, S.E., Shevkoplyas, S.S., Slone, R.D., Xue, J., Qiao, Y., Weisberg, S., Roodhouse, K., et al. (2012). The core apoptotic executioner proteins CED-3 and CED-4 promote initiation of neuronal regeneration in Caenorhabditis elegans. PLoS Biol *10*, e1001331.

Quinn, L.M., Dorstyn, L., Mills, K., Colussi, P.A., Chen, P., Coombe, M., Abrams, J., Kumar, S., and Richardson, H. (2000). An essential role for the caspase dronc in developmentally programmed cell death in Drosophila. J. Biol. Chem. *275*, 40416–40424.

Reddien, P.W., and Horvitz, H.R. (2000). CED-2/CrkII and CED-10/Rac control phagocytosis and cell migration in Caenorhabditis elegans. Nat. Cell Biol. *2*, 131–136.

Reddien, P.W., and Horvitz, H.R. (2004). The engulfment process of programmed cell death in caenorhabditis elegans. Annu. Rev. Cell Dev. Biol. *20*, 193–221.

Reddien, P.W., Cameron, S., and Horvitz, H.R. (2001). Phagocytosis promotes programmed cell death in C. elegans. Nature *412*, 198–202.

Schoenmann, Z., Assa-Kunik, E., Tiomny, S., Minis, A., Haklai-Topper, L., Arama, E., and Yaron, A. (2010). Axonal degeneration is regulated by the apoptotic machinery or a NAD+-sensitive pathway in insects and mammals. J. Neurosci. *30*, 6375–6386.

Sokolowski, J.D., and Mandell, J.W. (2011). Phagocytic clearance in neurodegeneration. Am. J. Pathol. *178*, 1416–1428.

Su, H.P., Nakada-Tsukui, K., Tosello-Trampont, A.-C., Li, Y., Bu, G., Henson, P.M., and Ravichandran, K.S. (2002). Interaction of CED-6/GULP, an adapter protein involved in engulfment of apoptotic cells with CED-1 and CD91/low density lipoprotein receptor-related protein (LRP). J. Biol. Chem. *277*, 11772–11779.

Tanaka, T., Ueno, M., and Yamashita, T. (2009). Engulfment of axon debris by microglia requires p38 MAPK activity. J. Biol. Chem. *284*, 21626–21636.

Tao, J., and Rolls, M.M. (2011). Dendrites have a rapid program of injury-induced degeneration that is molecularly distinct from developmental pruning. J. Neurosci. *31*, 5398–5405.

Tosello-Trampont, A.-C., Nakada-Tsukui, K., and Ravichandran, K.S. (2003). Engulfment of apoptotic cells is negatively regulated by Rho-mediated signaling. J. Biol. Chem. *278*, 49911–49919.

Venegas, V., and Zhou, Z. (2007). Two alternative mechanisms that regulate the presentation of apoptotic cell engulfment signal in Caenorhabditis elegans. Mol. Biol.

Cell *18*, 3180–3192.

Williams, D.W., Kondo, S., Krzyzanowska, A., Hiromi, Y., and Truman, J.W. (2006). Local caspase activity directs engulfment of dendrites during pruning. Nat. Neurosci. *9*, 1234–1236.

Wu, Y.C., and Horvitz, H.R. (1998a). C. elegans phagocytosis and cell-migration protein CED-5 is similar to human DOCK180. Nature *392*, 501–504.

Wu, Y.C., and Horvitz, H.R. (1998b). The C. elegans cell corpse engulfment gene ced-7 encodes a protein similar to ABC transporters. Cell *93*, 951–960.

Wu, Ghosh-Roy, Yanik, Zhang, Jin, Y., and Chisholm (2007). Caenorhabditis elegans neuronal regeneration is influenced by life stage, ephrin signaling, and synaptic branching. Proc Natl Acad Sci U A.

Wu, Y.-C., Tsai, M.-C., Cheng, L.-C., Chou, C.-J., and Weng, N.-Y. (2001). C. elegans CED-12 acts in the conserved CrkII/DOCK180/Rac pathway to control cell migration and cell corpse engulfment. Dev. Cell *1*, 491–502.

Zhang, Q., Cox, D., Tseng, C.-C., Donaldson, J.G., and Greenberg, S. (1998). A requirement for ARF6 in Fcγ receptor-mediated phagocytosis in macrophages. J. Biol. Chem. *273*, 19977–19981.

Zhou, Z., Hartwieg, E., and Horvitz, H.R. (2001a). CED-1 is a transmembrane receptor that mediates cell corpse engulfment in C. elegans. Cell *104*, 43–56.

Zhou, Z., Caron, E., Hartwieg, E., Hall, A., and Horvitz, H.R. (2001b). The C. elegans PH domain protein CED-12 regulates cytoskeletal reorganization via a Rho/Rac GTPase signaling pathway. Dev. Cell *1*, 477–489.

Ziegenfuss, J.S., Doherty, J., and Freeman, M.R. (2012). Distinct molecular pathways mediate glial activation and engulfment of axonal debris after axotomy. Nat. Neurosci. *15*, 979–987.

Zou, W., Lu, Q., Zhao, D., Li, W., Mapes, J., Xie, Y., and Wang, X. (2009). Caenorhabditis elegans myotubularin MTM-1 negatively regulates the engulfment of apoptotic cells. PLoS Genet. *5*, e1000679.

Supplemental Materials

Figure 3S.1. *ced-3* caspase pathway in beta-spectrin mutants. (A) and (B) contain three separate data sets illustrating that mutations in the killing phase of the apoptosis pathway do not increase dorsal cord coverage on their own. The increase in dorsal cord coverage is only seen when both the engulfment pathway (*ced-1*) and the caspase pathway are mutated (Figure 3.3). (C) If fragmentation is impaired in *ced-1*; *ced-3* double mutants then we would expect to see an increase in the number of large detached axon segments. This analysis includes a survey of all broken axons in the worm rather than looking at just the dorsal cord. However, there is no difference in the number of large axon segments per worm in the ced-1, killing phase double mutants compared to *ced-1* alone. (n.s. Kruskal-Wallis test) (D) If *ced-3* mutants are impaired for axon fragmentation, then we would expect to see a decrease in the amount of axonal debris. Axonal debris is slightly decreased in *ced-1*; *ced-3* mutants and significantly decreased in *ced-1*; *ced-9* double mutants compared to *ced-1* alone. ($p= 0.04$ One-way ANOVA with Dunnett's multiple comparisons against *ced-1* $*p< 0.05$) (E) The average number of commissures per worm is increased in *ced-1*; *ced-3* double mutants. ($p= 0.035$ One-Way ANOVA with Dunnett's multiple comparisons against *ced-1* $*p< 0.05$). All worms contain *unc-70(s1502)* and all worms in C-E are also *ced-1(e1735)*. N= total number of worms. [An increase in commissures plus an increase in dorsal cord coverage seems to suggest one of two things i) *ced-3* increases regeneration in *ced-1* mutants. However, this would be the opposite of what the Driscoll lab has shown for the role of *ced-3* in regeneration. ii) Loss of *ced-3* inhibits the breaking of beta-spectrin axons in *ced-1* mutants.]

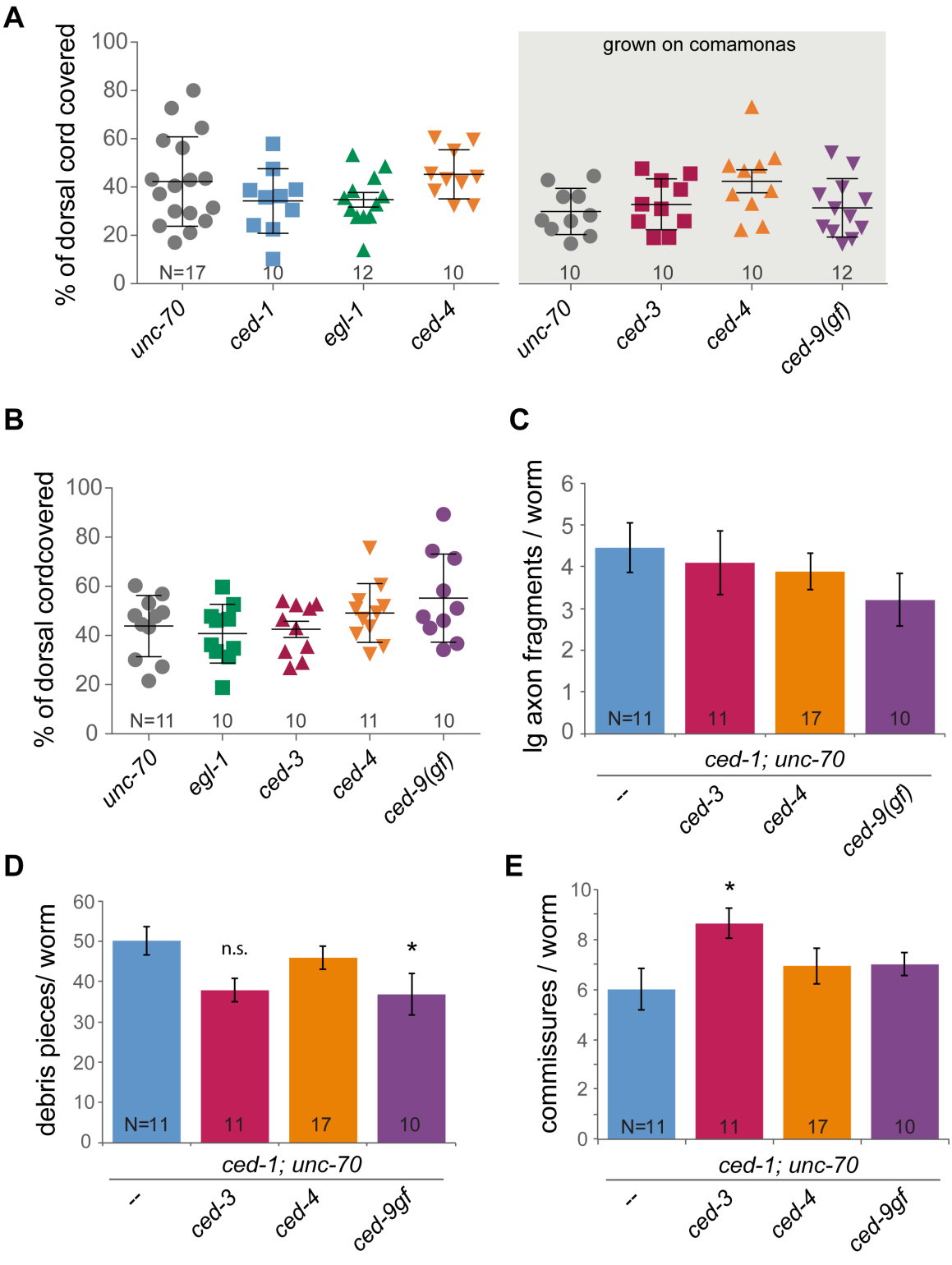
A
% of dorsal cord covered
100
80
60
40
20
0
N=17
10
12
10
unc-70
ced-1
egl-1
ced-4
grown on comamonas
10
10
10
12
unc-70
ced-3
ced-4
ced-9(gf)
B
% of dorsal cordcovered
N=11
10
10
11
10
unc-70
egl-1
ced-3
ced-4
ced-9(gf)
C
lg axon fragments / worm
6
5
4
3
2
1
0
N=11
11
17
10
ced-1; unc-70
--
ced-3
ced-4
ced-9(gf)
D
debris pieces/ worm
60
50
40
30
20
10
0
n.s.
*
N=11
11
17
10
ced-1; unc-70
--
ced-3
ced-4
ced-9gf
E
commissures / worm
10
8
6
4
2
0
*
N=11
11
17
10
ced-1; unc-70
--
ced-3
ced-4
ced-9gf

Figure 3S.2. Axotomy of ALA and GABA motor neuron axons. (A) The number of large axon segments remaining after axotomy of the ALA axon is unchanged across the *ced* genotypes. (B) *ced-1* is required for the clearance of GABA commissure debris following axotomy. GABA motor neurons extend axons from the ventral nerve cord across the lateral side of the worm (commissures) up to the dorsal side where they branch out to form the dorsal nerve cord. Individual commissures were cut with a laser just below the midline of the worm, four commissures per worm. The worms were allowed to recover for 48 hrs and then reimaged. The amount of debris from degenerating commissures was quantified. The worm in the image is shifted so that its dorsal side is facing towards the objective. Examples of commissure debris are indicated with the dashed circle. The asterisk marks autofluorescence from the gut. (C) *ced-1(e1735)* mutants had nearly 8-fold greater amounts of debris compared to the wild type ($p = 0.0036$, two-tailed Mann-Whitney test).

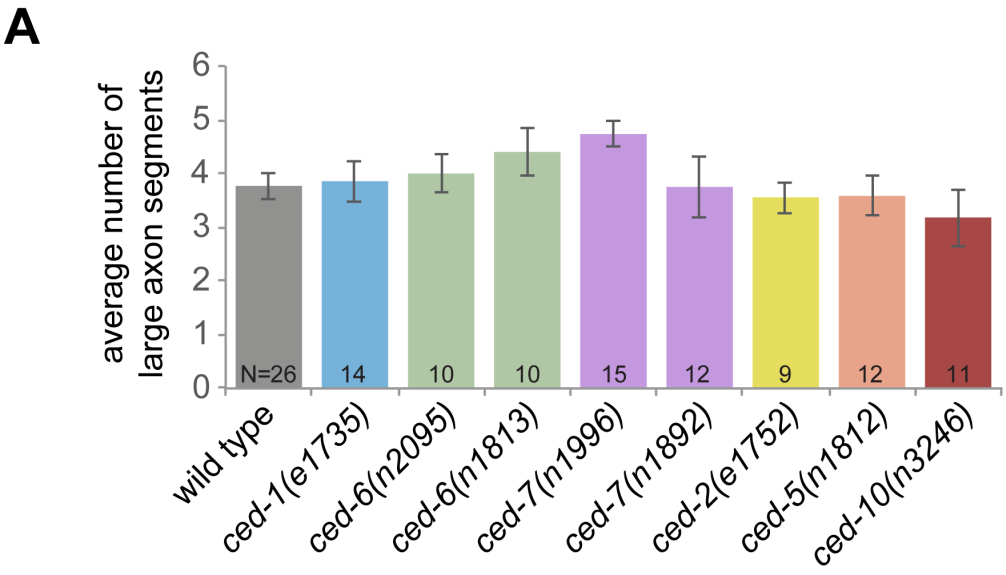
A
average number of large axon segments
0
1
2
3
4
5
6
N=26
14
10
10
15
12
9
12
11
wild type
ced-1(e1735)
ced-6(n2095)
ced-6(n1813)
ced-7(n1996)
ced-7(n1892)
ced-2(e1752)
ced-5(n1812)
ced-10(n3246)

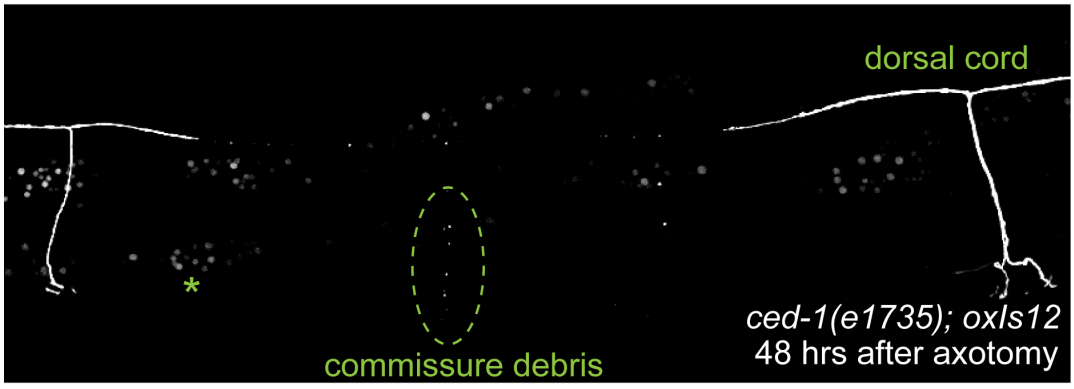
B
dorsal cord
*
commissure debris
ced-1(e1735); oxIs12
48 hrs after axotomy

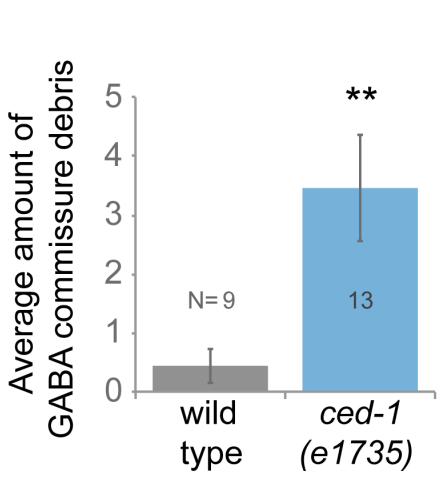
C
Average amount of GABA commissure debris
0
1
2
3
4
5
**
N= 9
13
wild type
ced-1 (e1735)

Figure 3S.3. *ced-1* rescuing construct is functional. (A) The *ced-1::rfp* mosSCI inserts were crossed into *ced-1(e1735)*; *oxIs12*. The images were taken from strains that were homozygous for *ced-1(e1735)* but still heterozygous for the *ced-1::rfp* inserts. *ced-1::rfp* was expressed under the *eft-3* promoter (ubiquitous expression) and *dpy-7* promoter (hypodermis). NonRFP embryos had apoptotic cell corpses (arrowheads), whereas embryos positive for RFP were rescued for corpse engulfment. Images were acquired on a wide-field microscope. The strains were homozygosed for the mosSCI inserts prior to the axotomy experiments. (B) The number of large axon segments remaining 24 hrs after axotomy of the ALA axon is unchanged across genotypes.

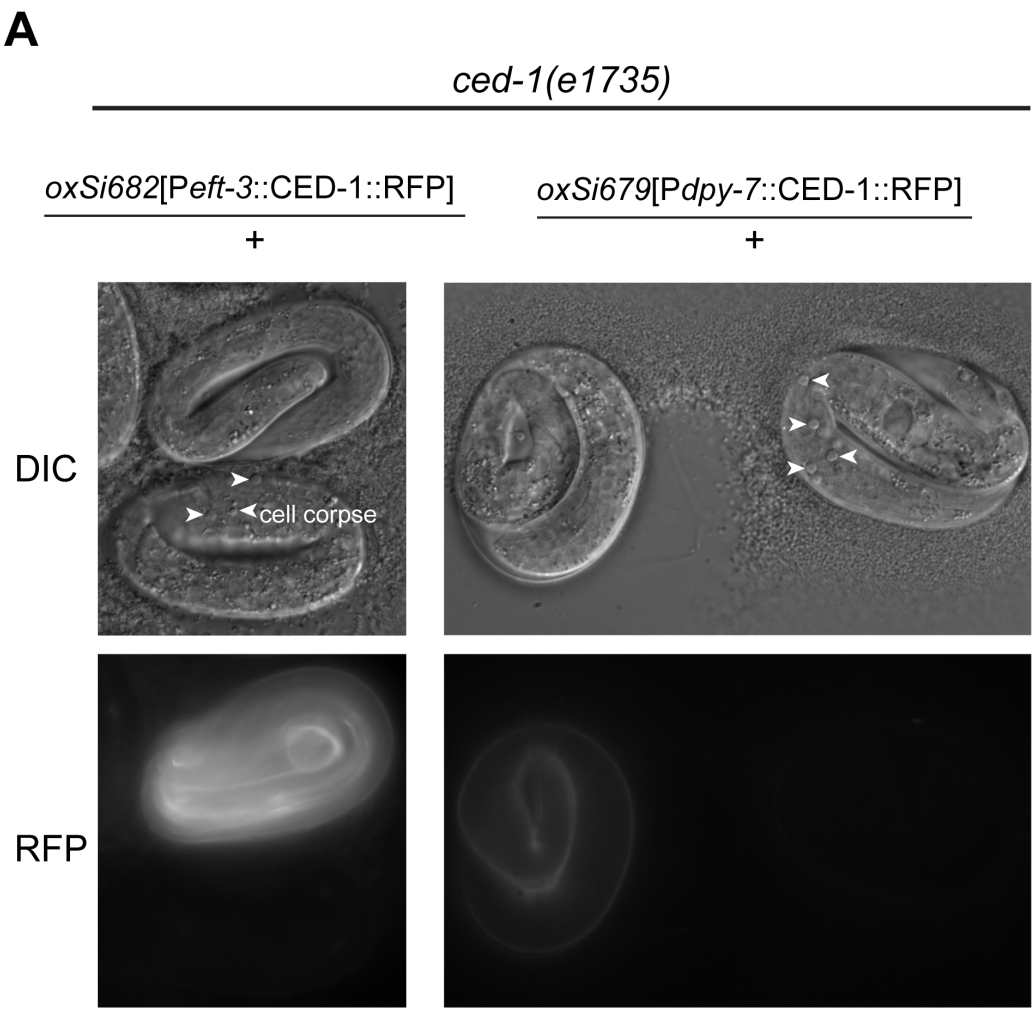
A
ced-1(e1735)
oxSi682[Peft-3::CED-1::RFP]
+
oxSi679[Pdpy-7::CED-1::RFP]
+
DIC
RFP
cell corpse

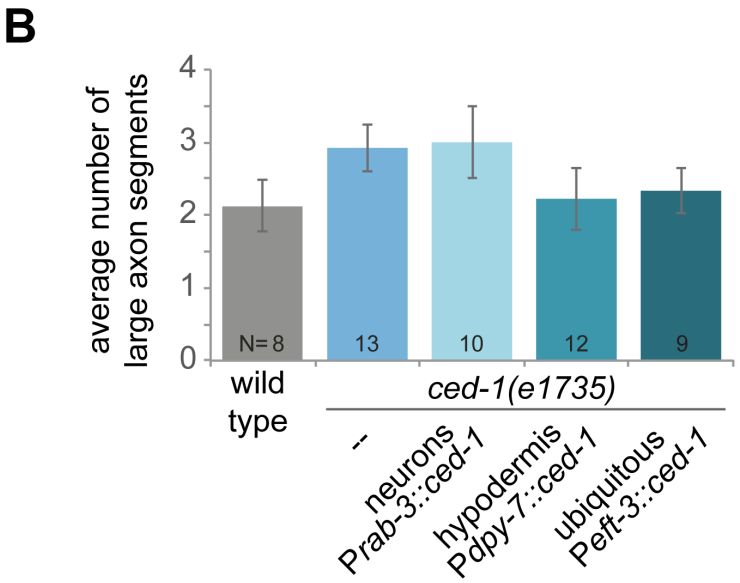
B
average number of large axon segments
0
1
2
3
4
N=8
13
10
12
9
wild type
ced-1(e1735)
--
neurons Prab-3::ced-1
hypodermis Pdpy-7::ced-1
ubiquitous Peft-3::ced-1

CHAPTER 4

SUMMARY AND FUTURE DIRECTIONS

The aim of this dissertation was two-fold; one, to establish *C. elegans* as a model system for studying axon degeneration, and two, to uncover molecular mechanisms mediating axon degeneration. Axons degenerate in *C. elegans* by undergoing the same morphological changes that are seen in Wallerian degeneration. In other words, they swell, bead, dissociate, and are cleared away. Axon degeneration in the worm includes other common characteristics. After an injury, an axon will degenerate depending on the location of its mitochondria. The presence of mitochondria robustly suppresses axon degeneration in *C. elegans* (Chapter 2). Studies from other model systems, including mammals and flies, have similarly demonstrated that mitochondria regulate axon protection (Fang et al., 2012; Misko et al., 2012; Schon and Przedborski, 2011). When an axon degenerates, other cells clear away the fragmented pieces by engulfment. The engulfment of axon debris in *C. elegans* is regulated by *ced-1* and *ced-6* (Chapter 3), similar to what has been observed in *Drosophila* (Awasaki et al., 2006; Hoopfer et al., 2006; Macdonald et al., 2006). Thus, the nematode *C. elegans* is a useful model system for studying conserved mechanisms of axon degeneration following axotomy.

In addition, the data presented in this dissertation delineate several advancements. In Chapter 3, we show that epithelial cells engulf degenerating axons and that this process is uniquely regulated compared to engulfment during apoptosis and during glia-mediated engulfment of degenerating axons. Namely, the *ced-2* and *ced-10* cytoskeleton-rearranging pathway is not involved in clearing degenerating axons by epithelial cells, suggesting that these cells employ a novel mechanism for engulfment. The data also reveal a specific role for *ced-7* during neurodegenerative disease and not following an injury. In Chapter 2, we identify *ric-7* as a novel regulator of mitochondria distribution in *C. elegans* neurons. Using *ric-7* as a tool to study degeneration, we demonstrate that mitochondria are not required for the break down of axons following injury. The presence of mitochondria robustly protects axons in both mutants and the wild type, highlighting the critical need for mitochondria in axon maintenance.

Mitochondria-Dependent Mechanism of Axon Protection

The presence of mitochondria strongly suppresses axon degeneration in *C. elegans*. Some studies have suggested that mitochondria are a required participant in the destruction of axons (Barrientos et al., 2011; Keller et al., 2011). However, our results demonstrate that mitochondria are dispensable for the execution of axon degeneration; instead, they are actively involved in preventing degeneration from occurring. How might mitochondria be acting to suppress axon degeneration? They could be protective through some direct property of the organelle itself, such as energy supply or calcium buffering. Alternatively,

molecules associated with mitochondria may be involved in halting axon destruction pathways. In the latter model, the mitochondria's function is to localize the antidegeneration signal along the axon.

Oxidative phosphorylation

Energy supply is unlikely to be the rate-limiting step of axon degeneration. Mitochondria dysfunction has been frequently associated with neurodegenerative disease and the topic has received much attention. ATP supply from mitochondria is critical to the cell and complete abolishment of oxidative phosphorylation is cell lethal. However, moderate perturbations do not seem to make neurons susceptible to neurodegeneration. Nonlethal mutations in humans are not associated with neurodegenerative diseases (Schon and Przedborski, 2011). Strong hypomorphic alleles in electron transport chain subunits did not exhibit elevated axon degeneration following injury in *C. elegans* (Figure S4.4). Furthermore, some studies suggest that neurons can rely heavily on glycolysis in the absence of oxidative phosphorylation (Calupca et al., 1999; Fünfschilling et al., 2013; Misko et al., 2012; Rangaraju et al., 2014; Tekk k et al., 2003; Winkler et al., 2000).

Calcium buffering

Several pieces of evidence support a role for mitochondria in buffering calcium during degeneration. In general, calcium is a well-known mediator of degeneration and is tightly regulated by the cell (reviewed in Wang et al., 2012;

Zündorf and Reiser, 2011). Application of calcium channel blockers or calcium chelators abates axon degeneration (Barrientos et al., 2011; George et al., 1998; Knöferle et al., 2010). During homeostatic conditions, the amount of calcium in mitochondria is quite low, but they are capable of taking up large amounts of calcium when necessary (Montero et al., 2000; Pivovarova et al., 1999). Isolated mitochondria from Wld^S mice are able to load significantly greater amounts of calcium, suggesting that the calcium capacity of mitochondria might be related to the protective effects of Wld^S (Avery et al., 2012). Mitochondria uptake calcium through the voltage dependent anion channel (VDAC) and the mitochondria calcium uniporter (MCU) (Calì et al., 2012). Blocking these channels with DIDS and Ruthenium Red reduced axon degeneration in severed sciatic nerves (Barrientos et al., 2011). However, VDAC has also been identified in the ER and Ruthenium Red targets multiple proteins, including Ryanodine receptors and TRP channels (Ding et al., 1998; Dray et al., 1990; Shoshan-Barmatz et al., 2004).

Thus far, the evidence supporting an essential role for mitochondria in buffering calcium during axon degeneration remains relatively indirect. Experiments using specific knockdown of MCU are needed. Also, live imaging of mitochondrial calcium levels would reveal the temporal and spatial characteristics of calcium uptake following an axon injury. Smooth endoplasmic reticulum (ER) is located along the entire length of axons (including in *ric-7* mutants, Figure 4.1); thus, it is intriguing that mitochondria would have an essential role in buffering

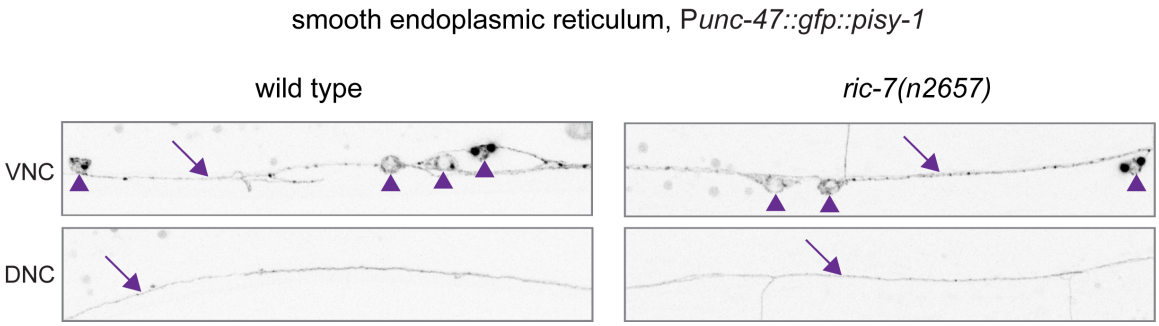

Figure 4.1. Endoplasmic reticulum is located throughout axons. Worms are expressing GFP-tagged PISY-1 in the GABA neurons under the *unc-47* promoter. Worms were imaged with their ventral or dorsal side facing the objective. The black and white fluorescent images are inverted. ER can be seen throughout the entire length of axons in both the ventral nerve cord (VNC) and dorsal nerve cord (DNC). ER localization is normal in *ric-7* mutants (right column). Arrowheads mark cell bodies and arrows point to axons.

calcium after an injury. Imaging of two color calcium reporters is needed to elucidate the calcium dynamics between these two organelles. Using mitochondria-localized GCaMP and ER-localized R-GECO, the calcium flux in each of these organelles can be simultaneously observed in response to an axon injury. Do both organelles respond to the increase in cytosolic calcium? Are their buffering capacities temporally distinct?

If *ric-7* mutant axons have enhanced degeneration due to reduced calcium buffering, the following predictions can be made for future experiments. 1) In wild-type axons, mito-GCaMP6 fluorescence should increase following axotomy. 2) Worms with cell-specific knockdown of the MCU channel should have enhanced levels of degeneration, similar to *ric-7*. 3) Blocking calcium entry into the axon should suppress degeneration in *ric-7* mutants. Thus far, blocking the L-type voltage gated calcium channel EGL-19 with the drug Nemadipine-A and the *egl-19(n582)* mutation were unable to suppress degeneration in *ric-7* mutants.

unc-2 mutants remain to be tested and perhaps both channels need to be impaired in order to prevent axon degeneration.

Novel mechanisms of protection

Lastly, mitochondria may be serving a protective function by localizing an unidentified axon-survival factor along axons. These three proposed mechanisms of protection are not mutually exclusive and more than one may be at play in abating degeneration. *C. elegans* is an ideal model system in which to screen for novel regulators of degeneration. Both beta-spectrin and *ric-7* mutants will lend themselves well to forward genetic screens.

RIC-7 Mechanism

Why are mitochondria absent in *ric-7* mutant axons? In *ric-7* mutants, mitochondria are unable to exit the neuronal cell bodies. There are three simple models that could explain this phenotype. 1) Fission. The mitochondria are unable to divide within the cell body. RIC-7 may promote mitochondrial fission and the smaller mitochondria are then able to transport down the narrow axons. 2) Anchor removal. The mitochondria within the cell body may be tethered in place. RIC-7 could be involved in releasing the mitochondria from their anchor before they can transport down axons. 3) Transport. RIC-7 may be involved in associating mitochondria with the kinesin motor.

Fission

The first model predicts that RIC-7 is contributing to mitochondrial fission. Fission is a highly regulated process of dividing mitochondria in two through the constriction of membranes at the fission site (reviewed in Bliek et al., 2013). Drp1 (dynamin-related protein 1) is a well-characterized mediator of mitochondrial fission, originally characterized in yeast (Dnm1) and mammalian cells (Bleazard et al., 1999; Otsuga et al., 1998; Smirnova et al., 1998). Dnm1/Drp1 accumulates at fission sites and forms spirals around the mitochondrial outer membrane. As the spiral tightens due to GTPase activity, the membranes on either side of the spiral are pinched off from one another (Ingerman et al., 2005).

The fission model predicts that *ric-7* mutants will phenocopy *drp-1* mutants and that mitochondria exit from cell bodies is dependent upon fission. To address these questions, we examined *drp-1* loss of function in GABA motor neurons. Null mutations in *drp-1* are lethal, so a dominant negative version of the protein DRP-1(K40S) was cell-specifically expressed at high concentrations. The mitochondria distribution in DRP-1(K40S) neurons is strikingly dissimilar to that of *ric-7* mutants. In dominant negative DRP-1(K40S) worms, the mitochondria extend out of the cell body as long continuous tubules (Figure 4.2). The tubules are of varying lengths, but often cover the entire ventral length of the GABA motor neuron axons. Thus, instead of a loss of axonal mitochondria, DRP-1(K40S) animals have an excess of mitochondria in their proximal axons. These contrasting phenotypes indicate that *ric-7* is not required for fission, and that fission is not a prerequisite for exit of mitochondria from neuronal cell bodies.

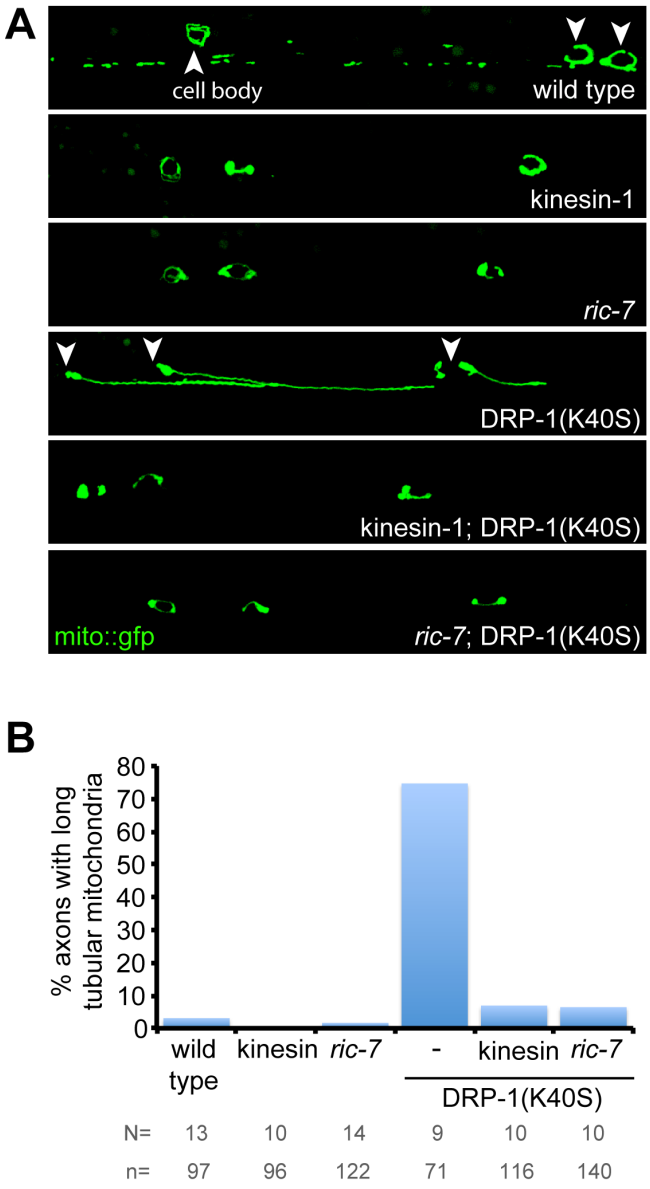

Figure 4.2. *ric-7* phenocopies transport mutants and not fission mutants. (A) Mitochondria are distributed throughout the ventral nerve cord in the wild type but are absent from axons in both kinesin-1/*unc-116(rh24sb79)* and *ric-7(n2657)* mutants. Mitochondria are present in the axons of worms overexpressing a dominant negative form of DRP-1(K40S), but they are long, continuous tubules that extend along the ventral cord. If transport is blocked, then the tubules no longer extend out of the cell body 'kinesin-1; DRP-1(K40S)'. Similarly, removing *ric-7* also prevents extension of mitochondria tubules in DRP-1(K40S) worms. (B) The percent of GABA motor neurons with long tubular mitochondria. N = the number of worms, n = the number of neurons assayed.

Anchor removal

The second model postulates that RIC-7 is acting to displace a mitochondrial tether within the cell body. Once the mitochondria are released from their tether, they can be transported down axons. *anc-1* is required to anchor mitochondria in both hypodermal and muscle cells (Hedgecock and Thomson, 1982; Starr and Han, 2002). The muscle mitochondria in an *anc-1* mutant can be seen floating around the cell during muscle contractions. Unanchored mitochondria also tend to be spherical and clustered together, whereas muscle mitochondria are typically a network of interconnected tubules. Because *anc-1* appears to be expressed in all adult somatic cells (Starr and Han, 2002), it is likely that ANC-1 is anchoring mitochondria within neurons as well. If RIC-7's function is to displace the anchor, then genetically ablating the anchor should free the mitochondria and make them available for transport. While the mitochondria in wild-type neuronal cell bodies typically form a ring around the nucleus, the mitochondria in *anc-1(n1614)* mutants are often clustered to one or both sides of the nucleus (not quantified, Figure 4.3C), suggesting that *anc-1* might be required for mitochondria stability in GABA motor neuron cell bodies. However, *anc-1* does not rescue the localization of mitochondria in *ric-7* mutants (Figure 4.3D). This suggests that RIC-7 does not release mitochondria from a cell body anchor. Very little is known about how mitochondria are stabilized at specific locations within neurons. It remains plausible that RIC-7 is regulating an unidentified mitochondria anchor. Such an anchor should be identifiable from future *ric-7* suppressor screens.

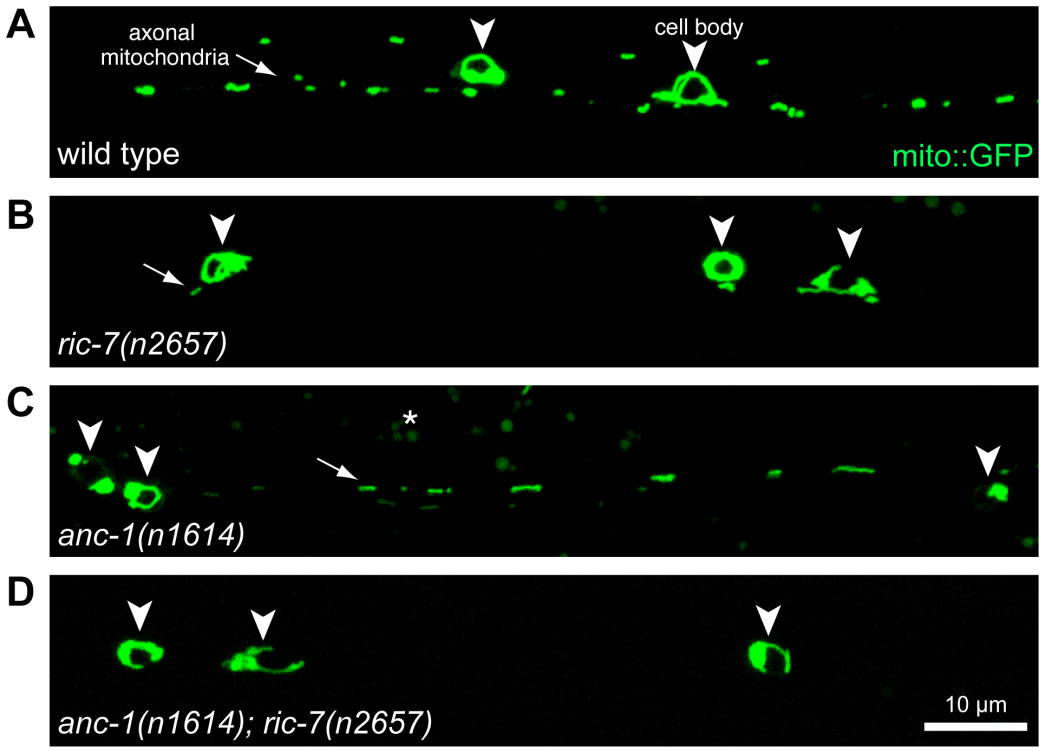

Figure 4.3. *anc-1* does not suppress *ric-7*. (A) In wild-type worms, mitochondria are located in cell bodies (arrowheads) and along axons (arrow). (B) In *ric-7* mutants, the mitochondria are sequestered to the cell bodies. (C) Mitochondria are located along axons in *anc-1* mutants. The mitochondria in the cell bodies to the far right and far left appear to be clustered at one or both ends of the nucleus. The asterisk indicates autofluorescence from the gut. (D) In *anc-1*; *ric-7* double mutants, the mitochondria are still trapped within the cell bodies. All worms are expressing P*unc-47*::Tom20::GFP 'mito::GFP'. Worms were imaged with their ventral nerve cord facing the objective.

Transport

Thus far, the data support the third model for RIC-7 function, namely that it is required for mitochondrial transport. Much like kinesin-1 mutants, there is a near total loss of mitochondria in *ric-7* mutant axons. Instead, the mitochondria appear to be trapped and accumulated within the neuron cell bodies. On occasion, there will be one or two mitochondria that have exited the cell body; however, they are typically located at very short distances from the cell body (arrow, Figure 4.3B). This suggests that the mitochondria are not able to move very far along the axon, even if they do manage to exit the cell body. The few mitochondria that exit the cell body in kinesin-1 mutants are similarly localized. It is possible that these mitochondria are being carried small distances by myosin motors, which are known to locally transport mitochondria along actin (Zinsmaier et al., 2009).

Further support for the role of RIC-7 in transport comes from the dominant negative DRP-1 experiments. The long mitochondria tubules in DRP-1(K40S) worms could be extending along the axons by pushing their way out as mitochondria biogenesis continues in the cell body, in other words, by passive displacement. Alternatively, the long tubules could be transported down the axon. The data strongly support the latter scenario. Long tubular mitochondria do not extend out of cell bodies in kinesin-1; DRP-1(K40S) double mutants (Figure 4.2). This demonstrates that the mitochondrial tubule extension is dependent upon transport by kinesin motors. The mitochondrial tubules are also absent in *ric-7*; DRP-1(K40S) double mutants, suggesting that *ric-7* is also involved in

mitochondrial transport (Figure 4.2).

In addition, *ric-7* can be acutely rescued. Expressing *ric-7* under a heat shock promoter can rapidly restore mitochondria transport in the GABA motor neurons of *ric-7(n2657)* mutants. L4 worms were heat shocked for 1 hr at 32°C. Time-lapse confocal recordings were then taken over the next hour. Each worm was recoded for 10 minutes. After heat shock, mobile mitochondria were seen in 9 out of 12 worms and all worms had mitochondria restored in their proximal axons (Figure 4.4). Worms carrying the rescue array but without heat shock treatment were not rescued for axonal mitochondria (0/30 worms). Such rapid rescue of transport implies that there may not be many steps between RIC-7's function and transport of mitochondria. Taken together, the data thus far suggest that RIC-7 plays a role prior to or during mitochondrial transport.

Mitochondrial Transport

Miro and Milton

There are three known adaptors for mitochondrial transport; Miro, Milton, and Syntabulin (Guo et al., 2005; Stowers et al., 2002). Miro contains two EF-hand motifs flanked by GTPase domains, and is inserted into the mitochondrial outer membrane at its C-terminus (Fransson et al., 2003; Frederick et al., 2004). Milton can bind to both Miro and kinesin (Glater et al., 2006); thus, together these two proteins create a bridge between mitochondria and kinesin. Miro can be regulated by calcium via the EF-hand motifs (Saotome et al., 2008). There are

Figure 4.4. Acute rescue of *ric-7* using a heat shock promoter. (A) The *ric-7* rescue construct was placed under a heat shock promoter (P*hsp16-41*). (B) L4 worms were heat shocked for 1 hr in a 32°C water bath. Worms were then mounted on 10% agarose pads and immobilized with microbeads. Mitochondria transport in the ventral nerve cord of GABA motor neurons was recorded on a Nikon spinning disk confocal. All worms were imaged for 10 min and within the first hour after heat shock. (C) Mitochondria transport is rapidly restored in ventral nerve cord axons following heat shock. The orange arrowhead points to a mitochondrion that is transporting down the axon. The other two mitochondria are stable. (D) Kymographs representing an entire individual experiment. The y-axis is time and the x-axis represents the location of the mitochondria along the axon. Straight vertical lines correspond to mitochondria that were stable throughout the recording. Slanted lines correspond to mobile mitochondria. The majority of mitochondria in a wild type are stable, whereas a greater percentage of mitochondria can be seen transporting in *ric(n2657)*; *hsp::ric-7* following heat shock. (E) The percent of mitochondria that are mobile over 10 min in the GABA motor neuron ventral nerve cord. Mean (black horizontal line) +/- SEM. On average, 27% of mitochondria are mobile in wild-type worms. There is a slight increase in mobility following heat shock. A greater percentage of mitochondria are mobile following heat shock rescue of *ric-7(n2657)* mutants. The average percent of mitochondria that are mobile is the same in the constitutive rescued worms [*ric-7(n2657)*; P*unc-47*::RFP::RIC-7, 'RIC-7(+)'] compared to wild type. The number of animals is indicated above. N= number of animals. n= number of time lapse recordings. (F) Heat shock induced rescue of *ric-7* restores the total number of mitochondria per 50 µm to wild-type levels. Without heat shock, 0/30 worms were rescued for mitochondria localization in axons. Time-lapse recordings were not taken of these animals, but from previous experiments, we know that the number of mitochondria per 50 µm is close to zero in *ric-7(n2657)* (see Figure 3.2). The same n values apply as in the graph above.

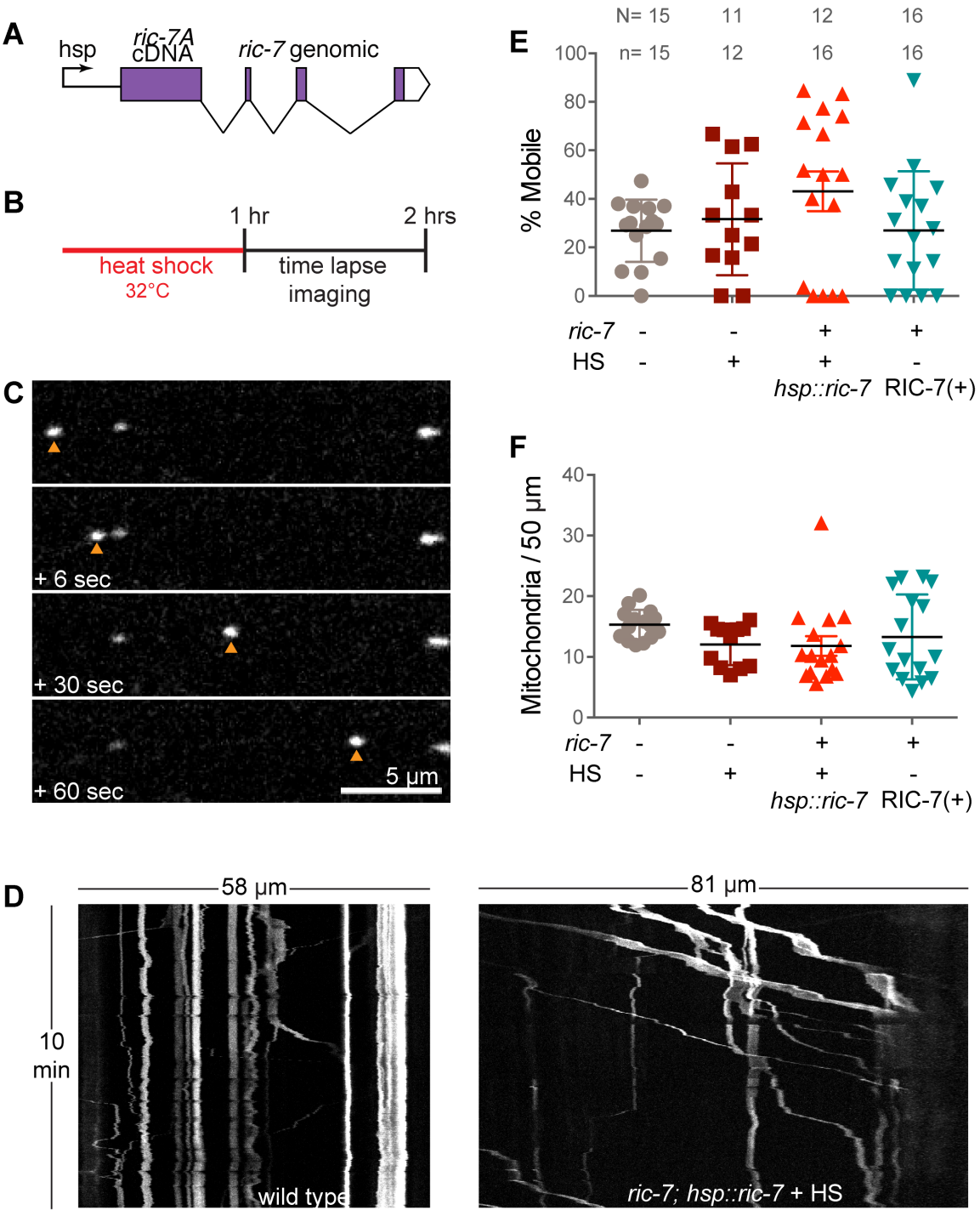
A
hsp
ric-7A cDNA
ric-7 genomic
B
1 hr
2 hrs
heat shock
32°C
time lapse
imaging
C
+ 6 sec
+ 30 sec
+ 60 sec
5 µm
D
58 µm
10 min
wild type
81 µm
ric-7; hsp::ric-7 + HS
E
N= 15 11 12 16
n= 15 12 16 16
% Mobile
ric-7 - - + +
HS - + + -
hsp::ric-7 RIC-7(+)
F
Mitochondria / 50 µm
ric-7 - - + +
HS - + + -
hsp::ric-7 RIC-7(+)

two different models for how calcium is negatively regulating transport through Miro. In one study, Miro was shown to bind directly to the kinesin motor KIF5 and this interaction is inhibited in the presence of calcium (MacAskill et al., 2009). Thus, in the presence of calcium mitochondria disassociate from kinesin. However, a second study using *Drosophila* Milton within mammalian systems proposes a different model (Wang and Schwarz, 2009). They show that human Miro cannot bind to rat KHC (kinesin heavy chain) unless *Drosophila* Milton is present. In the presence of calcium, the kinesin motor domain dissociates from microtubules and binds to Miro. They also show that all mitochondria, even stationary ones, are associated with kinesin. Together the data suggest that calcium mediated transport arrest is due to kinesin dissociation from microtubules rather than from a mitochondria transport complex (Wang and Schwarz, 2009).

Syntabulin

Syntabulin is a single adaptor protein that binds to kinesin 1 and can associate peripherally with the mitochondria membrane (Cai, 2005; Su et al., 2004). Cultured neurons expressing siRNA against syntabulin have reduced numbers of mitochondria in processes and disrupted mitochondrial transport (Cai, 2005; Ma et al., 2009). Axons expressing siRNA against syntabulin have an increase in stable mitochondria and a dramatic decrease in the percent of mitochondria that are transporting anterogradely (Cai, 2005). It is not known how the function of syntabulin overlaps with, or differentiates from, that of Miro and

Milton. Syntabulin also has a reduction in syntaxin and active zone puncta in axons (Cai et al., 2007; Su et al., 2004). It would be interesting to know if these two results are related. Could it be that there are reduced mitochondria in axons because there are fewer synapses, or vice versa? Syntabulin exists solely in vertebrates and appears to be rapidly diverging, with only 44% identity between mice and zebrafish, compared to 80% for Miro.

Mitochondrial transport in *C. elegans*

Miro and Milton do not have a confirmed function in mitochondrial transport in *C. elegans*. There are three genes that encode Miro homologs in the worm. These genes appear to be the result of a duplication of the Miro gene since they are nearly identical. Deletion mutations in each are viable; however, RNAi against *miro* is lethal, suggesting that they act redundantly. We have examined a deletion mutant for *miro-1* and the mitochondria are transported into the GABA motor neuron axons. It is possible that the removal of all three *miro* genes would result in a severe mitochondrial trafficking defect if the worms were viable.

The Milton homolog in the worm is T27A3.1, which is 32% identical to the mouse TRAK1 (trafficking protein kinesin-binding) and 24% identical to *Drosophila* Milton. The mutation *tm1572* contains a 706 nt deletion beginning in the middle of the conserved coiled-coil domain that has been shown to bind Kinesin (Smith et al., 2006), followed by a frameshift and a premature stop codon a few amino acids later. Thus, the *tm1572* allele is likely to be a null mutation due

to nonsense-mediated decay. Surprisingly, the mutant does not exhibit a profound defect in mitochondria localization in motor neurons. On occasion, there are increased gaps between mitochondria in the dorsal nerve cord (Figure 4.5), but in general, the mitochondria are able to transport out into axons. While Milton mutants have very severe losses of mitochondria in the fly, knock down of both TRAK1 and 2 in mammalian neurons results in transport abnormalities but not a total loss of mitochondria (Brickley and Stephenson, 2011; van Spronsen et al., 2013). The mammalian TRAK proteins are weakly homologous to Drosophila Milton, with just 22% identity (MacAskill et al., 2009). It is likely that T27A3.1 is more similar in function to TRAK than *Drosophila* Milton.

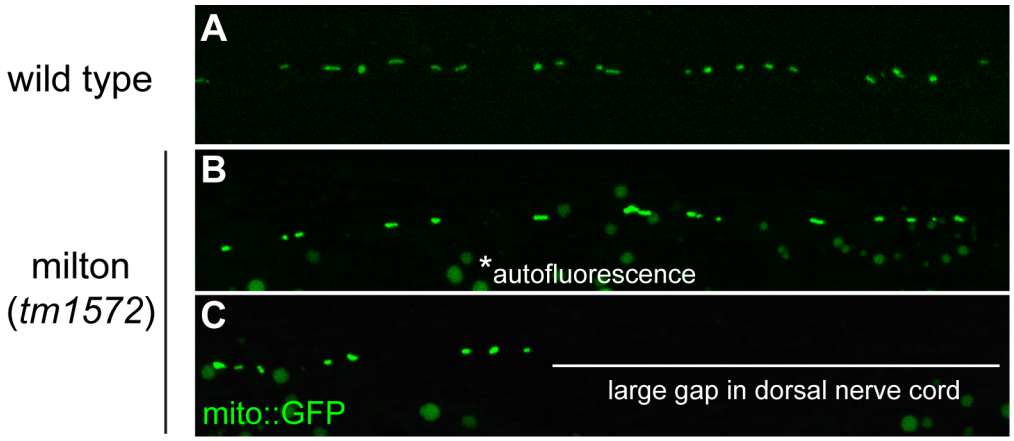

Figure 4.5. *C. elegans* milton mutants have minor defects in mitochondrial localization. mito::GFP is expressed in the GABA neurons. Worms were imaged with their dorsal side facing the objective. The dorsal nerve cord represents the most distal portion of the GABA motor neuron axons. (A) In wild-type worms, mitochondria are evenly distributed along the dorsal nerve cord. (B) In milton mutants, the mitochondria are usually properly localized. (C) Occasionally, gaps in the coverage of the dorsal nerve cord are observed.

Since RNAi against *miro* is lethal and it is highly conserved from humans to yeast, it seems very likely that *miro* will also be required for mitochondrial transport in *C. elegans*. But how is Miro interacting with kinesin if the closest Milton homologue is not involved? Can *C. elegans* MIRO directly bind to Kinesin/UNC-116 as demonstrated by the Kittery lab (MacAskill et al., 2009)? Or could another protein be serving the function of Milton in *C. elegans*, such as RIC-7? If RIC-7 is serving as a bridge between the kinesin motor and the mitochondria, then we should be able to see RFP::RIC-7 transporting along with mitochondria. In *C. elegans* GABA motor neurons, 27% of mitochondria in the ventral nerve cord are mobile. However, RFP::RIC-7 was not seen transporting along the axons. Future genetic screens and biochemistry experiments are needed in order to resolve RIC-7's mechanism. Establishing the interaction partners for RIC-7 may uncover a novel mechanism for regulating mitochondrial transport in neurons.

Mitochondrial Transport and Neurodegeneration

Many neurodegenerative disorders have been linked to mitochondrial defects, as discussed in Chapter 1. It is not clear whether these defects are secondary effects of disease or whether they could be causative for degeneration. Recent studies, including the work in this dissertation, demonstrate that defects in mitochondria localization are sufficient to induce degeneration (Chapter 2; Fang et al., 2012; Iijima-Ando et al., 2012; Misko et al., 2012). These results argue that the disruption of mitochondria transport or localization is

causative for degeneration. Of the mitochondrial defects associated with neurodegenerative disease, many are related to the transport and localization of mitochondria.

Transport machinery mutations

Some diseases are associated with mutations in the transport machinery. Mitochondria transport is disrupted in the absence of the kinesin KIF5A (Karle et al., 2012) and the mammalian homolog for Milton has been shown to interact with KIF5A (Brickley et al., 2005). Human mutations in KIF5A have been identified in families with the hereditary neurodegenerative diseases, spastic paraplegia and Charcot-Marie-Tooth type 2 (Crimella et al., 2012; Musumeci et al., 2011; Reid et al., 2002). Mutations in the dynactin subunit p150Glued are associated with both sporadic and familial forms of ALS (Münch et al., 2004). Notably, the mammalian Milton homolog TRAK has recently been shown to bind p150Glued and regulate retrograde transport of mitochondria (van Spronsen et al., 2013).

Mitofusin2

Disruption of the mitochondrial fusion protein Mitofusin2 (Mfn2) causes the neurodegenerative disease Charcot-Marie-Tooth type 2 in humans (Cartoni and Martinou, 2009). However, mitochondria transport may be more relevent to their pathology than fusion. Both mutants and knockouts of Mfn2 have reduced mitochondria transport (Baloh et al., 2007; Misko et al., 2010, 2012). Fusion

defective mitochondria may have altered transport due to the propensity for dysfunctional mitochondria to be transported back to the cell body (Miller and Sheetz, 2004). However, the mutant Mfn 2 mitochondria do not display defects in membrane potential or ATP levels (Baloh et al., 2007; Misko et al., 2012). In addition, Mfn2 can directly interact with the transport adaptor proteins Miro and Milton (Misko et al., 2010), and mutant Mfn2 leads to reduced mitochondria velocity and increased pause times (Misko et al., 2010). Together the data suggest that Mfn2 may have a role in regulating mitochondria transport dynamics. Most recently, it was demonstrated that cultured DRG neurons with mutant Mfn2 undergo degeneration due to impairments in mitochondria distribution and not fusion (Misko et al., 2012).

ALS, Alzheimer's, and Huntington's diseases

In general, mitochondria transport defects have been identified in many neurodegenerative disease patients and models, including ALS, Alzheimer's, and Huntington's. The most common source of familial ALS are mutations in Cu/Zn superoxide dismutase-1 (SOD1). SOD1 mutant axons have reduced numbers of mitochondria due to a decrease in anterograde and an increase in retrograde transport (De Vos et al., 2007). A subsequent study showed that mobility is reduced in both anterograde and retrograde directions when neurons were expressing mutant human SOD1 (Magrané et al., 2009). Fibroblasts from Alzheimer's patients have fewer and mislocalized mitochondria (Wang et al., 2008), and postmortem analysis of the hippocampus in patients revealed that

mitochondria are largely absent from axons (Wang et al., 2009). An amyloid beta precursor protein (AβPP) mouse model revealed a strong reduction in anterograde transport of mitochondria (Calkins et al., 2011). There is also strong evidence implicating a key role for transport in Huntington's disease. Expressing mutant huntingtin (mHtt) in cultured neurons led to aggregates of mHtt in axons, with which mitochondria were preferentially colocalized. Mitochondria that were associated with mHtt aggregates were dramatically less mobile, whereas those not associated with aggregates had wild-type levels of mobility (Chang et al., 2006). The velocity of mitochondria transport is also reduced in response to mutated Htt and to the knockout (Orr et al., 2008; Trushina et al., 2004).

However, many of these findings are complicated by other defects, such as a general disruption of axonal transport (Gunawardena et al., 2003; Lee et al., 2004). It was not clear whether the lack of mitochondria is sufficient for degeneration. Our results demonstrate that mitochondrial mislocalization is sufficient for degeneration. It is possible that mitochondrial dynamics have a key underlying role in neurodegenerative diseases. Perhaps more disorders are associated with defective mitochondrial transport over mitochondria dysfunction than we currently realize.

Mitochondrial transport as a therapeutic target

Could mitochondrial transport be a therapeutic target for treating neurodegnerative disease? If axons are highly susceptible to the mislocalization or aberrant transport of mitochondria, then perhaps augmenting their mobility

could be neuroprotective. Forcing mitochondria into axons by directly linking them to kinesin with a chimeric protein robustly suppressed axon degeneration in *ric-7* mutants (Figure 2.4). This suggests that enhancing transport can effectively treat a mitochondria mislocalization disorder. The axon protective chimeric protein Wld^S has also been linked to mitochondria transport. Wld^S has many effects on the cell, one of which is to increase the number of mobile mitochondria following an injury compared to wild type (Avery et al., 2012; O'Donnell et al., 2013). It is not known whether the increase in transport is required for the protective effects of Wld^S.

Removal of HDAC6 (histone deacetylase) can also promote transport through an increase in microtubule acetylation (Chen et al., 2010; Dompierre et al., 2007; Hubbert et al., 2002; Matsuyama et al., 2002). Both kinesin and dynein can bind more efficiently to acetylated microtubules and transport is generally increased in these mutants (Dompierre et al., 2007). Mitochondrial transport is reduced in a HSPB1 Charcot-Marie-Tooth mouse model and inhibiting HDAC6 improved both mitochondria transport and motor performance (d' Ydewalle et al., 2011). HDAC6 inhibitors are also able to augment mitochondrial transport in an Alzheimer's disease model (Kim et al., 2012) and HDAC6 knockout improved both memory and mitochondria localization in another AD mouse model (Govindarajan et al., 2013). It is not certain whether these mouse models are recovering due to a restoration of mitochondrial transport, or whether transport in general has to be increased for effective prevention of degeneration.

Another study indicates that increasing mitochondria transport is not likely

to be therapeutic. Mitochondria transport can be increased by removing syntaphilin, which blocks transport by anchoring mitochondria to microtubules in axons (Chen and Sheng, 2013; Chen et al., 2009). For example, 76% of hippocampal mitochondria are mobile in syntaphilin knockouts compared to 36% in the wild type (Kang et al., 2008). The ALS mouse model $SOD1^{G93A}$ has a 50% reduction in mitochondria mobility in cultured DRG neurons and removing syntaphilin can increase mobility to above wild-type levels. However, removing syntaphilin did not prevent neurodegeneration of motor neurons in the ALS $SOD1^{G93A}$ mice (Zhu and Sheng, 2011). Thus, increasing mitochondria mobility may not be a reliable means to prevent degeneration. Evidence suggests that hyper-mobile mitochondria are unable to effectively buffer calcium after high stimulation (Kang et al., 2008). The mitochondria in the syntaphilin knock outs might be similarly unsuited for the demands of a neurodegnerative disease model.

The literature suggests that we are far from understanding the role of mitochondria transport in preventing degeneration. The stopping locations and exact distribution of mitochondria may be more important in preventing degeneration than their mobility (Misko et al., 2012). The transport dynamics of mitochondria in the Kinesin::Tom7 transport chimera experiments are unknown. Can mitochondria stabilization still be regulated when the organelle is forcibly linked to kinesin? Interestingly, of the three existing models for mitochondria stabilization, only one could presumably still function in these animals. The three models for stabilization are; i) syntaphilin-mediated anchoring to microtubules,

but there is no syntaphilin homolog in *C. elegans,* ii) dissociation of kinesin from the adaptor complex, and iii) kinesin motor domain dissociation from microtubules and binding to Miro. In *ric-7* mutants expressing the Kinesin::Tom7 transport chimera, kinesin is incapable of dissociating from mitochondria. However, the kinesin in the transport chimera could still presumably fold back and bind to MIRO on the mitochondria surface (Figure 4.6). If model ii is correct, all mitochondria should be mobile in these worms. If model iii is correct, only a portion of mitochondria should be mobile. Observing mitochondria transport and localization in *ric-7*; Kinesin::Tom7 worms can additionally answer questions about the importance of mitochondria localization in preventing degneration. Do the mitochondria have to be docked at synapses or located near the lesion site? Or do the mitochondria simply have to be present? In conclusion, *ric-7* mutants will continue to be a useful tool for studying the rules governing both mitochondria dynamics and axon degeneration.

Acknowledgments

We would like to thank Dane Maxfield, Fred Horndli, and Villu Maricq for the use of their spinning disc Nikon confocal and for all assistance with the time-lapse imaging. The milton and miro strains mentioned in this chapter were provided by the Mitani National BioResource Project for *C. elegans*.

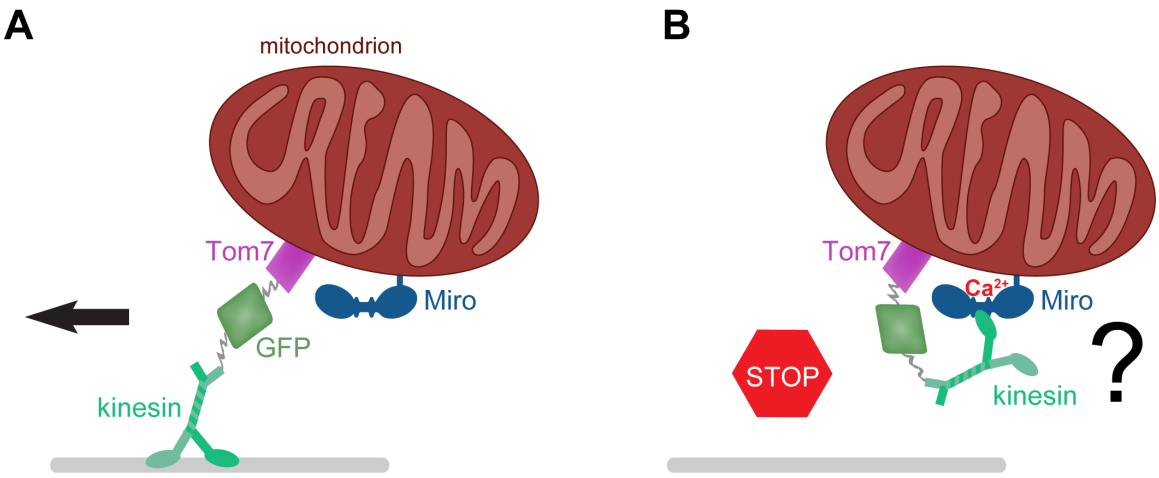

Figure 4.6. How are *C. elegans* mitochondria stabilized within axons? Previous studies demonstrate that mitochondria are stabilized within axons by syntaphilin, dissociation from the motor, or dissociation from microtubules. *C. elegans* do not have a syntaphilin homolog. (A) In *ric-7* mutants expressing the transport chimera Kinesin::Tom7, all axonal mitochondria are incapable of dissociating from the motor. Time-lapse imaging of mitochondria within this strain can determine whether all mitochondria are mobile. (B) If the model that the kinesin motor domain can dissociate from microtubules and bind to Miro is correct, then transport chimera mitochondria are predicted to be stable within *ric-7* mutant axons. *ric-7* mutants will continue to be a useful tool for the study of mitochondria dynamics. Miro structure is adapted from Schwartz *et al.* (2013).

References

Avery, M.A., Rooney, T.M., Pandya, J.D., Wishart, T.M., Gillingwater, T.H., Geddes, J.W., Sullivan, P.G., and Freeman, M.R. (2012). WldS prevents axon degeneration through increased mitochondrial flux and enhanced mitochondrial Ca2+ buffering. Curr. Biol. 1–5.

Awasaki, T., Tatsumi, R., Takahashi, K., Arai, K., Nakanishi, Y., Ueda, R., and Ito, K. (2006). Essential role of the apoptotic cell engulfment genes draper and ced-6 in programmed axon pruning during drosophila metamorphosis. Neuron *50*, 855–867.

Baloh, R.H., Schmidt, R.E., Pestronk, A., and Milbrandt, J. (2007). Altered axonal mitochondrial transport in the pathogenesis of Charcot-Marie-Tooth disease from mitofusin 2 mutations. J. Neurosci. Off. J. Soc. Neurosci. *27*, 422–430.

Barrientos, S.A., Martinez, N.W., Yoo, S., Jara, J.S., Zamorano, S., Hetz, C.,

Twiss, J.L., Alvarez, J., and Court, F.A. (2011). Axonal degeneration is mediated by the mitochondrial permeability transition pore. J. Neurosci. *31*, 966–978.

Bleazard, W., McCaffery, J.M., King, E.J., Bale, S., Mozdy, A., Tieu, Q., Nunnari, J., and Shaw, J.M. (1999). The dynamin-related GTPase Dnm1 regulates mitochondrial fission in yeast. Nat. Cell Biol. *1*, 298–304.

Bliek, A.M. van der, Shen, Q., and Kawajiri, S. (2013). Mechanisms of mitochondrial fission and fusion. Cold Spring Harb. Perspect. Biol. *5*, a011072.

Brickley, K., and Stephenson, F.A. (2011). Trafficking kinesin protein (TRAK)-mediated transport of mitochondria in axons of hippocampal neurons. J. Biol. Chem. *286*, 18079–18092.

Brickley, K., Smith, M.J., Beck, M., and Stephenson, F.A. (2005). GRIF-1 and OIP106, members of a novel gene family of coiled-coil domain proteins association in vivo and in vitro with kinesin. J. Biol. Chem. *280*, 14723–14732.

Cai, Q. (2005). Syntabulin-mediated anterograde transport of mitochondria along neuronal processes. J. Cell Biol. *170*, 959–969.

Cai, Q., Pan, P.-Y., and Sheng, Z.-H. (2007). Syntabulin-Kinesin-1 family member 5b-mediated axonal transport contributes to activity-dependent presynaptic assembly. J. Neurosci. *27*, 7284–7296.

Calì, T., Ottolini, D., and Brini, M. (2012). Mitochondrial Ca2+ and neurodegeneration. Cell Calcium *52*, 73–85.

Calkins, M.J., Manczak, M., Mao, P., Shirendeb, U., and Reddy, P.H. (2011). Impaired mitochondrial biogenesis, defective axonal transport of mitochondria, abnormal mitochondrial dynamics and synaptic degeneration in a mouse model of Alzheimer's disease. Hum. Mol. Genet. *20*, 4515–4529.

Calupca, M.A.M., Hendricks, G.M.G., Hardwick, J.C.J., and Parsons, R.L.R. (1999). Role of mitochondrial dysfunction in the Ca2+-induced decline of transmitter release at K+-depolarized motor neuron terminals. J. Neurophysiol. *81*, 498–506.

Cartoni, R., and Martinou, J.-C. (2009). Role of mitofusin 2 mutations in the physiopathology of Charcot-Marie-Tooth disease type 2A. Exp. Neurol. *218*, 268–273.

Chang, D.T.W., Rintoul, G.L., Pandipati, S., and Reynolds, I.J. (2006). Mutant huntingtin aggregates impair mitochondrial movement and trafficking in cortical neurons. Neurobiol. Dis. *22*, 388–400.

Chen, Y., and Sheng, Z.-H. (2013). Kinesin-1-syntaphilin coupling mediates activity-dependent regulation of axonal mitochondrial transport. J. Cell Biol. *202*,

351–364.

Chen, S., Owens, G.C., Makarenkova, H., and Edelman, D.B. (2010). HDAC6 regulates mitochondrial transport in hippocampal neurons. PloS One *5*, e10848.

Chen, Y.-M., Gerwin, C., and Sheng, Z.-H. (2009). Dynein light chain LC8 regulates syntaphilin-mediated mitochondrial docking in axons. J. Neurosci. *29*, 9429–9438.

Crimella, C., Baschirotto, C., Arnoldi, A., Tonelli, A., Tenderini, E., Airoldi, G., Martinuzzi, A., Trabacca, A., Losito, L., Scarlato, M., et al. (2012). Mutations in the motor and stalk domains of KIF5A in spastic paraplegia type 10 and in axonal Charcot–Marie–Tooth type 2. Clin. Genet. *82*, 157–164.

Ding, J.M., Buchanan, G.F., Tischkau, S.A., Chen, D., Kuriashkina, L., Faiman, L.E., Alster, J.M., McPherson, P.S., Campbell, K.P., and Gillette, M.U. (1998). A neuronal ryanodine receptor mediates light-induced phase delays of the circadian clock. Nature *394*, 381–384.

Dompierre, J.P., Godin, J.D., Charrin, B.C., Cordelières, F.P., King, S.J., Humbert, S., and Saudou, F. (2007). Histone deacetylase 6 inhibition compensates for the transport deficit in Huntington's disease by increasing tubulin acetylation. J. Neurosci. Off. J. Soc. Neurosci. *27*, 3571–3583.

Dray, A., Forbes, C.A., and Burgess, G.M. (1990). Ruthenium red blocks the capsaicin-induced increase in intracellular calcium and activation of membrane currents in sensory neurones as well as the activation of peripheral nociceptors in vitro. Neurosci. Lett. *110*, 52–59.

Fang, Y., Soares, L., Teng, X., Geary, M., and Bonini, N.M. (2012). A Novel Drosophila Model of Nerve Injury Reveals an Essential Role of Nmnat in Maintaining Axonal Integrity. Curr. Biol. 1–6.

Fransson, A., Ruusala, A., and Aspenström, P. (2003). Atypical Rho GTPases have roles in mitochondrial homeostasis and apoptosis. J. Biol. Chem. *278*, 6495–6502.

Frederick, R.L., McCaffery, J.M., Cunningham, K.W., Okamoto, K., and Shaw, J.M. (2004). Yeast Miro GTPase, Gem1p, regulates mitochondrial morphology via a novel pathway. J. Cell Biol. *167*, 87–98.

Fünfschilling, U., Supplie, L.M., Mahad, D., Boretius, S., Saab, A.S., Edgar, J., Brinkmann, B.G., Kassmann, C.M., Tzvetanova, I.D., Möbius, W., et al. (2013). Glycolytic oligodendrocytes maintain myelin and long-term axonal integrity. Nature *485*, 517–521.

George, E.B., Glass, J.D., and Griffin, J.W. (1998). Axotomy-induced axonal degeneration is mediated by calcium influx through ion-specific channels. J.

Neurosci. Off. J. Soc. Neurosci. *15*, 6445–6452.

Glater, E.E., Megeath, L.J., Stowers, R.S., and Schwarz, T.L. (2006). Axonal transport of mitochondria requires milton to recruit kinesin heavy chain and is light chain independent. J. Cell Biol. *173*, 545–557.

Govindarajan, N., Rao, P., Burkhardt, S., Sananbenesi, F., Schlüter, O.M., Bradke, F., Lu, J., and Fischer, A. (2013). Reducing HDAC6 ameliorates cognitive deficits in a mouse model for Alzheimer's disease. EMBO Mol. Med. *5*, 52–63.

Gunawardena, S., Her, L.-S., Brusch, R.G., Laymon, R.A., Niesman, I.R., Gordesky-Gold, B., Sintasath, L., Bonini, N.M., and Goldstein, L.S.B. (2003). Disruption of axonal transport by loss of huntingtin or expression of pathogenic polyQ proteins in Drosophila. Neuron *40*, 25–40.

Guo, X., Macleod, G.T., Wellington, A., Hu, F., Panchumarthi, S., Schoenfield, M., Marin, L., Charlton, M.P., Atwood, H.L., and Zinsmaier, K.E. (2005). The GTPase dMiro is required for axonal transport of mitochondria to Drosophila synapses. Neuron *47*, 379–393.

Hedgecock, E.M., and Thomson, J.N. (1982). A gene required for nuclear and mitochondrial attachment in the nematode Caenorhabditis elegans. Cell *30*, 321–330.

Hoopfer, E., Mclaughlin, T., Watts, R., Schuldiner, O., Oleary, D., and Luo, L. (2006). Wlds protection distinguishes axon degeneration following injury from naturally occurring developmental pruning. Neuron *50*, 883–895.

Hubbert, C., Guardiola, A., Shao, R., Kawaguchi, Y., Ito, A., Nixon, A., Yoshida, M., Wang, X.-F., and Yao, T.-P. (2002). HDAC6 is a microtubule-associated deacetylase. Nature *417*, 455–458.

Iijima-Ando, K., Sekiya, M., Maruko-Otake, A., Ohtake, Y., Suzuki, E., Lu, B., and Iijima, K.M. (2012). Loss of axonal mitochondria promotes tau-mediated neurodegeneration and Alzheimer's disease–related tau phosphorylation via PAR-1. PLoS Genet. *8*, e1002918.

Ingerman, E., Perkins, E.M., Marino, M., Mears, J.A., McCaffery, J.M., Hinshaw, J.E., and Nunnari, J. (2005). Dnm1 forms spirals that are structurally tailored to fit mitochondria. J. Cell Biol. *170*, 1021–1027.

Kang, J.-S., Tian, J.-H., Pan, P.-Y., Zald, P., Li, C., Deng, C., and Sheng, Z.-H. (2008). Docking of axonal mitochondria by syntaphilin controls their mobility and affects short-term facilitation. Cell *132*, 137–148.

Karle, K.N., Möckel, D., Reid, E., and Schöls, L. (2012). Axonal transport deficit in a KIF5A(-/-) mouse model. Neurogenetics *13*, 169–179.

Keller, L.C., Cheng, L., Locke, C.J., Müller, M., Fetter, R.D., and Davis, G.W. (2011). Glial-derived prodegenerative signaling in the drosophila neuromuscular system. Neuron *72*, 760–775.

Kim, C., Choi, H., Jung, E.S., Lee, W., Oh, S., Jeon, N.L., and Mook-Jung, I. (2012). HDAC6 inhibitor blocks amyloid beta-induced impairment of mitochondrial transport in hippocampal neurons. PLoS ONE *7*, e42983.

Knöferle, J., Koch, J.C., Ostendorf, T., Michel, U., Planchamp, V., Vutova, P., Tönges, L., Stadelmann, C., Brück, W., Bähr, M., et al. (2010). Mechanisms of acute axonal degeneration in the optic nerve in vivo. Proc. Natl. Acad. Sci. *107*, 6064–6069.

Lee, W.-C.M., Yoshihara, M., and Littleton, J.T. (2004). Cytoplasmic aggregates trap polyglutamine-containing proteins and block axonal transport in a Drosophila model of Huntington's disease. Proc. Natl. Acad. Sci. U. S. A. *101*, 3224–3229.

Ma, H., Cai, Q., Lu, W., Sheng, Z.-H., and Mochida, S. (2009). KIF5B motor adaptor syntabulin maintains synaptic transmission in sympathetic neurons. J. Neurosci. Off. J. Soc. Neurosci. *29*, 13019–13029.

MacAskill, A.F., Rinholm, J.E., Twelvetrees, A.E., Arancibia-Carcamo, I.L., Muir, J., Fransson, A., Aspenstrom, P., Attwell, D., and Kittler, J.T. (2009). Miro1 Is a calcium sensor for glutamate receptor-dependent localization of mitochondria at synapses. Neuron *61*, 541–555.

Macdonald, J., Beach, M., Porpiglia, E., Sheehan, A., Watts, R., and Freeman, M. (2006). The Drosophila cell corpse engulfment receptor draper mediates glial clearance of severed axons. Neuron *50*, 869–881.

Magrané, J., Hervias, I., Henning, M.S., Damiano, M., Kawamata, H., and Manfredi, G. (2009). Mutant SOD1 in neuronal mitochondria causes toxicity and mitochondrial dynamics abnormalities. Hum. Mol. Genet. *18*, 4552–4564.

Matsuyama, A., Shimazu, T., Sumida, Y., Saito, A., Yoshimatsu, Y., Seigneurin-Berny, D., Osada, H., Komatsu, Y., Nishino, N., Khochbin, S., et al. (2002). In vivo destabilization of dynamic microtubules by HDAC6-mediated deacetylation. EMBO J. *21*, 6820–6831.

Miller, K.E., and Sheetz, M.P. (2004). Axonal mitochondrial transport and potential are correlated. J. Cell Sci. *117*, 2791–2804.

Misko, A.A., Jiang, S.S., Wegorzewska, I.I., Milbrandt, J.J., and Baloh, R.H.R. (2010). Mitofusin 2 is necessary for transport of axonal mitochondria and interacts with the Miro/Milton complex. J. Neurosci. Off. J. Soc. Neurosci. *30*, 4232–4240.

Misko, A.L., Sasaki, Y., Tuck, E., Milbrandt, J., and Baloh, R.H. (2012).

Mitofusin2 mutations disrupt axonal mitochondrial positioning and promote axon degeneration. J. Neurosci. Off. J. Soc. Neurosci. *32*, 4145–4155.

Montero, M., Alonso, M.T., Carnicero, E., Cuchillo-Ibáñez, I., Albillos, A., García, A.G., García-Sancho, J., and Alvarez, J. (2000). Chromaffin-cell stimulation triggers fast millimolar mitochondrial Ca2+ transients that modulate secretion. Nat. Cell Biol. *2*, 57–61.

Münch, C., Sedlmeier, R., Meyer, T., Homberg, V., Sperfeld, A.D., Kurt, A., Prudlo, J., Peraus, G., Hanemann, C.O., Stumm, G., et al. (2004). Point mutations of the p150 subunit of dynactin (DCTN1) gene in ALS. Neurology *63*, 724–726.

Musumeci, O., Bassi, M.T., Mazzeo, A., Grandis, M., Crimella, C., Martinuzzi, A., and Toscano, A. (2011). A novel mutation in KIF5A gene causing hereditary spastic paraplegia with axonal neuropathy. Neurol. Sci. *32*, 665–668.

O'Donnell, K.C., Vargas, M.E., and Sagasti, A. (2013). WldS and PGC-1 regulate mitochondrial transport and oxidation state after axonal injury. J. Neurosci. *33*, 14778–14790.

Orr, A.L., Li, S., Wang, C.E., Li, H., Wang, J., Rong, J., Xu, X., Mastroberardino, P.G., Greenamyre, J.T., and Li, X.J. (2008). N-terminal mutant huntingtin associates with mitochondria and impairs mitochondrial trafficking. J. Neurosci. *28*, 2783–2792.

Otsuga, D., Keegan, B.R., Brisch, E., Thatcher, J.W., Hermann, G.J., Bleazard, W., and Shaw, J.M. (1998). The Dynamin-related GTPase, Dnm1p, controls mitochondrial morphology in yeast. J. Cell Biol. *143*, 333–349.

Pivovarova, N.B., Hongpaisan, J., Andrews, S.B., and Friel, D.D. (1999). Depolarization-induced mitochondrial Ca accumulation in sympathetic neurons: spatial and temporal characteristics. J. Neurosci. *19*, 6372–6384.

Rangaraju, V., Calloway, N., and Ryan, T.A. (2014). Activity-driven local atp synthesis is required for synaptic function. Cell *156*, 825–835.

Reid, E., Kloos, M., Ashley-Koch, A., Hughes, L., Bevan, S., Svenson, I.K., Graham, F.L., Gaskell, P.C., Dearlove, A., Pericak-Vance, M.A., et al. (2002). A kinesin heavy chain (KIF5A) mutation in hereditary spastic paraplegia (SPG10). Am. J. Hum. Genet. *71*, 1189–1194.

Saotome, M., Safiulina, D., Szabadkai, G., Das, S., Fransson, Å., Aspenstrom, P., Rizzuto, R., and Hajnóczky, G. (2008). Bidirectional Ca2+-dependent control of mitochondrial dynamics by the Miro GTPase. Proc. Natl. Acad. Sci. *105*, 20728–20733.

Schon, E.A., and Przedborski, S. (2011). Mitochondria: the next (neurode)

generation. Neuron *70*, 1033–1053.

Shoshan-Barmatz, V., Zalk, R., Gincel, D., and Vardi, N. (2004). Subcellular localization of VDAC in mitochondria and ER in the cerebellum. Biochim. Biophys. Acta BBA - Bioenerg. *1657*, 105–114.

Smirnova, E., Shurland, D.-L., Ryazantsev, S.N., and Bliek, A.M. van der (1998). A human dynamin-related protein controls the distribution of mitochondria. j. cell biol. *143*, 351–358.

Smith, M.J., Pozo, K., Brickley, K., and Stephenson, F.A. (2006). Mapping the GRIF-1 binding domain of the kinesin, KIF5C, substantiates a role for GRIF-1 as an adaptor protein in the anterograde trafficking of cargoes. J. Biol. Chem. *281*, 27216–27228.

Van Spronsen, M., Mikhaylova, M., Lipka, J., Schlager, M.A., van den Heuvel, D.J., Kuijpers, M., Wulf, P.S., Keijzer, N., Demmers, J., Kapitein, L.C., et al. (2013). TRAK/Milton motor-adaptor proteins steer mitochondrial trafficking to axons and dendrites. Neuron *77*, 485–502.

Starr, D.A., and Han, M. (2002). Role of ANC-1 in tethering nuclei to the actin cytoskeleton. Science *298*, 406–409.

Stowers, R.S., Megeath, L.J., Górska-Andrzejak, J., Meinertzhagen, I.A., and Schwarz, T.L. (2002). Axonal transport of mitochondria to synapses depends on milton, a novel Drosophila protein. Neuron *36*, 1063–1077.

Su, Q., Cai, Q., Gerwin, C., Smith, C.L., and Sheng, Z.-H. (2004). Syntabulin is a microtubule-associated protein implicated in syntaxin transport in neurons. Nat. Cell Biol. *6*, 941–953.

Tekk k, S.B., Brown, A.M., and Ransom, B.R. (2003). Axon Function Persists During Anoxia in Mammalian White Matter. J. Cereb. Blood Flow Metab. 1340–1347.

Trushina, E., Dyer, R.B., Badger, J.D., Ure, D., Eide, L., Tran, D.D., Vrieze, B.T., Legendre-Guillemin, V., McPherson, P.S., Mandavilli, B.S., et al. (2004). Mutant huntingtin impairs axonal trafficking in mammalian neurons in vivo and in vitro. Mol. Cell. Biol. *24*, 8195–8209.

De Vos, K.J., Chapman, A.L., Tennant, M.E., Manser, C., Tudor, E.L., Lau, K.-F., Brownlees, J., Ackerley, S., Shaw, P.J., Mcloughlin, D.M., et al. (2007). Familial amyotrophic lateral sclerosis-linked SOD1 mutants perturb fast axonal transport to reduce axonal mitochondria content. Hum. Mol. Genet. *16*, 2720–2728.

Wang, X., and Schwarz, T.L. (2009). The mechanism of Ca2+-dependent regulation of kinesin-mediated mitochondrial motility. Cell *136*, 163–174.

Wang, J.T., Medress, Z.A., and Barres, B.A. (2012). Axon degeneration: molecular mechanisms of a self-destruction pathway. J. Cell Biol. *196*, 7–18.

Wang, X., Su, B., Fujioka, H., and Zhu, X. (2008). Dynamin-like protein 1 reduction underlies mitochondrial morphology and distribution abnormalities in fibroblasts from sporadic Alzheimer's disease patients. Am. J. Pathol. *173*, 470–482.

Wang, X., Su, B., Lee, H., Li, X., Perry, G., Smith, M.A., and Zhu, X. (2009). Impaired balance of mitochondrial fission and fusion in Alzheimer's disease. J. Neurosci. Off. J. Soc. Neurosci. *29*, 9090–9103.

Winkler, B.S., Arnold, M.J., Brassell, M.A., and Puro, D.G. (2000). Energy metabolism in human retinal Müller cells. Invest. Ophthalmol. Vis. Sci. *41*, 3183–3190.

D' Ydewalle, C., Krishnan, J., Chiheb, D.M., Van Damme, P., Irobi, J., Kozikowski, A.P., Berghe, P.V., Timmerman, V., Robberecht, W., and Van Den Bosch, L. (2011). HDAC6 inhibitors reverse axonal loss in a mouse model of mutant HSPB1-induced Charcot-Marie-Tooth disease. Nat. Med. *17*, 968–974.

Zhu, Y.-B., and Sheng, Z.-H. (2011). Increased axonal mitochondrial mobility does not slow amyotrophic lateral sclerosis (ALS)-like disease in mutant SOD1 mice. J. Biol. Chem. *286*, 23432–23440.

Zinsmaier, K.E., Babic, M., and Russo, G.J. (2009). Mitochondrial transport dynamics in axons and dendrites. Results Probl. Cell Differ. *48*, 107–139.

Zündorf, G., and Reiser, G. (2011). Calcium dysregulation and homeostasis of neural calcium in the molecular mechanisms of neurodegenerative diseases provide multiple targets for neuroprotection. Antioxid. Redox Signal. *14*, 1275–1288.